ESD-TR-69-280

ANALYSIS OF REAL-TIME REFRACTION CORRECTION METHODS FOR THREE MISSILE FLIGHTS FROM THE AIR FORCE WESTERN TEST RANGE

Lyall G. Rowlandson
John R. Herlihy

July 1969

AEROSPACE INSTRUMENTATION PROGRAM OFFICE
ELECTRONIC SYSTEM DIVISION
AIR FORCE SYSTEMS COMMAND
UNITED STATES AIR FORCE
L.G. Hanscom Field, Bedford, Mass

(Prepared under contract No. F19628-68-C-0209 by Syracuse University Reseach Corporation, Merrill Lane, University Heights, Syracuse, New York)

LEGAL NOTICE

When U. S. Government drawings, specifications or other data are used for any purpose other than a definitely related government procurement operation, the government thereby incurs no responsibility nor any obligation whatsoever; and the fact that the government may have formulated, furnished, or in any way supplied the said drawings, specifications, or other data is not to be regarded by implication or otherwise as in any manner licensing the holder or any other person or conveying any rights or permission to manufacture, use, or sell any patented invention that may in any way be related thereto.

OTHER NOTICES

Do not return this copy. Retain or destroy.

ESD-TR-69-280

ANALYSIS OF REAL-TIME REFRACTION CORRECTION METHODS FOR THREE MISSILE FLIGHTS FROM THE AIR FORCE WESTERN TEST RANGE

Lyall G. Rowlandson
John R. Herlihy

July 1969

AEROSPACE INSTRUMENTATION PROGRAM OFFICE
ELECTRONIC SYSTEM DIVISION
AIR FORCE SYSTEMS COMMAND
UNITED STATES AIR FORCE
L.G. Hanscom Field, Bedford, Mass

(Prepared under contract No. F19628-68-C-0209 by Syracuse University Reseach Corporation, Merrill Lane, University Heights, Syracuse, New York)

FOREWORD

This report is prepared for the

Aerospace Instrumentation Program Office
Electronics Systems Division
Air Force Systems Command of the United States Air Force
L. G. Hanscom Field
Bedford, Massachusetts

Air Force Program Monitor - Lt. C. Schafer, ESD/ESSIE

Project Number 6684, Task 6684.05

covering research over the period

1 January 1969 to 8 July 1969.

Prepared under Contract No. F19628-69-C-0209 by

Syracuse University Research Corporation
Merrill Lane, University Heights
Syracuse, New York.

This technical report has been reviewed and is approved.

GEORGE T GALT, Colonel USAF
Director of Aerospace Instrumentation
Program Office

ABSTRACT

An emphasis is placed on the real-time correction of refraction-induced tracking errors. With radar data from three missile trajectories the corrected range and angle data, using real-time equations, is compared with ray-traced data. It is shown that these equations can be effectively used to reduce the range and angle errors to about the resolution of the tracking radars; that is, approximately two feet in range and five thousandths of a degree in angle. It is also shown that the effect of an elevated layer on tracking angle errors can be compensated using these equations.

TABLE OF CONTENTS

TABLE OF CONTENTS

LIST OF ILLUSTRATIONS

LIST OF ILLUSTRATIONS

SECTION I

INTRODUCTION

In a previous report[1] an analysis was made of the refraction-induced errors produced by time and space variations of the medium. These apparent variations limit one's ability to define a single refractivity profile which can be used to compensate these errors in near-real-time. Within these restrictions a radiosonde profile obtained close to the time of launch and at a location in front of the tracking radar provides a first-order description of the propagation conditions.

To determine the significance of the refractivity fine structure obtained from the radiosonde requires ray-tracing analysis. Due to the time required to obtain ray-traced data for real-time corrections one must store the error data obtained from the tracings in advance and then reacquire this data or generate simple empirically-determined functions which can yield the equivalent error data in real-time. The ray-traced, storage approach requires making use of a large part of the tracking computer memory bank. If several radars are required to provide raw data into this central computer this approach generally becomes unacceptable.

The second method using functions fitted to the ray-traced error data has several variations. If the empirical functions are derived directly from error data the resulting equations can lose identification with the real-world parameters which produce refraction errors, such as the effect of the range, elevation angle, surface value of refractivity, etc. These equations are then mathematical expressions, probably polynomials, but can be made sufficiently simple to be used for real-time corrections. By preparing a library of these expressions for a wide range of measured refractivity profiles experience should permit one to select functions to meet most situations.

Another approach is to assume that on the average the refractivity profile can be expressed by a simple exponential function[2]. With suitable approximations equations can be developed for real-time range and angle corrections. To date, the development of these equations does not permit one to include an elevated layer in the model.

The following report describes the development and application of some new correction equations which can be used in real-time. These equations represent continuous functions which maintain a physical identification with the parameters which effect refraction-induced errors. Inherent in these equations is the ability to include the effect of an elevated layer thereby making these equations particularly useful for low-angle tracking. A comparison is presented of the differences between tracking parameters

determined from these real-time equations and the AFWTR post-flight ray-tracing analysis for two vehicle launches and with three AFWTR radars tracking each launch. In addition, one comparison is made with the GERTS real-time correction program. However, no inversion layer was present for this launch.

The comparative results indicate that meaningful corrections to refraction-induced tracking errors can be obtained with the SURC real-time equations. If accurate tracking data is required only above five degrees elevation angle these equations require only a single value of surface refractivity which can be obtained from the locally associated radiosonde launch station. To improve the accuracy below five degrees elevation angle the characteristics of the inversion layer, if present, need to be included.

These considerations indicate that if further investigations are necessary they should be directed toward the measurement of the residual errors within an experiment where corrected radar data is confronted with known target position data. Suitable test targets could be established by first using high altitude aircraft equipped with accurate radar altimeters for short range studies. Finally, using satellite targets of known trajectory, the long range errors at both low and high angles could be studied. However, in the light of presently available tracking accuracies using the FPS-16 radars it is believed that the bulk of residual errors will be largely due to the electromechanical characteristics of the radars and that the residual refraction errors will be almost impossible to detect in a systematic way. Therefore, further intensive investigations of the nature of all residual errors is deemed to be meaningless until the tracking system can resolve range to less than two feet and angles to less than 0.1 milliradians.

SECTION II

ANALYSIS

It was shown that for propagation in a simple exponential atmosphere the range error, ΔR, and true elevation angle, B_o, can be expressed by (figure 1).

$$\Delta R \simeq \frac{10^{-6} N_s}{c \sin \gamma} \left[1 - \frac{g}{k+g} \cdot e^{-(k^2 + 2kg)}\right] \tag{1}$$

$$B_o \simeq \sin^{-1} \left[\frac{1}{R} \int_o^R \sin (\theta_o - \tau)\, dR\right] \tag{2}$$

where the magnitude of the ray-bending, τ, is

$$\tau \simeq \frac{10^{-6} N_s}{\tan \gamma} \left[1 - \frac{g}{k+g}\, e^{-(k^2 + 2kg)}\right] \tag{3}$$

and

$$\sin \gamma = \sin \theta_o + \left[k_o + k_2 e^{-k_3 R}\right] e^{-k_1 \theta_o} \tag{4}$$

$$g = \sqrt{\frac{c r_o}{2}} \cdot \tan \gamma \tag{5}$$

$$k = R \sqrt{\frac{c}{2 r_o}} \cdot \cos \gamma \tag{6}$$

$$N = N_s\, e^{-c(h - H_s)} \tag{7}$$

The empirical constants, $k_o, \ldots, k_3$, were required at short ranges and small elevation angles to provide ray-bending calculations from (3) in agreement with the CRPL exponential model atmosphere. Their variation with station value of refractivity, N_s, is shown in figure 2.

Since the CRPL model was developed to correct ray-bending, the magnitude of the exponential decay constant, c, (7), tends to increase with N_s.[2] The range error, ΔR, being the integral of N tends to be directly dependent on the surface value, N_s. When the station value, N_s, exceeds about 340 units the effect of c, (1), causes the range error, ΔR, to decrease as N_s increases, which is abnormal. However, the error produced by this effect is very small compared with the position error produced by the effect of ray-bending. Therefore, it is meaningful to concentrate on the reduction of target position error produced by ray-bending and for this reason the

A4383

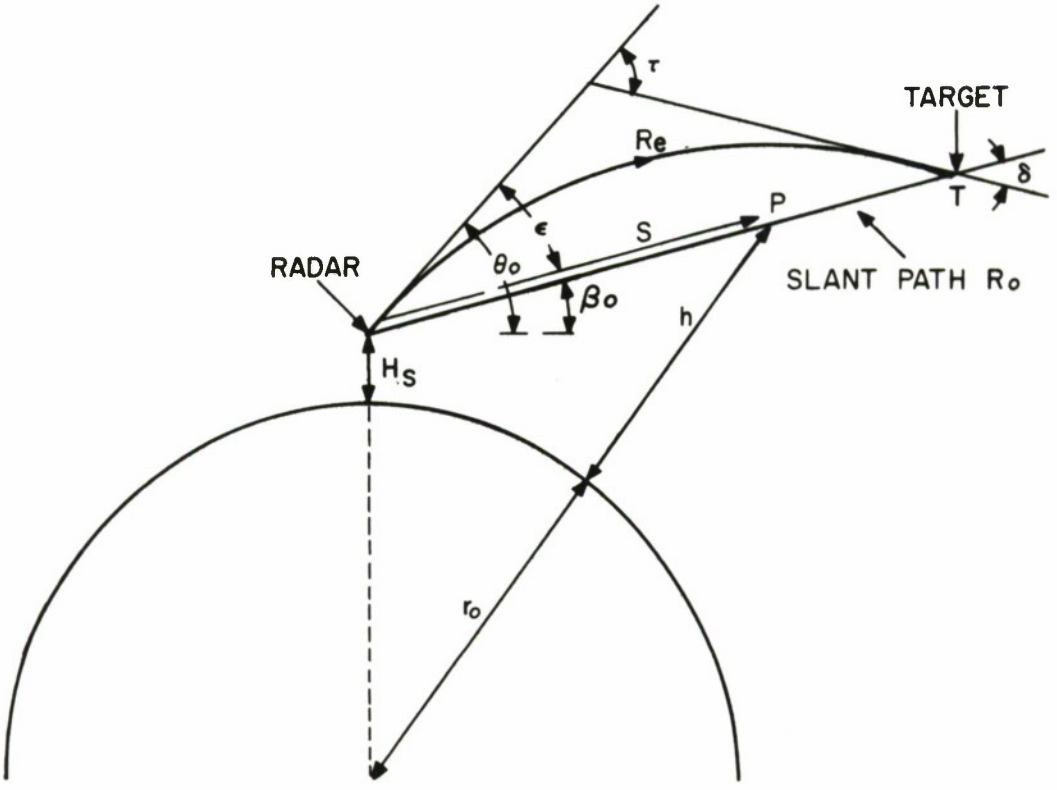

FIGURE 1. RAY GEOMETRY

FIGURE 2. VARIATION OF EMPIRICAL CONSTANTS WITH SURFACE REFRACTIVITY

CRPL model was adopted in this development. Furthermore, the velocity error is more seriously affected by ray-bending than by the range error.[3]

The true elevation angle, B_o, can be calculated directly with a digital computer by writing

$$\int_o^R \sin(\theta_o - \tau) \simeq \sum_{i=1}^{N} \sin(\theta_o - \tau_i) \cdot \delta R_i \tag{8}$$

where, τ_i, is evaluated at the mid-point of each interval, δR_i, using (3) and

$$\delta R_i = R/N \tag{9}$$

Since the bending, τ, is a logarithmic function of range, R, it is possible to greatly reduce the number of elements in the summation by expressing

$$\delta R_i = \frac{\Delta R_i - \Delta R_{i-1}}{2} \tag{10}$$

where

$$\Delta R_i = R\left[1 - \log_N (N - i + 1)\right] \tag{11}$$

$$i = 2, 3, \ldots, N$$

For example, whereas 25 intervals is required with (8) to maintain a comparative angle accuracy of 0.05 milliradians, the number of intervals can be reduced to 9 (N equals 10) with (10). This represents a considerable reduction in execution time.

The above equations can be used in real-time to determine tracking errors from measured radar parameters. Appendix I shows how the effect on ray-bending produced by an elevated layer can be included. This first-order layer correction still permits these SURC equations to be used in real-time.

SECTION III

COMPARISON OF TRACKING ERRORS BETWEEN SURC CALCULATIONS AND AFWTR RAY-TRACED RESULTS - OPERATION 5265

Figures 3 and 4 show the true elevation angle and range from the South Vandenberg tracker, (FPS-16, 023002) for a vehicle launched from the Vandenberg firing site. This angle and range data was obtained by correcting the raw radar data using the AFWTR (post-flight) ray-tracing program. It should be noted that this program was not used in real-time. The propagation conditions were defined by a radiosonde launch from South Vandenberg close to vehicle launch time. Figure 5 shows the lower part of the refractivity profile, and it is apparent that no effective layer was present above the height of the Tranquillan Peak radar. The radiosonde data for all associated radars and launches is included in Appendix II.

The raw radar range, R, and apparent elevation angle, θ_o, were used as real-time inputs (10 points per second) to the SURC equations where the program was set to run with no layer present. (See program description, Appendix III).

Figure 6 shows the difference between the corrected elevation angle data where the AFWTR data in all cases is subtracted from the SURC data. During the first 10 seconds of flight the true elevation angle difference (B_o) reaches a peak of about 0.0075 degrees (0.131 mr). This difference decreases rapidly to a negligible amount after the first 50 seconds of flight. Figure 7 shows the elevation angle error data, ϵ, obtained with the AFWTR ray-tracing program and figure 8, the same angle error data from the SURC equations. It is apparent that the largest angle difference (0.0075 degrees) in figure 6 is contributed by a perturbation in the AFWTR calculations. The refractivity profile, figure 5, does not show any discontinuity above the site elevation and the vehicles elevation and range are monotonically increasing (figures 3 and 4). Therefore, the perturbation shown in the AFWTR data appears to be due to some computational error in the ray-tracing program and not produced because of the propagation conditions.

Figure 9 shows the differences between the corrected ranges. These differences are so small (well below the range resolution of the radar) they can be considered to be negligible. These results show that the exponential model atmosphere does provide an accurate description of the radio propagation conditions for this particular set of tracking conditions.

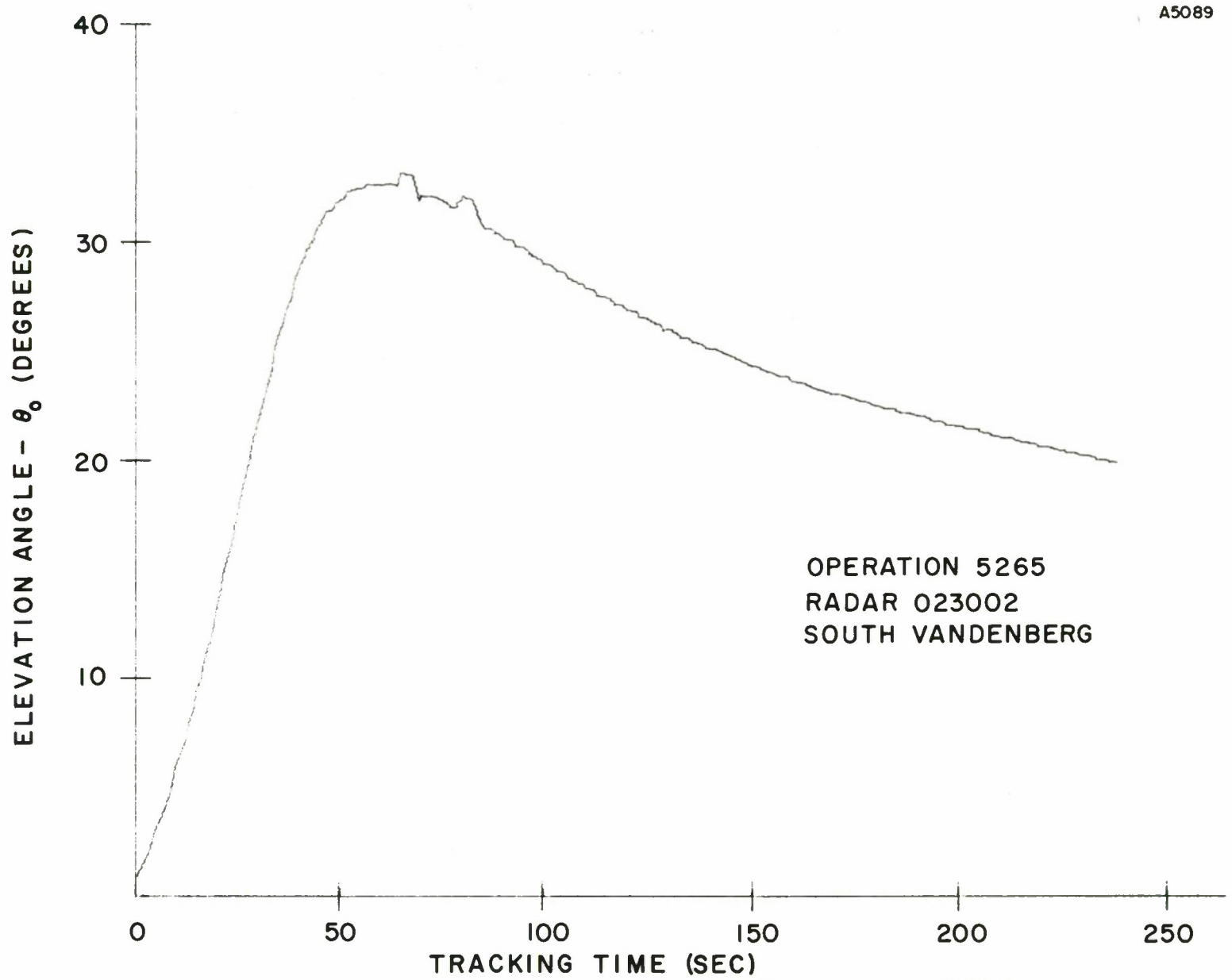

FIGURE 3. ELEVATION ANGLE VS. TIME (OP5265 SVBG)

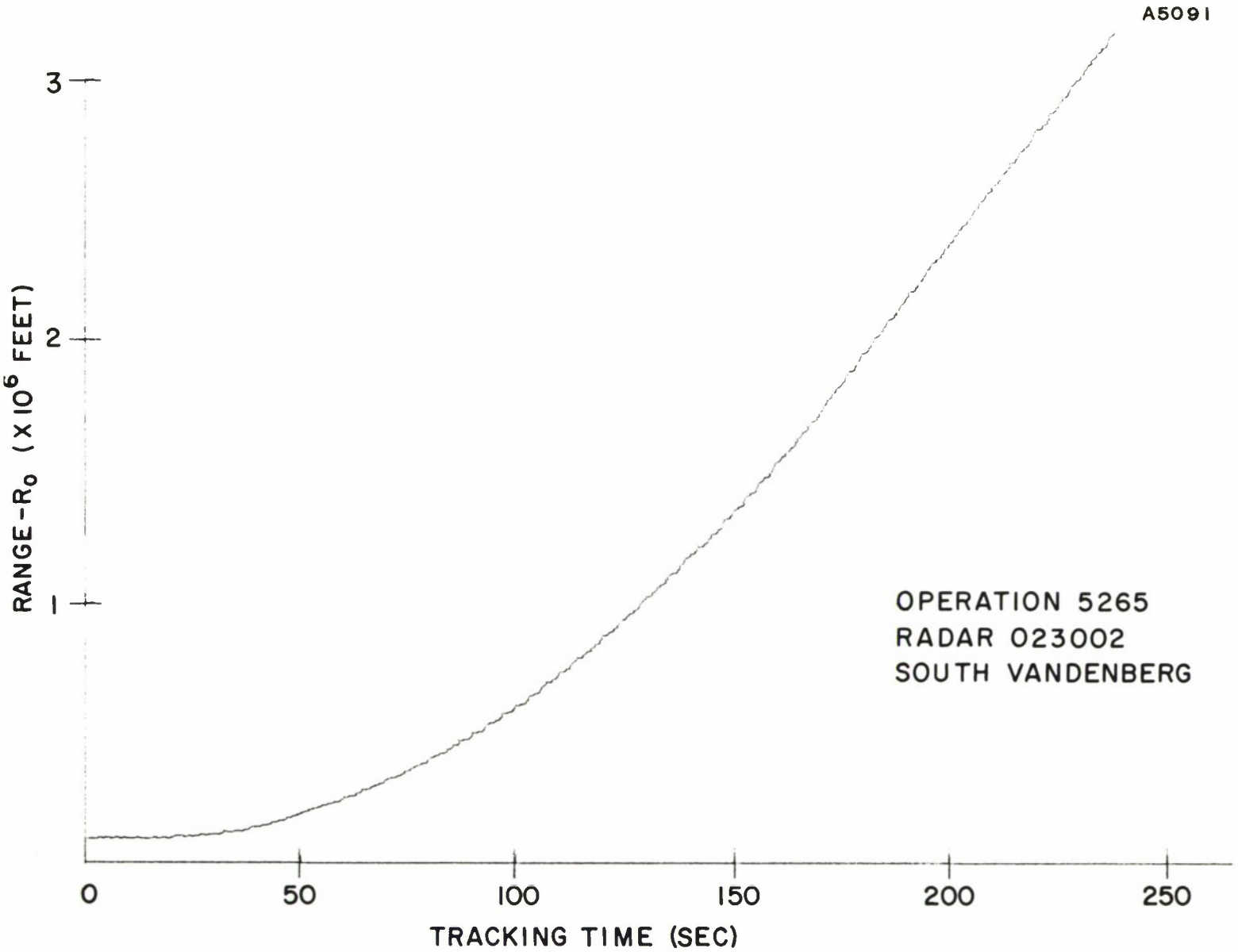

FIGURE 4. RANGE VS. TIME

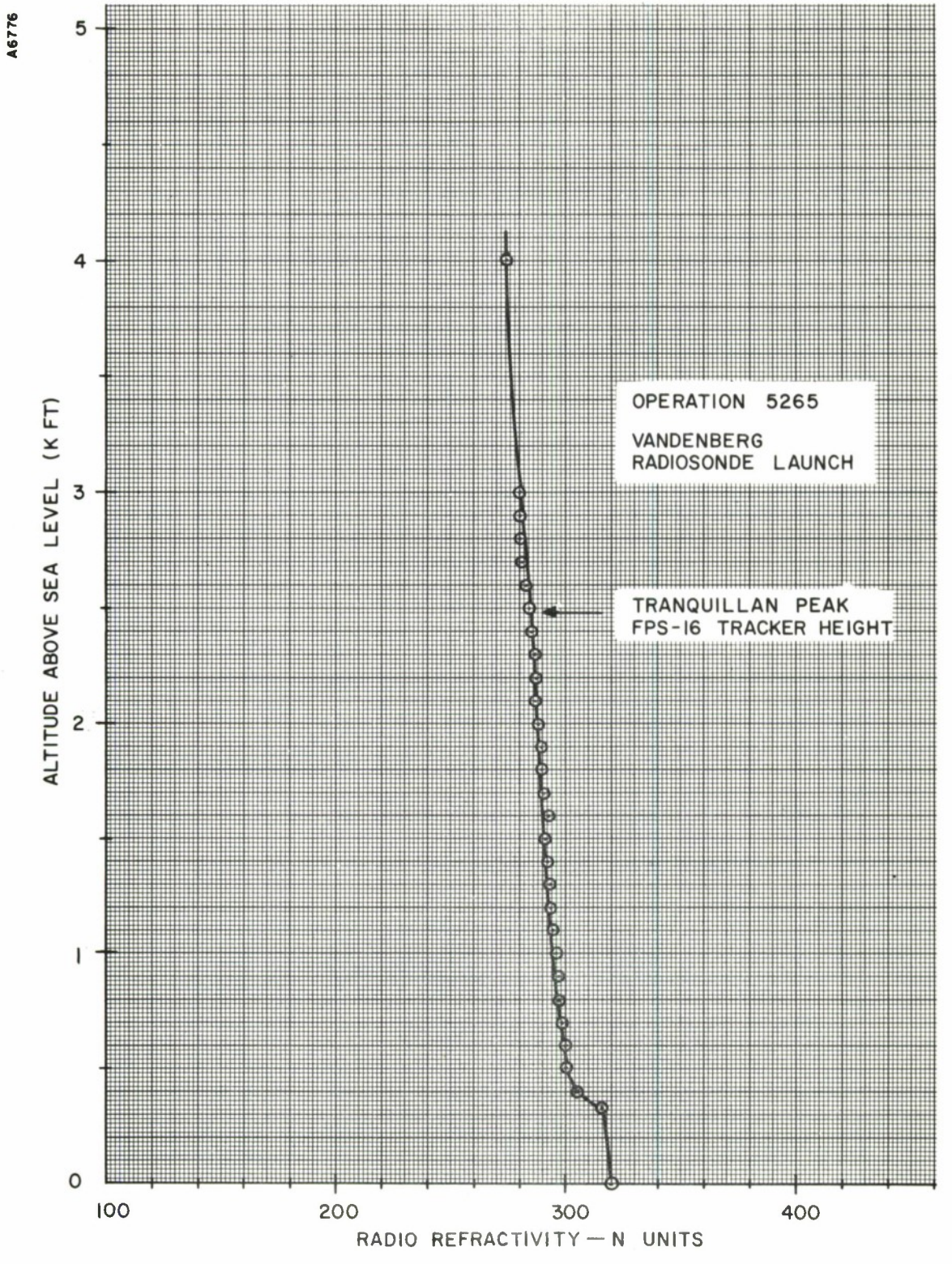

FIGURE 5. RADIO REFRACTIVITY PROFILE (SOUTH VANDENBERG)

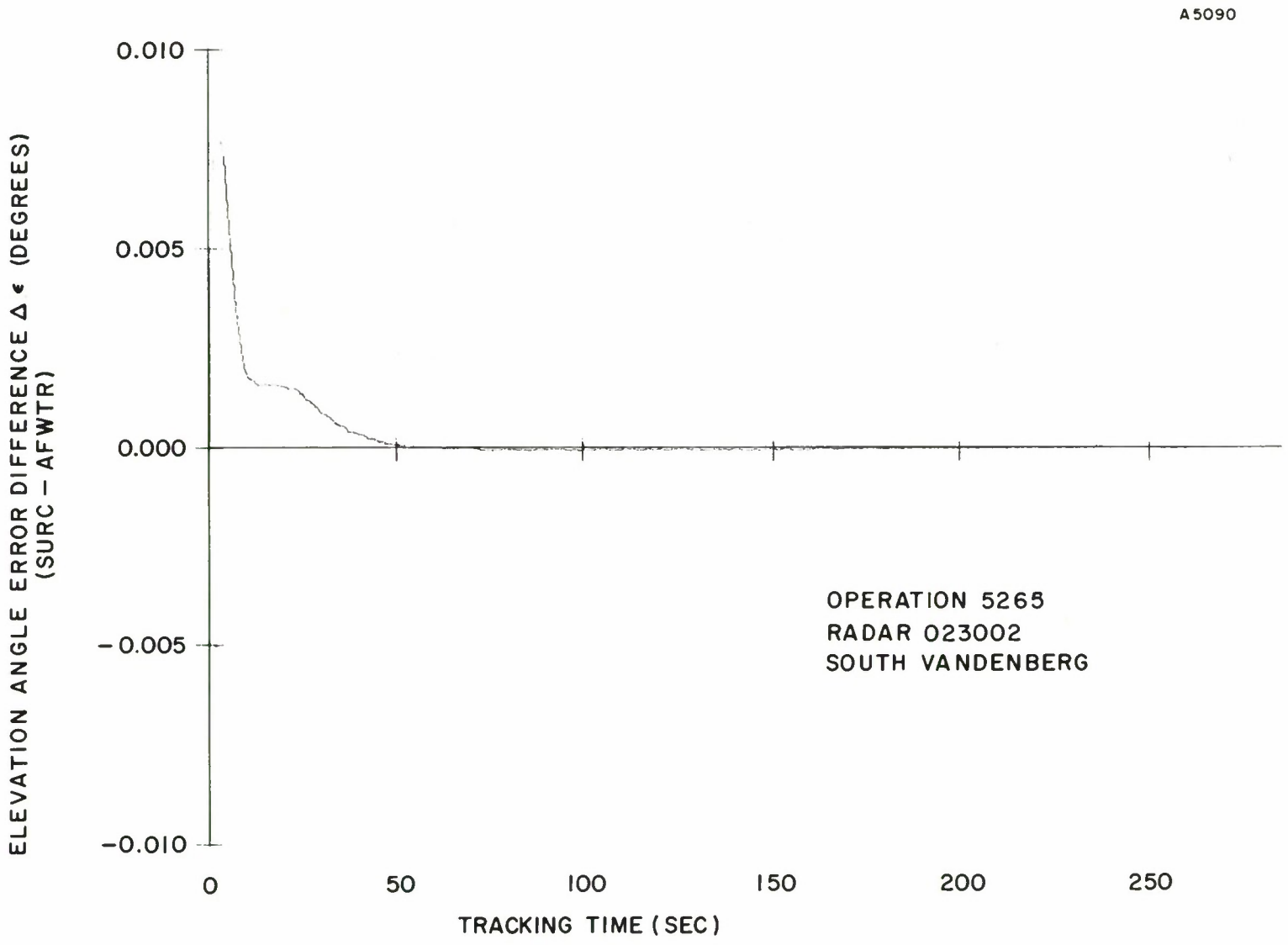

FIGURE 6. DIFFERENTIAL CORRECTED ELEVATION ANGLES VS. TIME

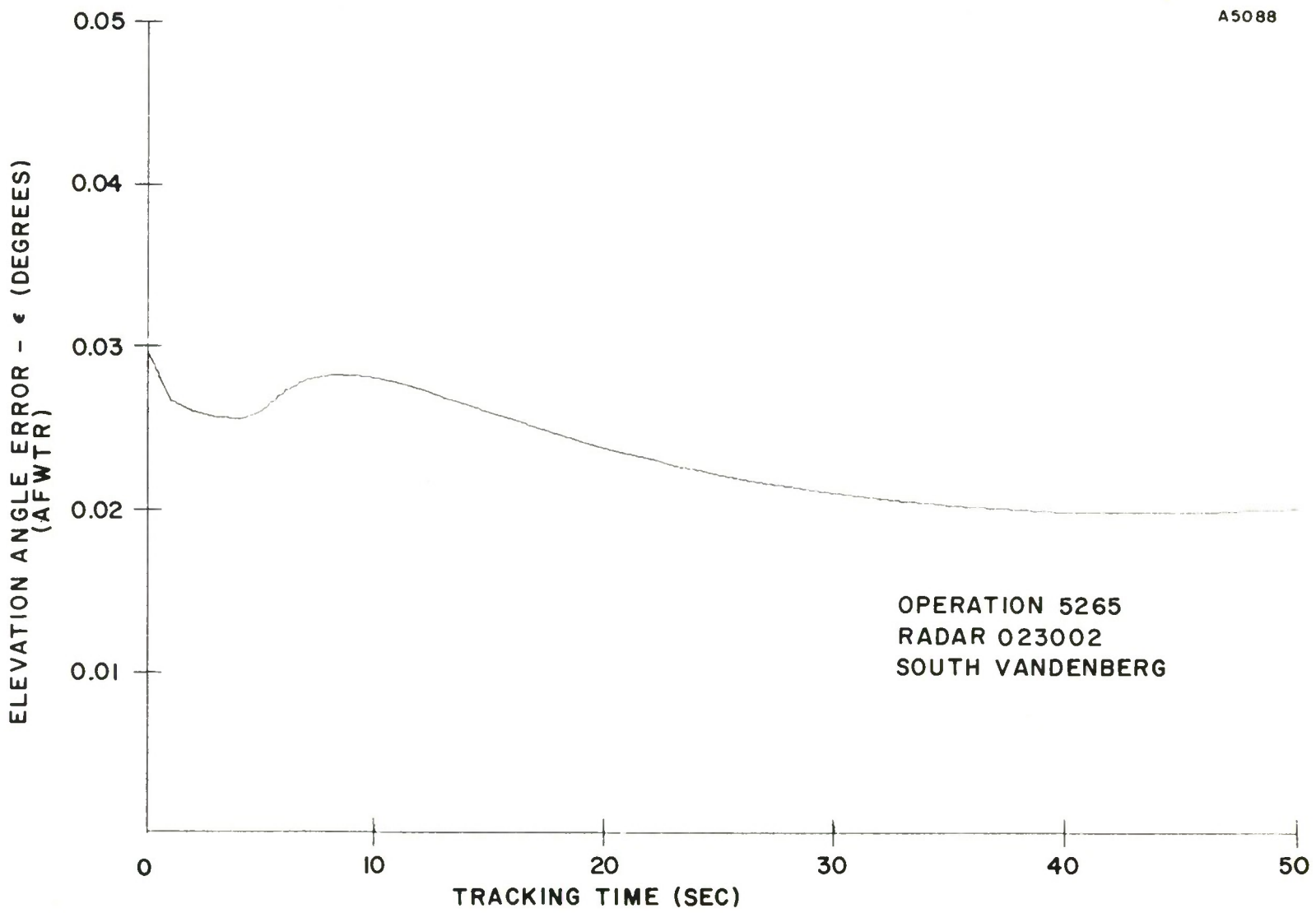

FIGURE 7. ELEVATION ANGLE ERROR VS. TIME (AFWTR)

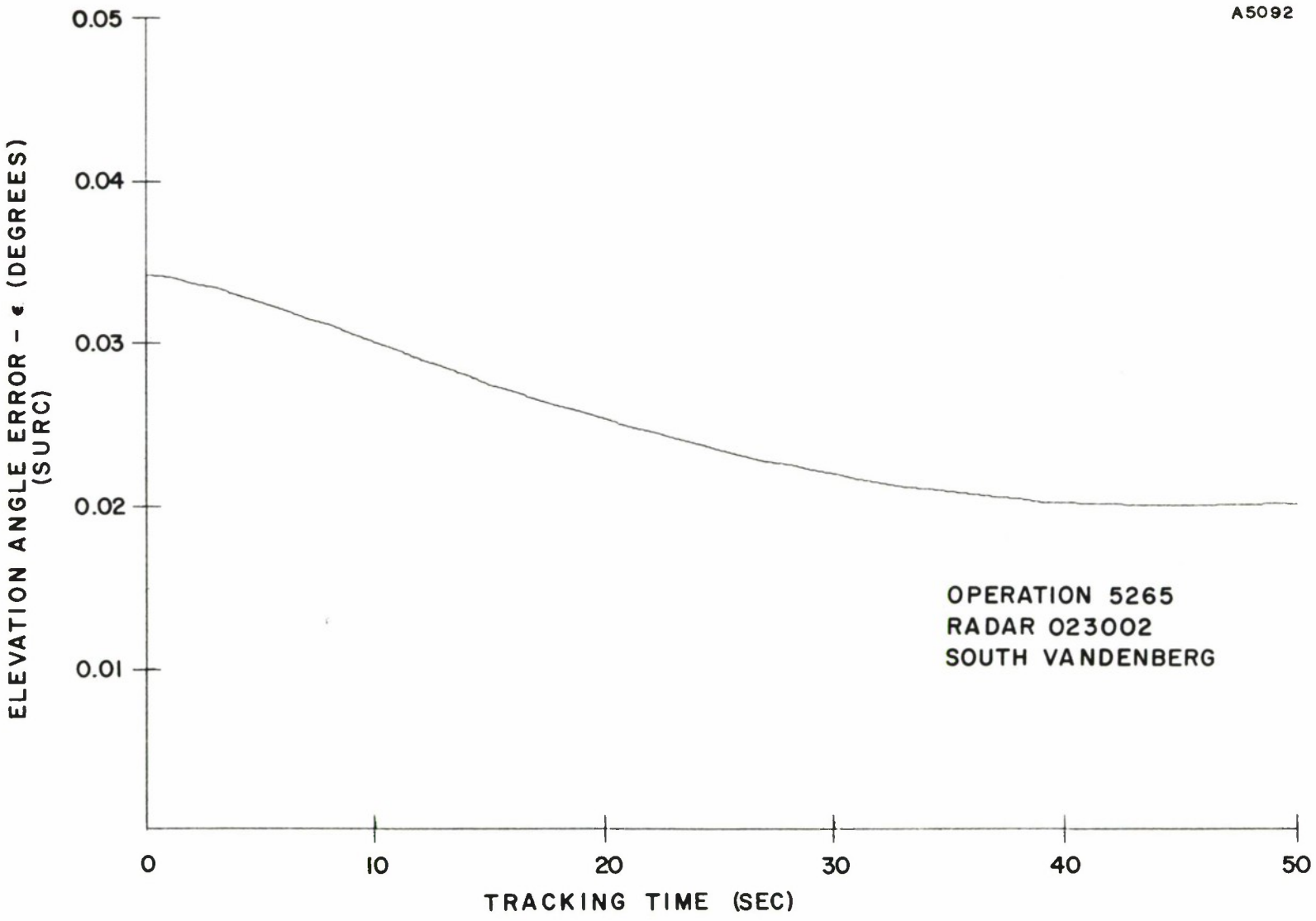

FIGURE 8. ELEVATION ANGLE ERROR VS. TIME (SURC)

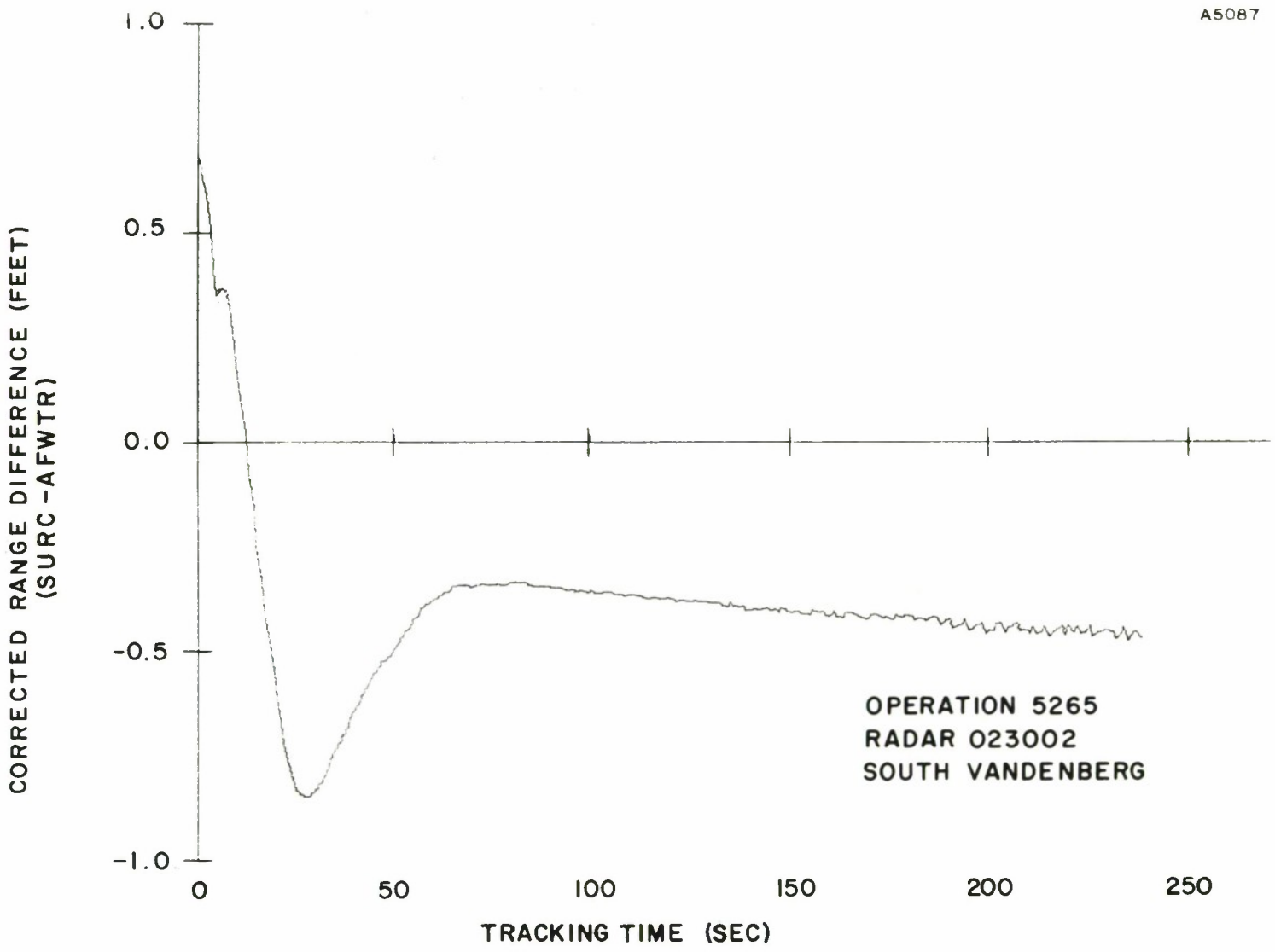

FIGURE 9. DIFFERENTIAL CORRECTED RANGES VS. TIME

Figures 10 and 11 show the tracking parameters from the radar (003003) at Point Mugu. Figure 12 shows the difference between the SURC and AFWTR elevation angle data. Initially, for tracking angles below five degrees (figure 10), the difference is about .015 degrees (0.26 mr) and thereafter decreases below 0.003 degrees (0.053 mr). Figure 13 shows the corrected range error difference and the maximum difference reaches about seven feet at low tracking angles and then decreases below 1.5 feet. Target position is most seriously affected by the angle errors and the angle difference (figure 12) of 0.015 degrees at a range of 500 KFT represents a height difference of 130 feet. At this time, the vehicle is around 30 KFT altitude. At 200 seconds the height difference is only 98 feet at a vehicle altitude of about one million feet.

Figures 14 through 17 show corresponding data for the Point Pillar radar (213001). This radar picks the vehicle up at a higher initial tracking angle and range due to the fact it is located far north of the firing site. The angle and range difference data is obviously negligible.

3.1 Some Comments on the Analysis of Operation 5265

Except for tracking elevation angles below five degrees the SURC real-time calculations are essentially in agreement with the post-flight, ray-traced, results provided by AFWTR. Of course, the greater differences in the elevation angle comparisons which occur at short ranges do not produce large position errors in height. These angle differences would be serious at long ranges if they remained above 0.006 degrees (0.1 mr). A more interesting comparison could be made when the radars are tracking at small elevation angles and very long ranges as the vehicle goes over the radar horizon. Unfortunately, the tracking data for operation 5265 terminated long before the radar horizon was reached.

A more interesting comparison is made in the analysis of Operation 2062, which follows, where one radar does track the vehicle almost to the radar horizon.

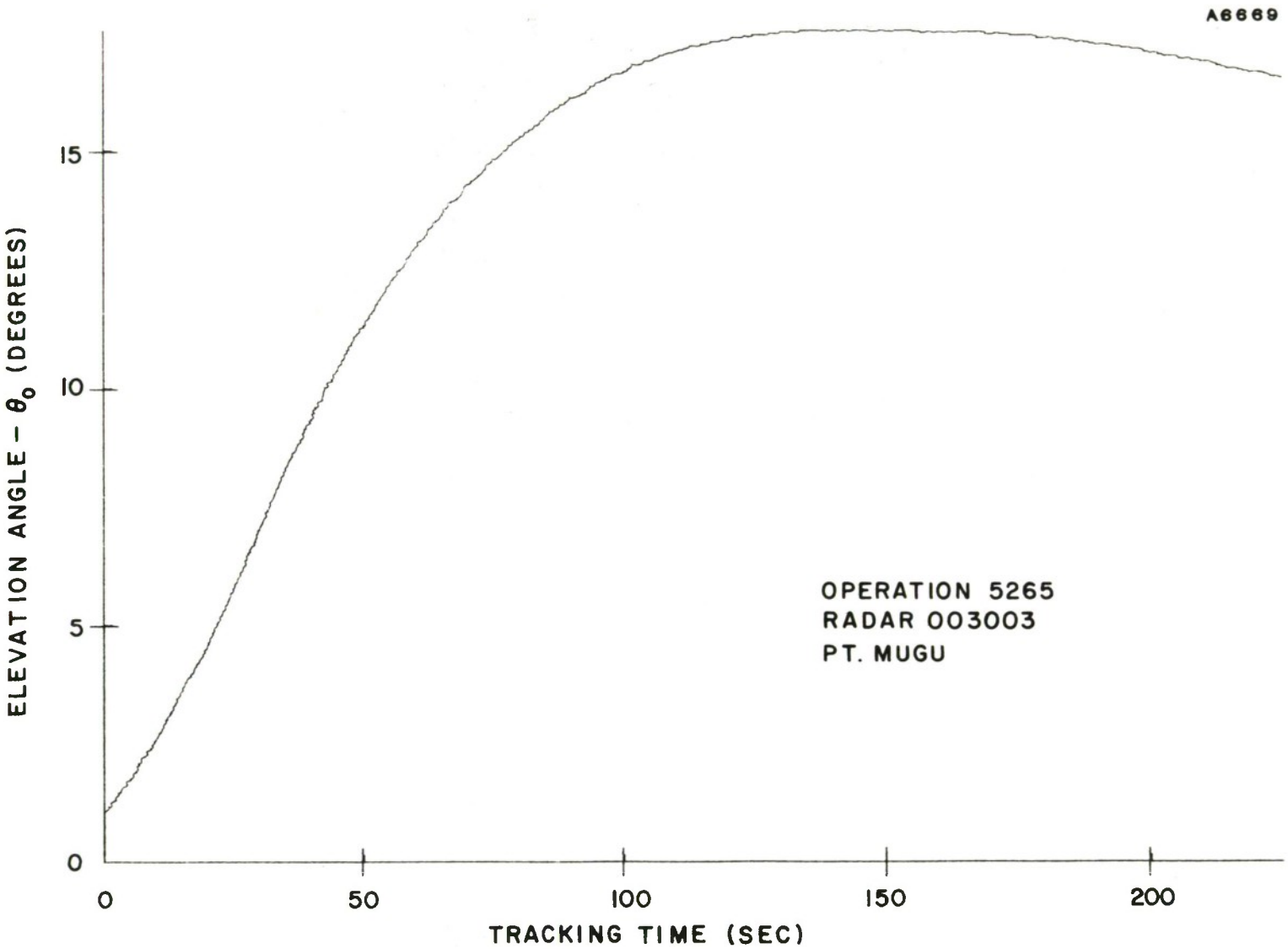

FIGURE 10. ELEVATION ANGLE VS. TIME (OP5265 PT. MUGU)

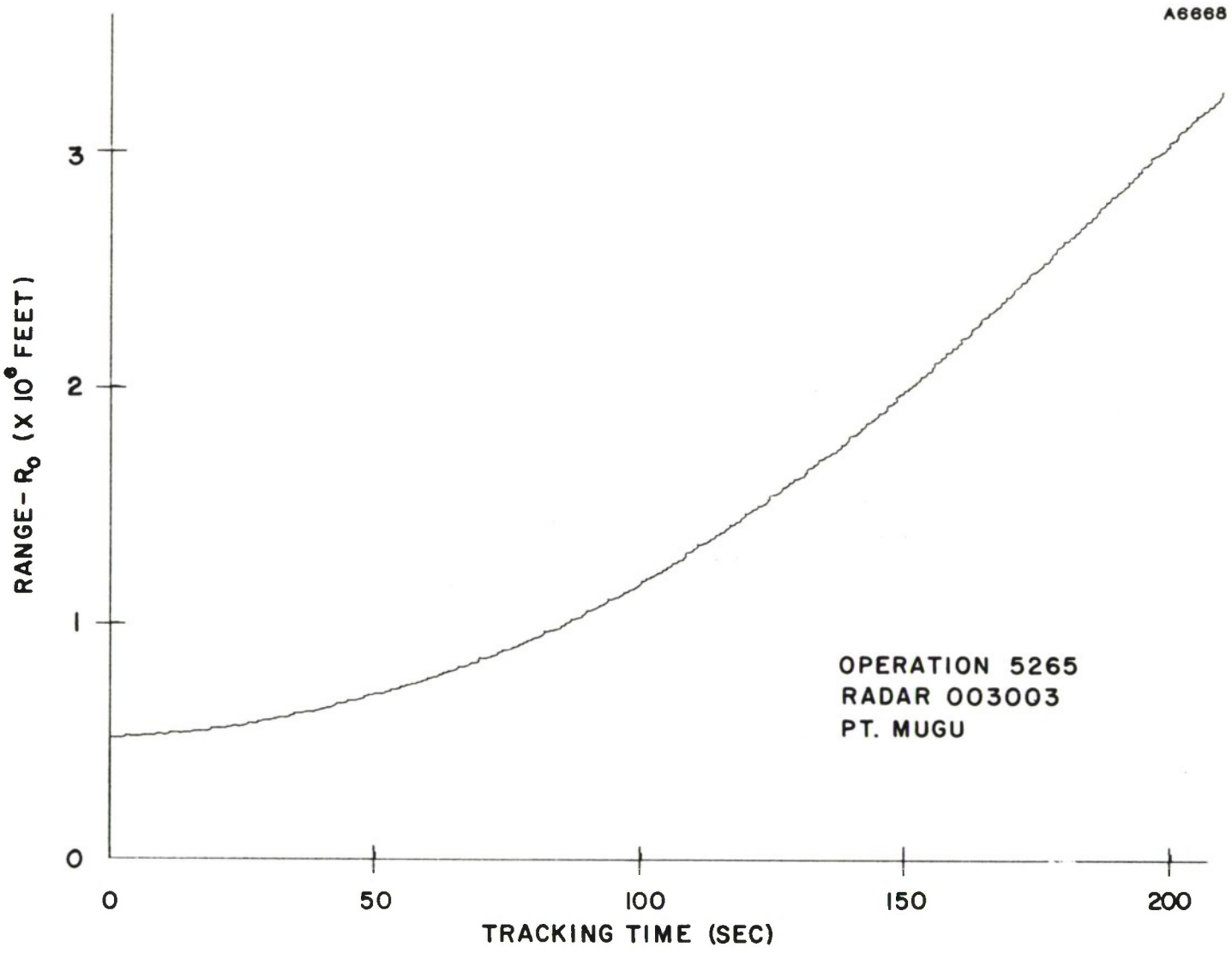

FIGURE 11. RANGE VS. TIME

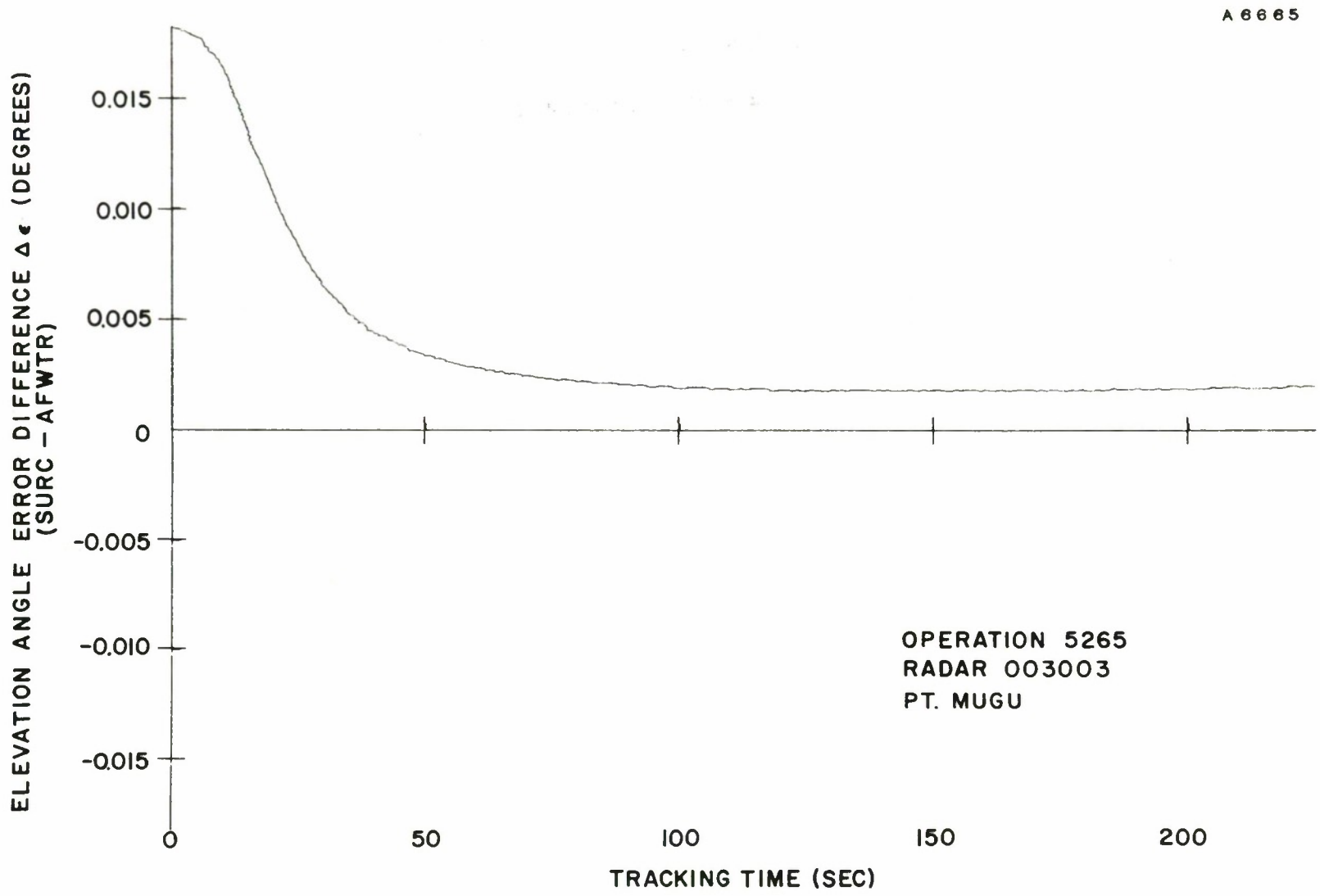

FIGURE 12. DIFFERENTIAL CORRECTED ELEVATION ANGLES VS. TIME

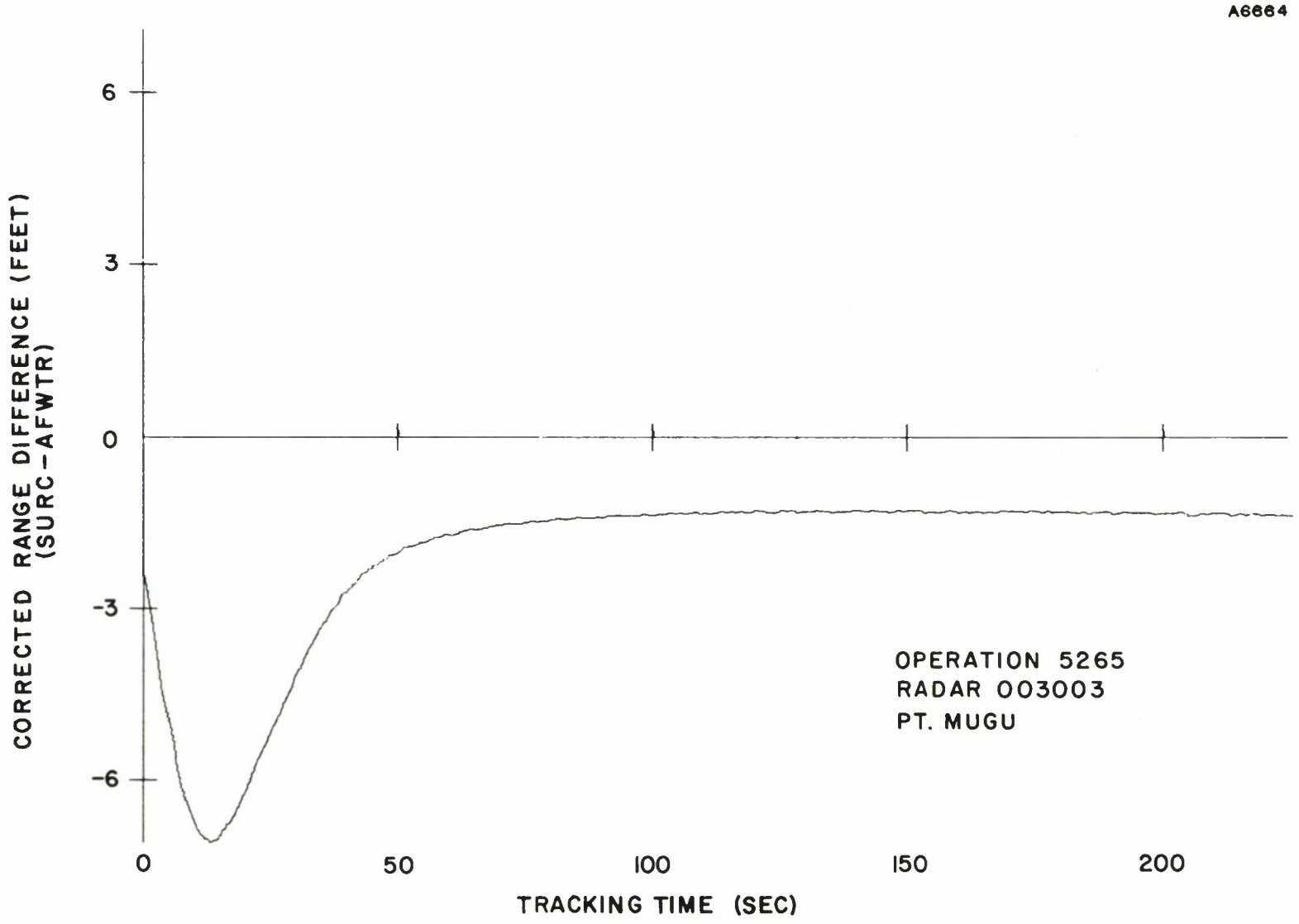

FIGURE 13. DIFFERENTIAL CORRECTED RANGES VS. TIME

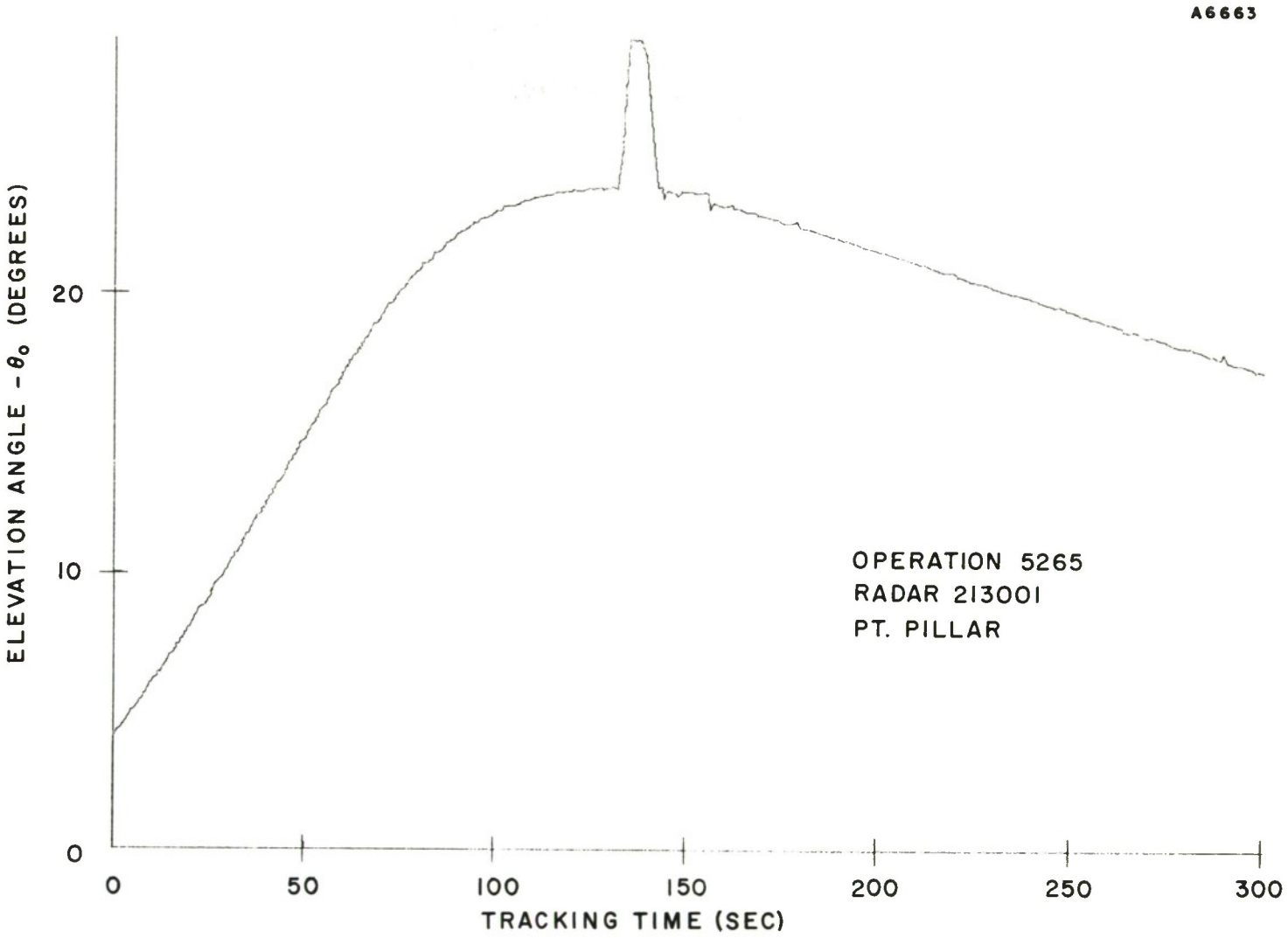

FIGURE 14. ELEVATION ANGLE VS. TIME (OP5265 PT. PILLAR)

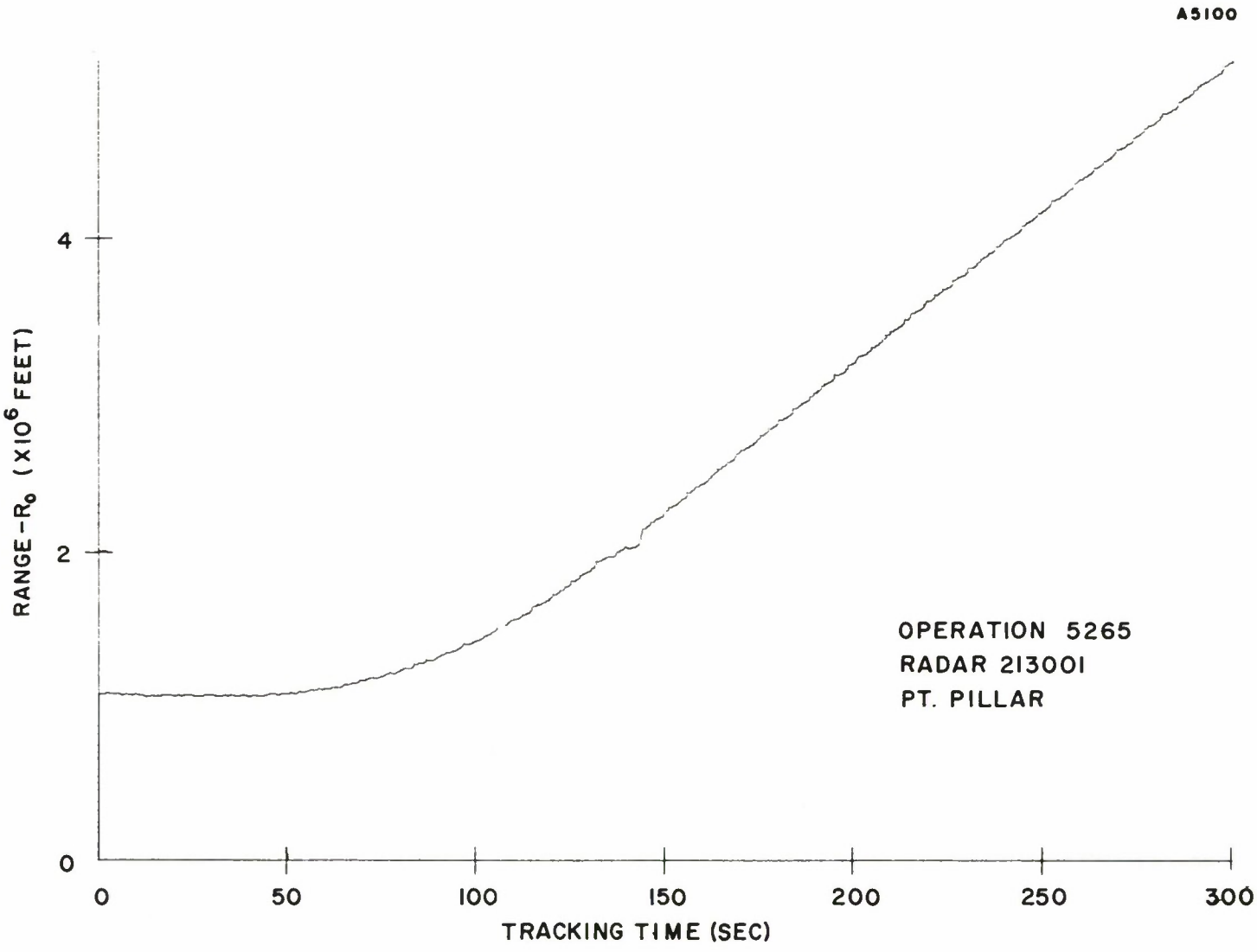

FIGURE 15. RANGE VS. TIME

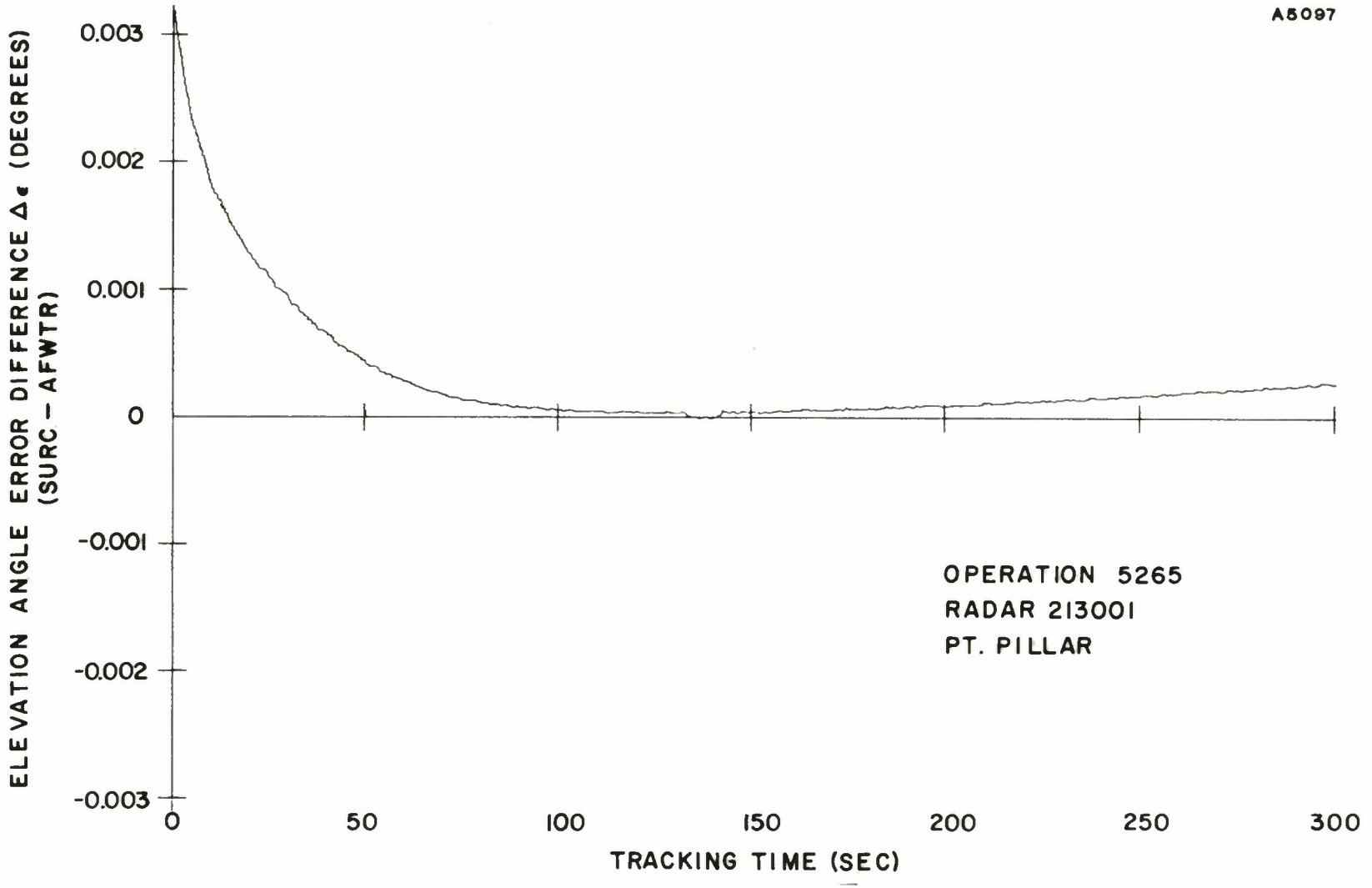

FIGURE 16. DIFFERENTIAL CORRECTED ELEVATION ANGLES VS. TIME

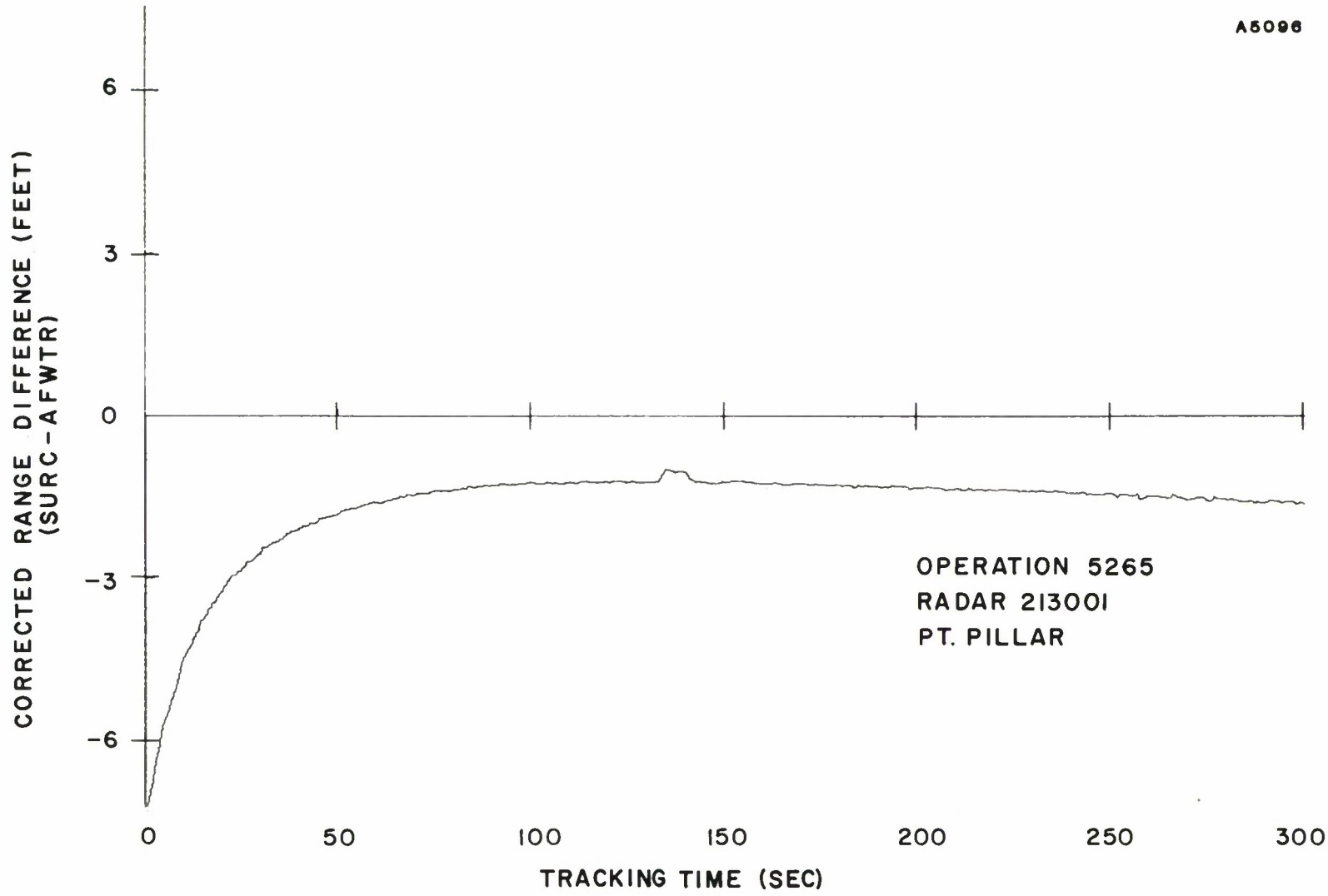

FIGURE 17. DIFFERENTIAL CORRECTED RANGES VS. TIME

SECTION IV

COMPARISON OF TRACKING ERRORS BETWEEN SURC CALCULATIONS AND AFWTR RAY-TRACED RESULTS - OPERATION 2062

Figures 18 through 23 show the tracking and difference data for Operation 2062 for the South Vandenberg tracker (023002). From figure 21 it may be noted that the corrected elevation angle data obtained from the AFWTR ray-traced program is perturbed within the first few seconds of flight. Figure 24 shows the associated radiosonde profile and it is apparent that the propagation conditions do not suggest a reason for this behavior. As noted before, the AFWTR calculations of the elevation angle error (figure 21) during the first few seconds of flight are not compatible with the smooth increase of elevation angle and range (figures 18 and 19).

The difference between SURC and AFWTR calculations of the corrected elevation angle (figure 22) and range (figure 23) are negligible after these first few seconds of flight.

Figures 25 through 28 show equivalent graphical results with the tracking radar located at Point Mugu (003001). As before, the difference between corrected elevation angles and ranges (figures 27 and 28) are negligible beyond 30 seconds of the flight. The radiosonde data (Appendix II) indicates a very weak layer might be present around 3 KFT. Since the layer was not introduced in the SURC equations one might expect that the elevation angle error, ϵ, would be larger using the AFWTR program. Therefore, during the first few seconds of tracking from Point Mugu the effect of a layer would cause the elevation angle difference (figure 27) to be larger. The results shown are, therefore, consistent with such propagation conditions.

Figures 29 through 32 show the results obtained with the tracker located at Point Pillar (213001). The comparative accuracies obtained throughout the first 300 seconds of tracking results are very good. The initial range error difference of about six feet (figure 23) is slightly larger than in previous cases. However, it should be noted that this time the vehicle was at a range of about one million feet (approximately 200 miles).

Figures 33 through 36 show results for the next 300 seconds of flight from Point Pillar where the vehicle is now heading towards the radar horizon. From figure 33 it may be seen that the elevation angle is decreasing towards five degrees and the range (figure 34) increasing beyond 10 million feet (approximately 2000 miles). A loss of signal occurs momentarily around 530 seconds.

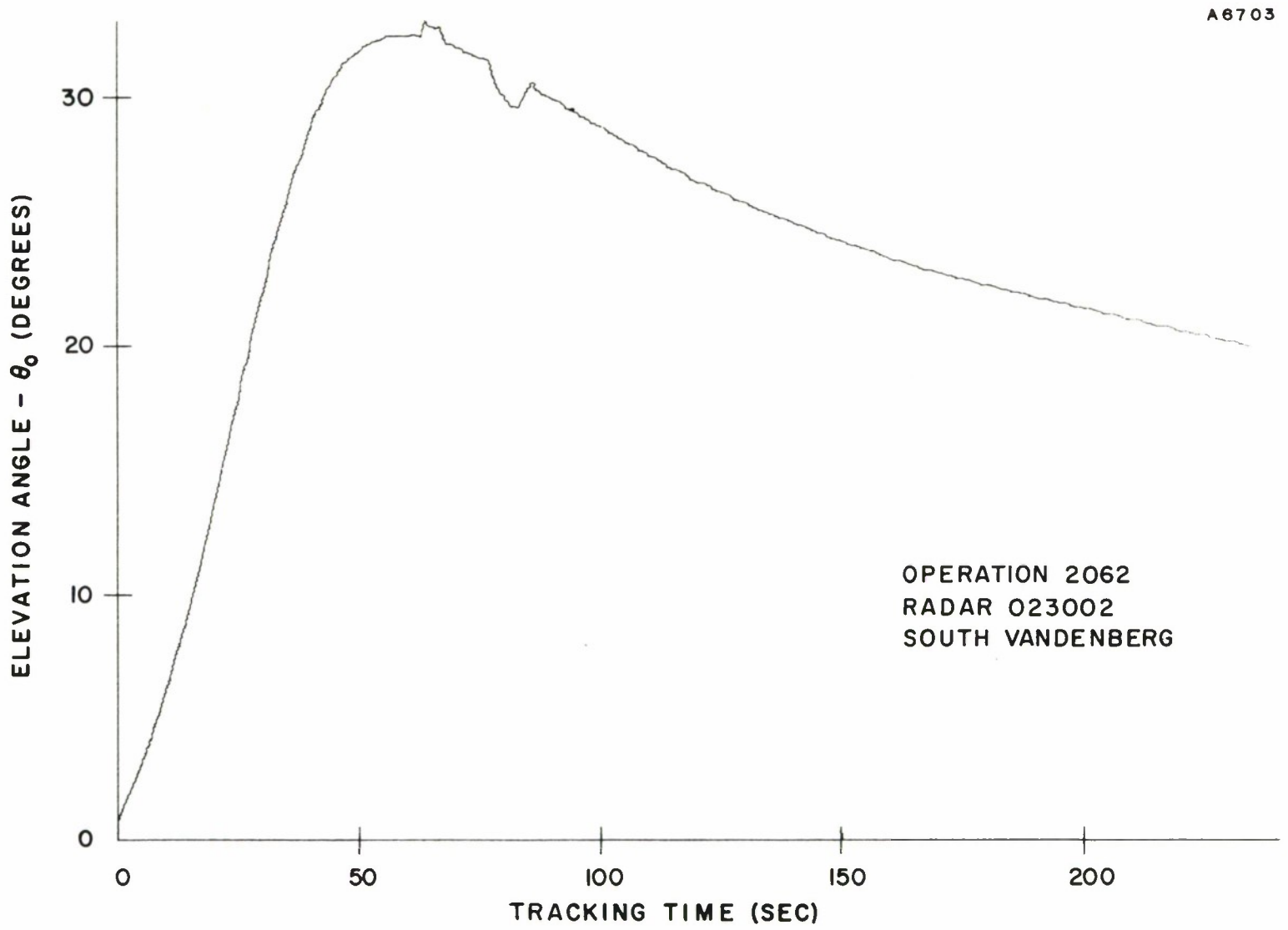

FIGURE 18. ELEVATION ANGLE VS. TIME (OP2062 SVBG)

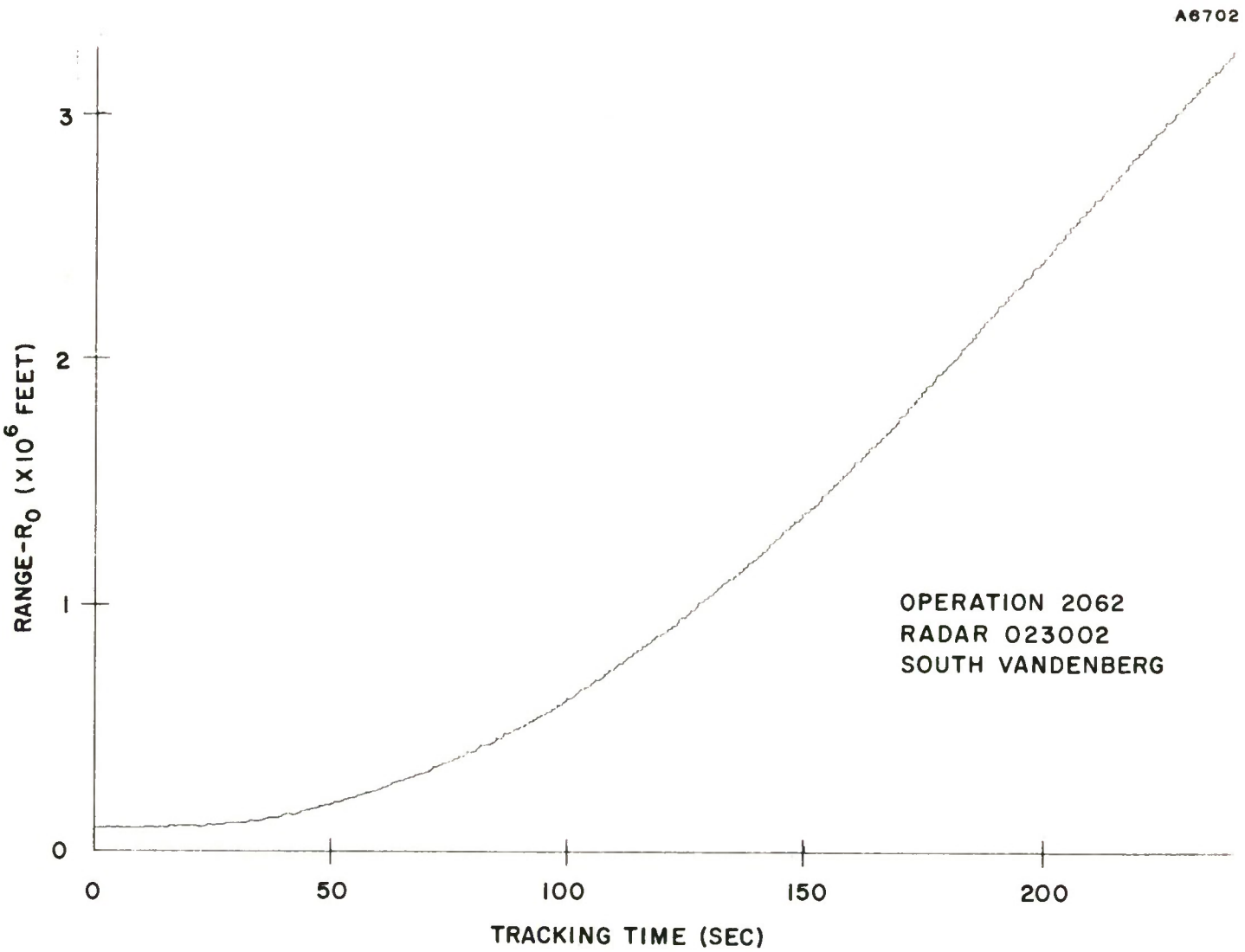

FIGURE 19. RANGE VS. TIME

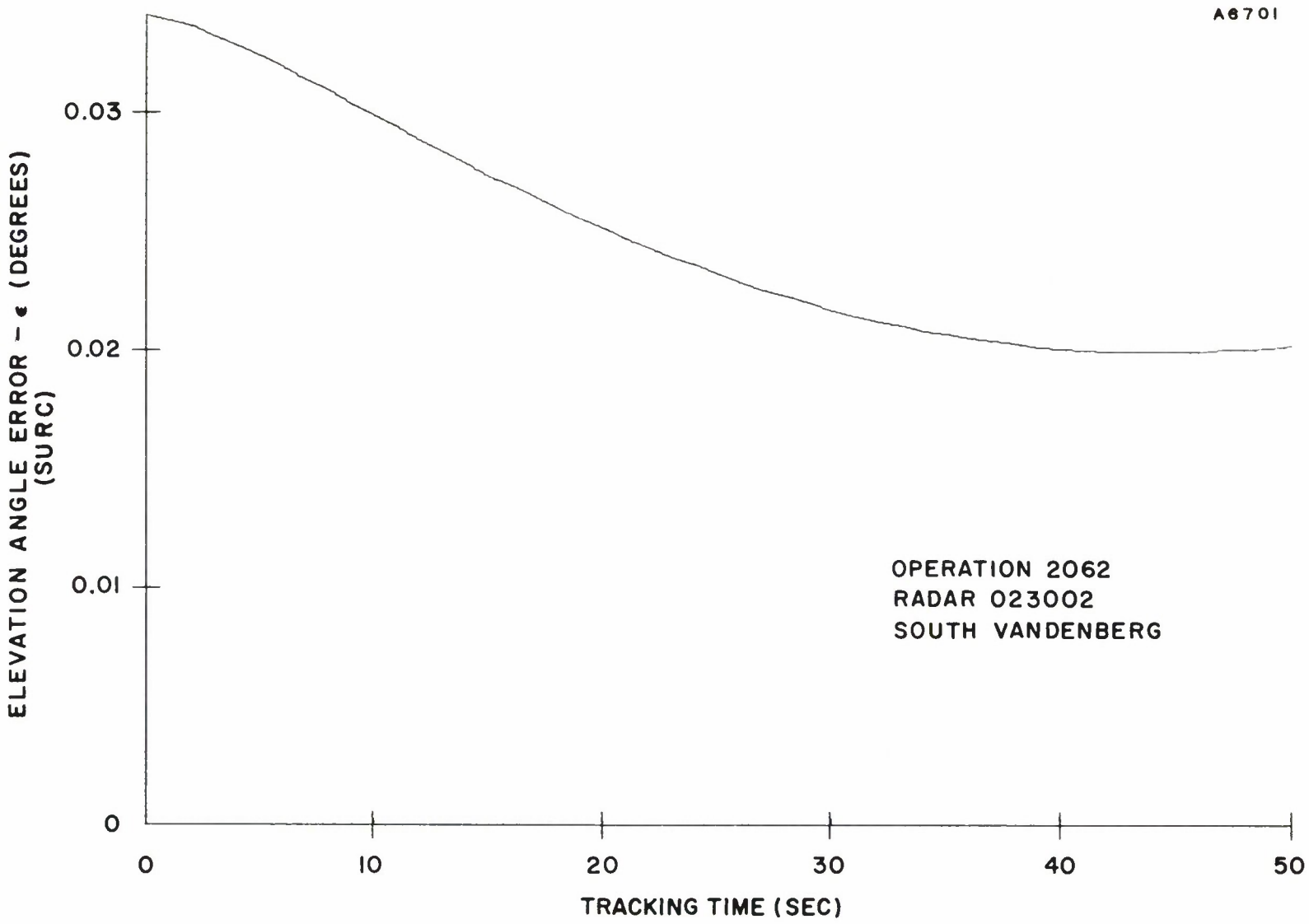

FIGURE 20. ELEVATION ANGLE ERROR VS. TIME (SURC)

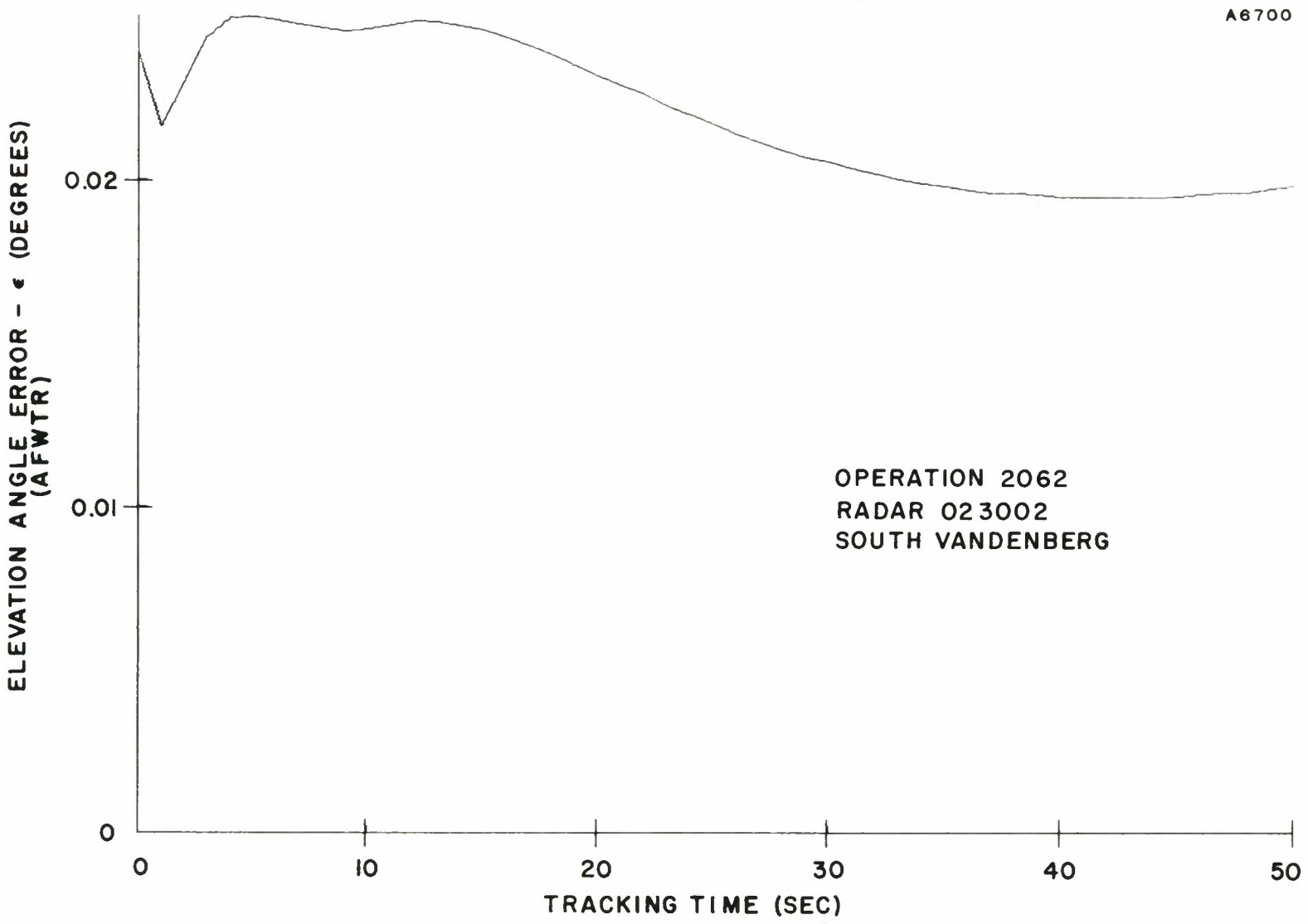

FIGURE 21. ELEVATION ANGLE ERROR VS. TIME (AFWTR)

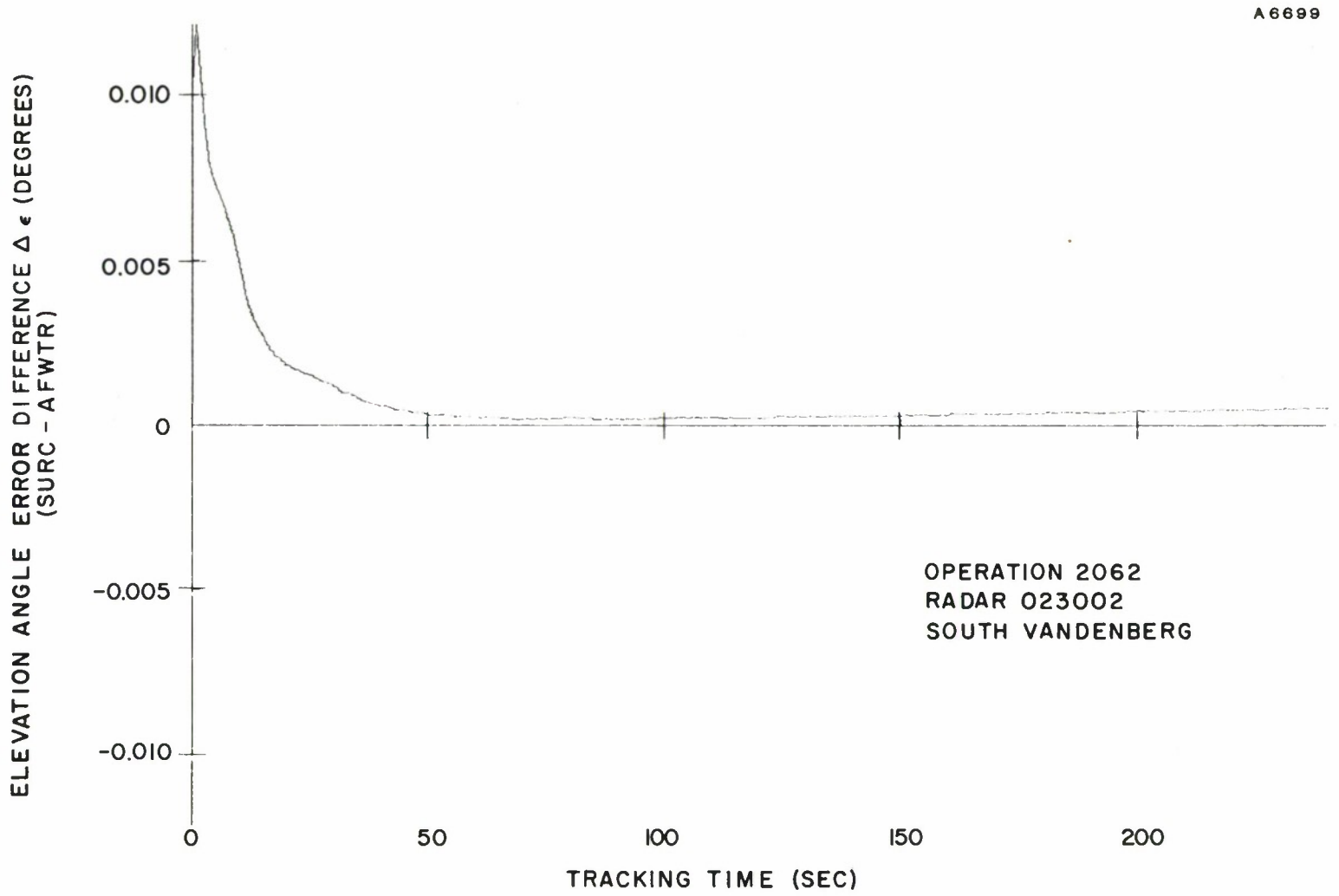

FIGURE 22. DIFFERENTIAL CORRECTED ELEVATION ANGLES VS. TIME

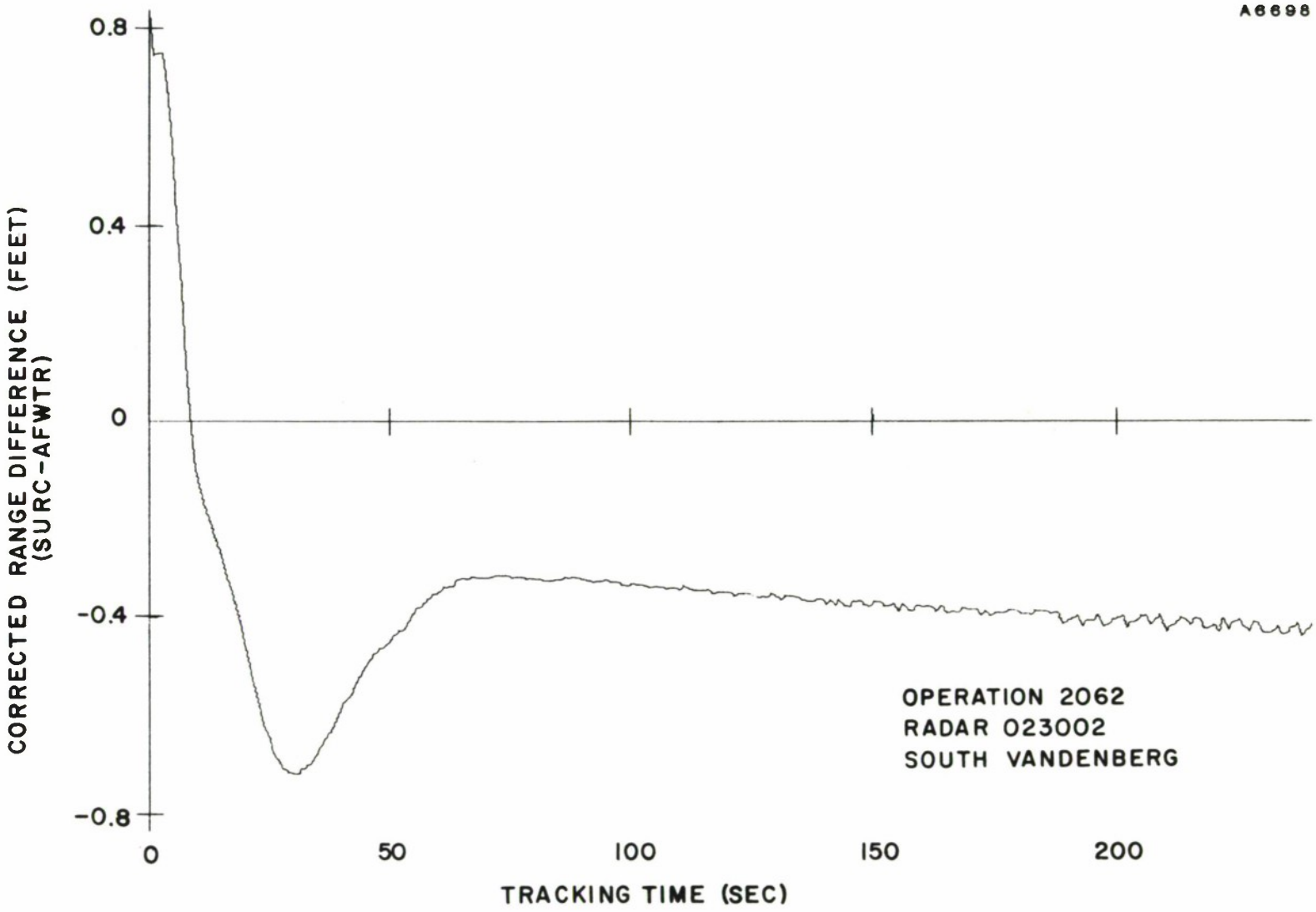

FIGURE 23. DIFFERENTIAL CORRECTED RANGES VS. TIME

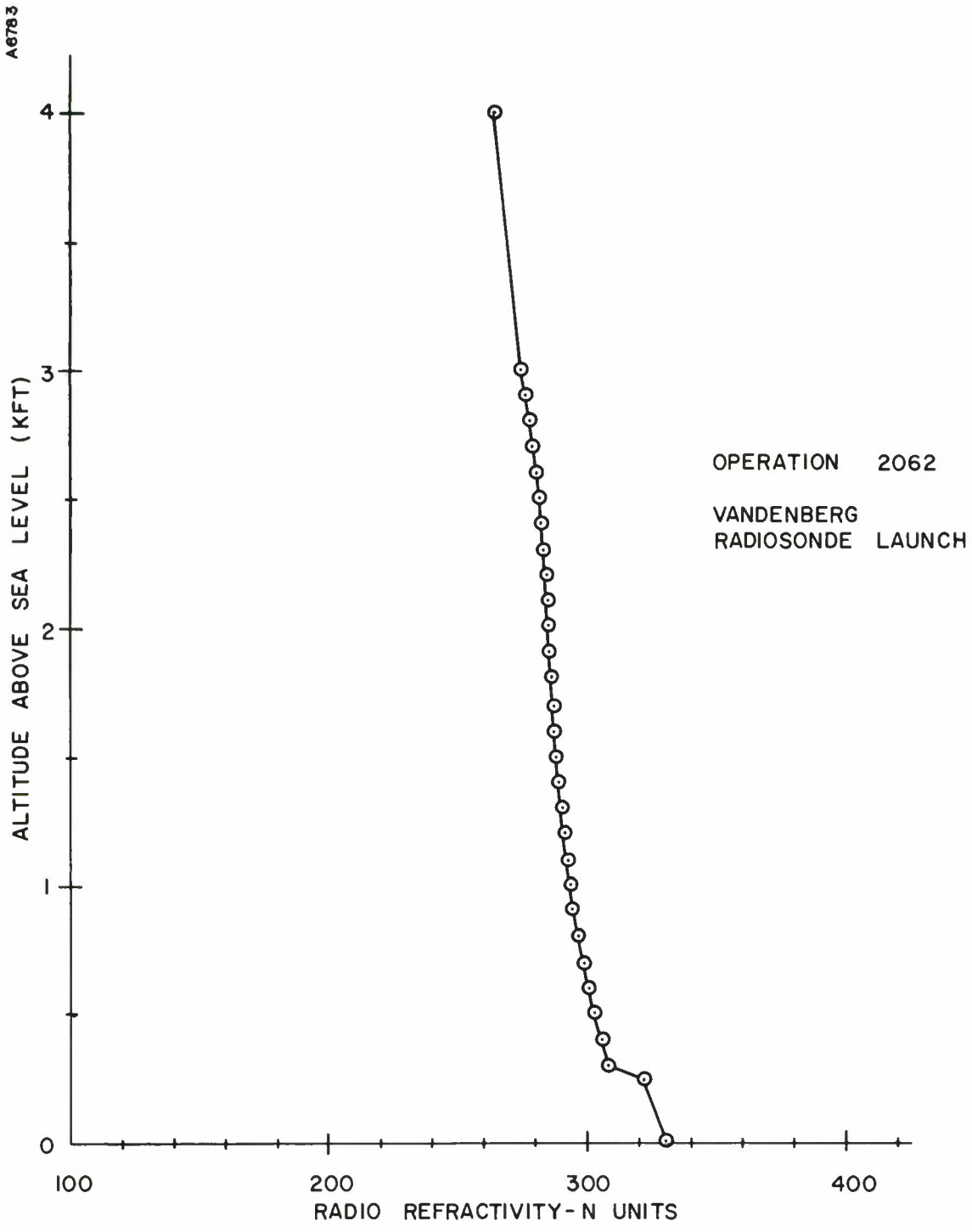

Figure 24. RADIO REFRACTIVITY PROFILE (SOUTH VANDENBERG)

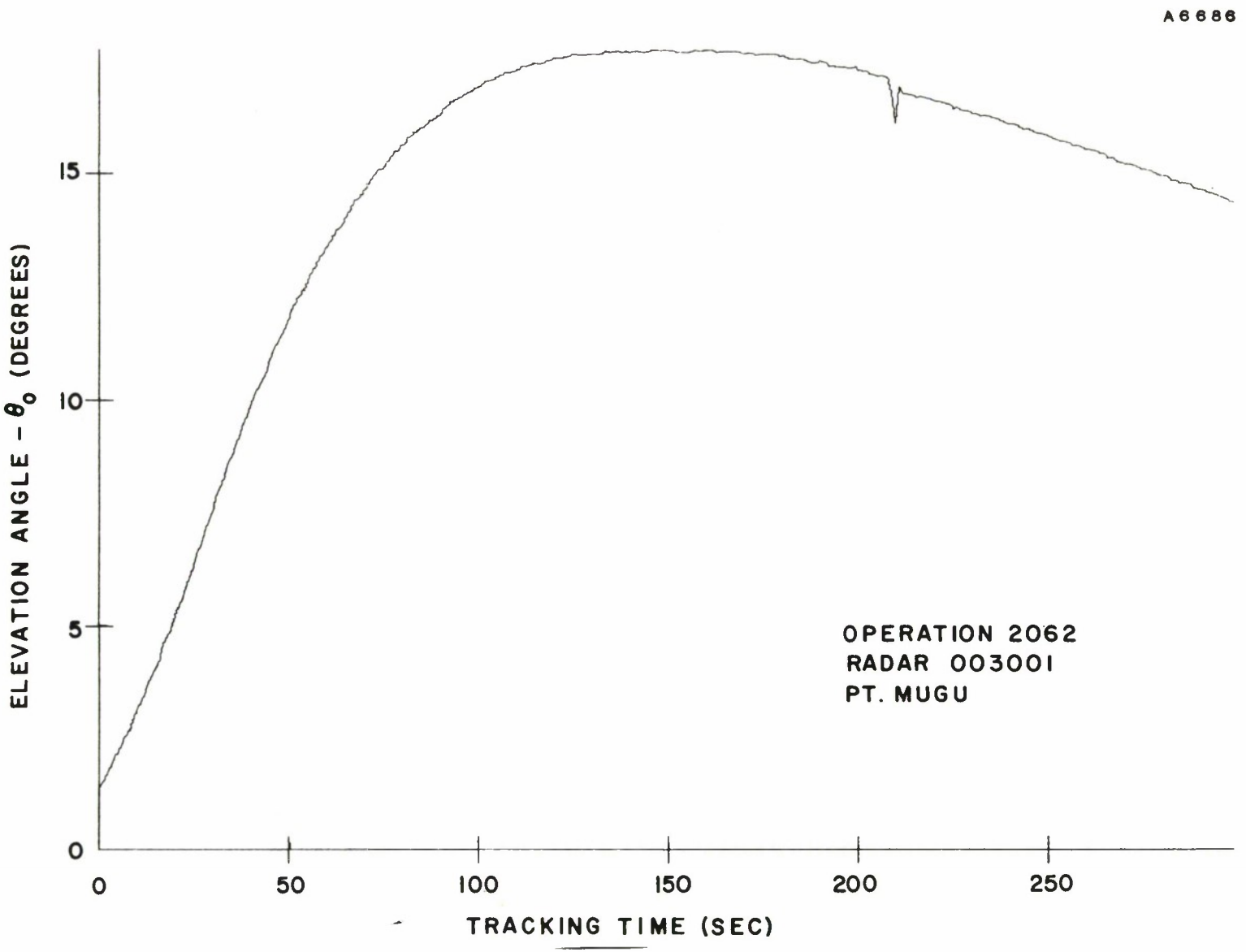

FIGURE 25. ELEVATION ANGLE VS. TIME (OP2062 PT. MUGU)

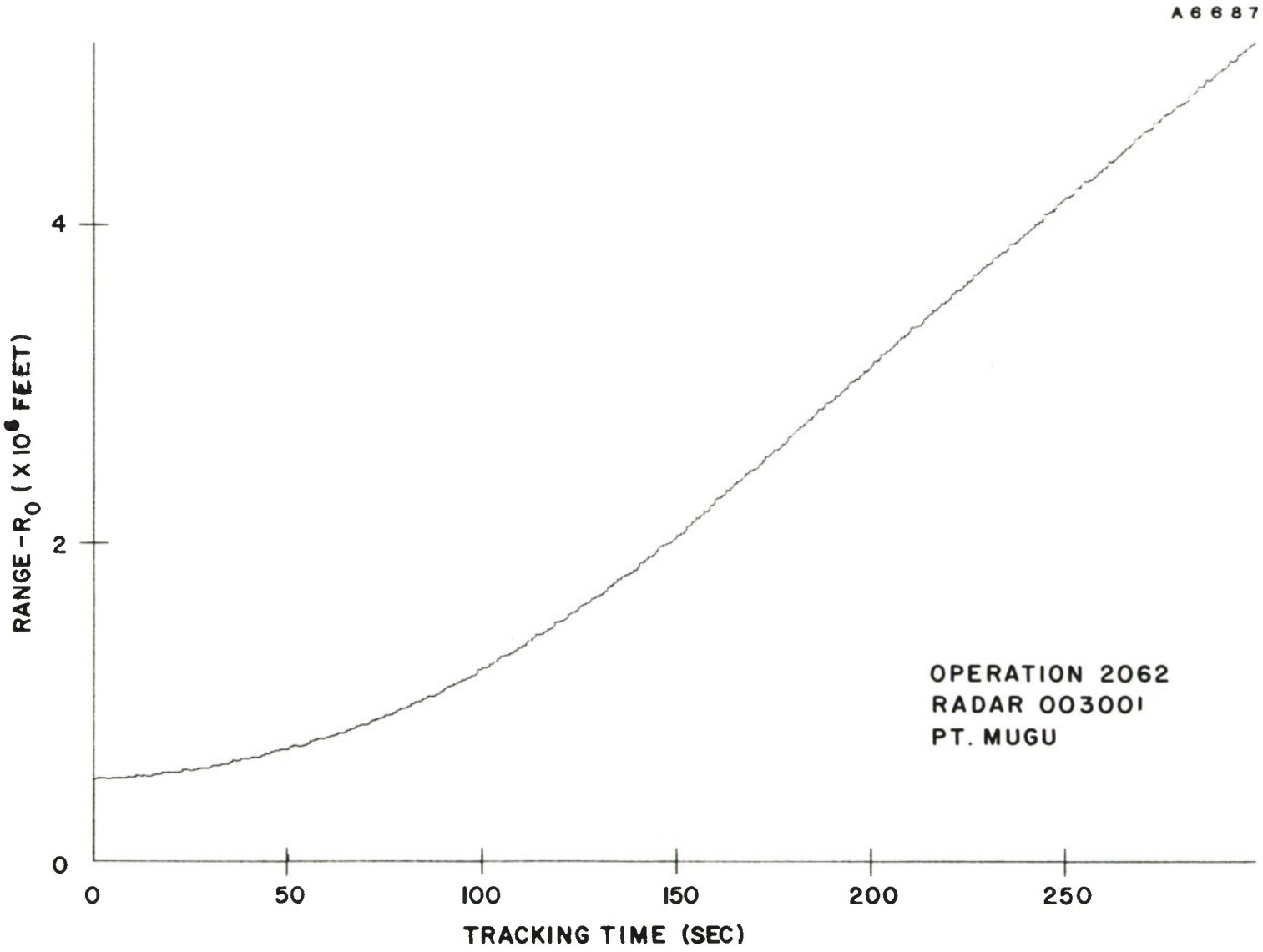

FIGURE 26. RANGE VS. TIME

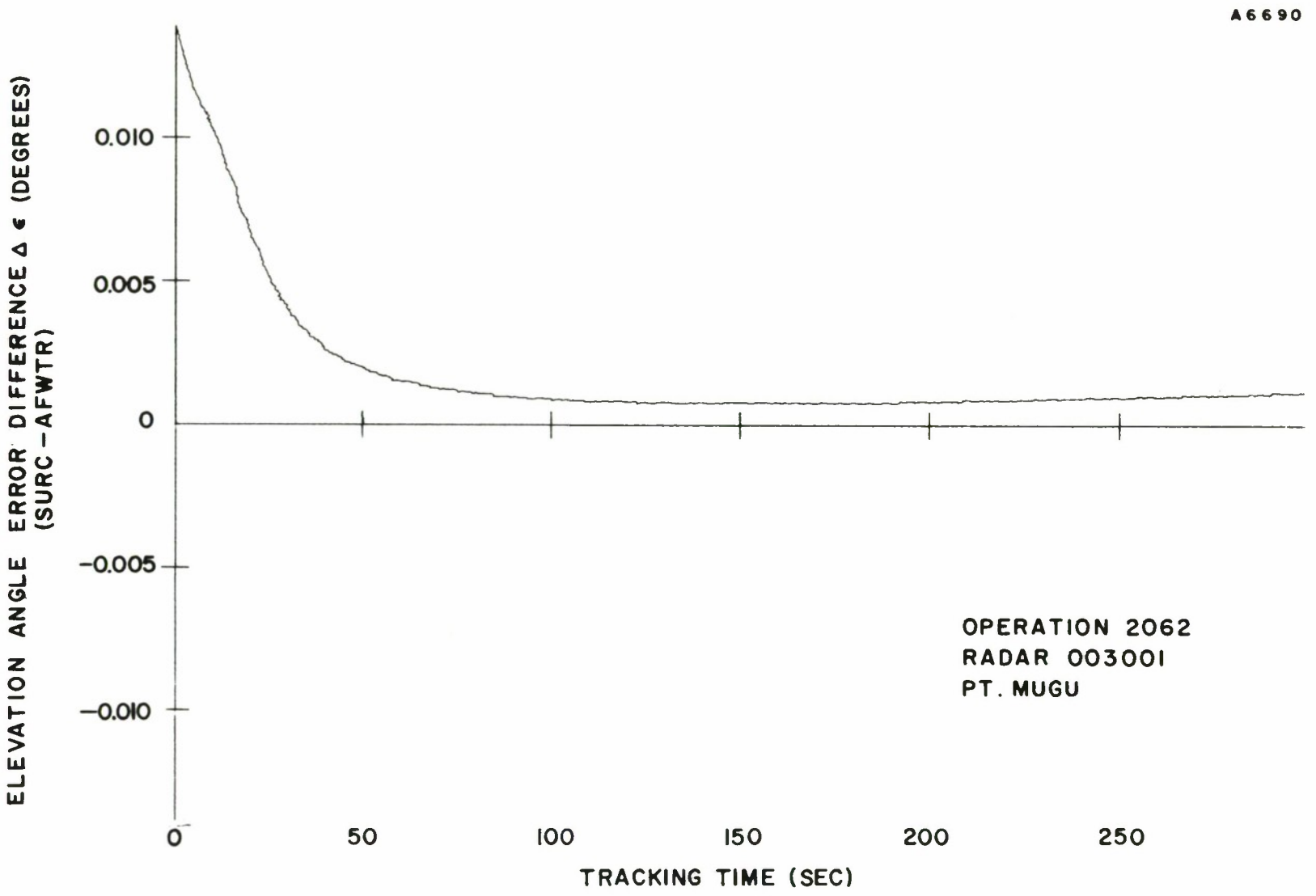

FIGURE 27. DIFFERENTIAL CORRECTED ELEVATION ANGLES VS. TIME

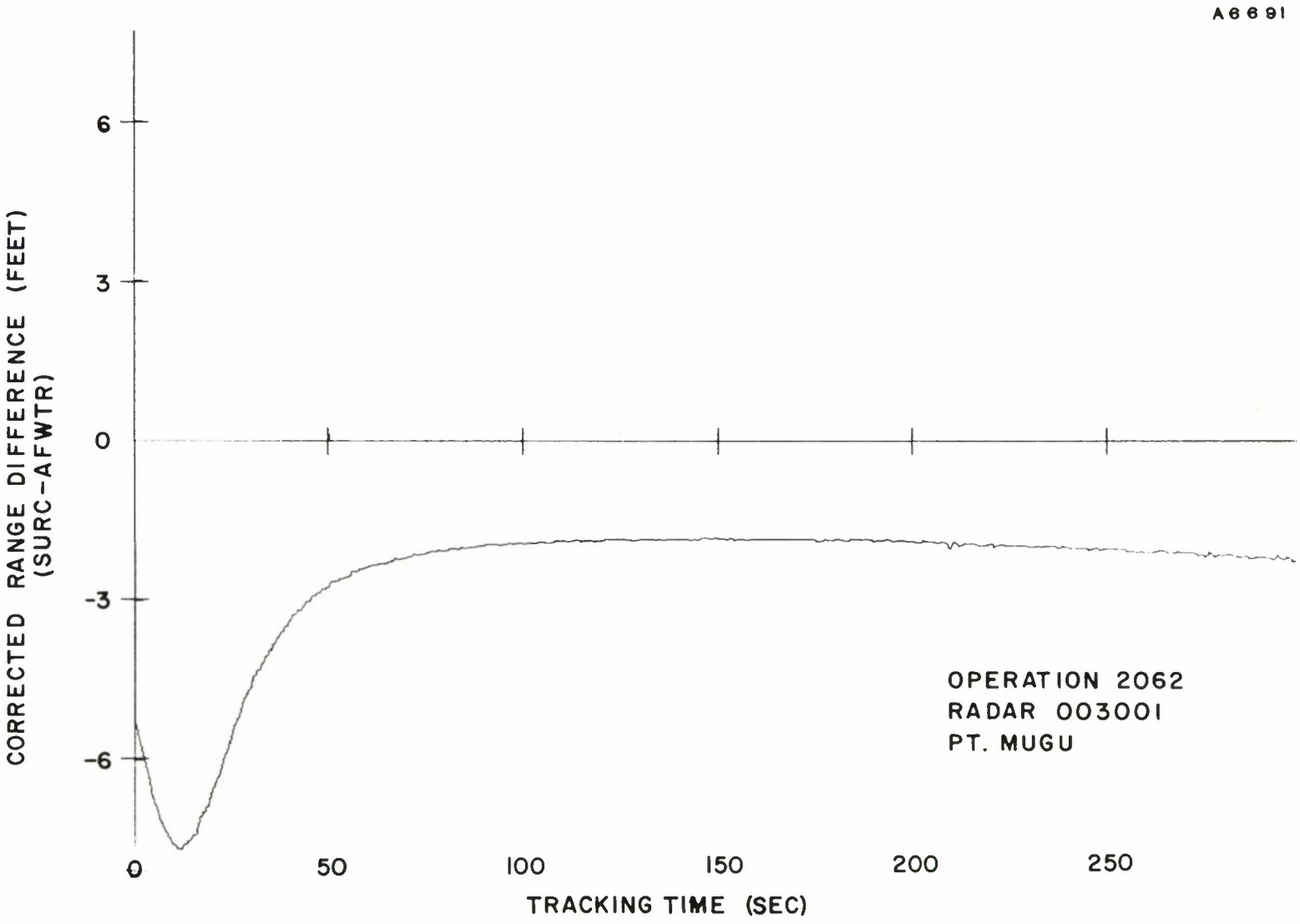

FIGURE 28. DIFFERENTIAL CORRECTED RANGES VS. TIME

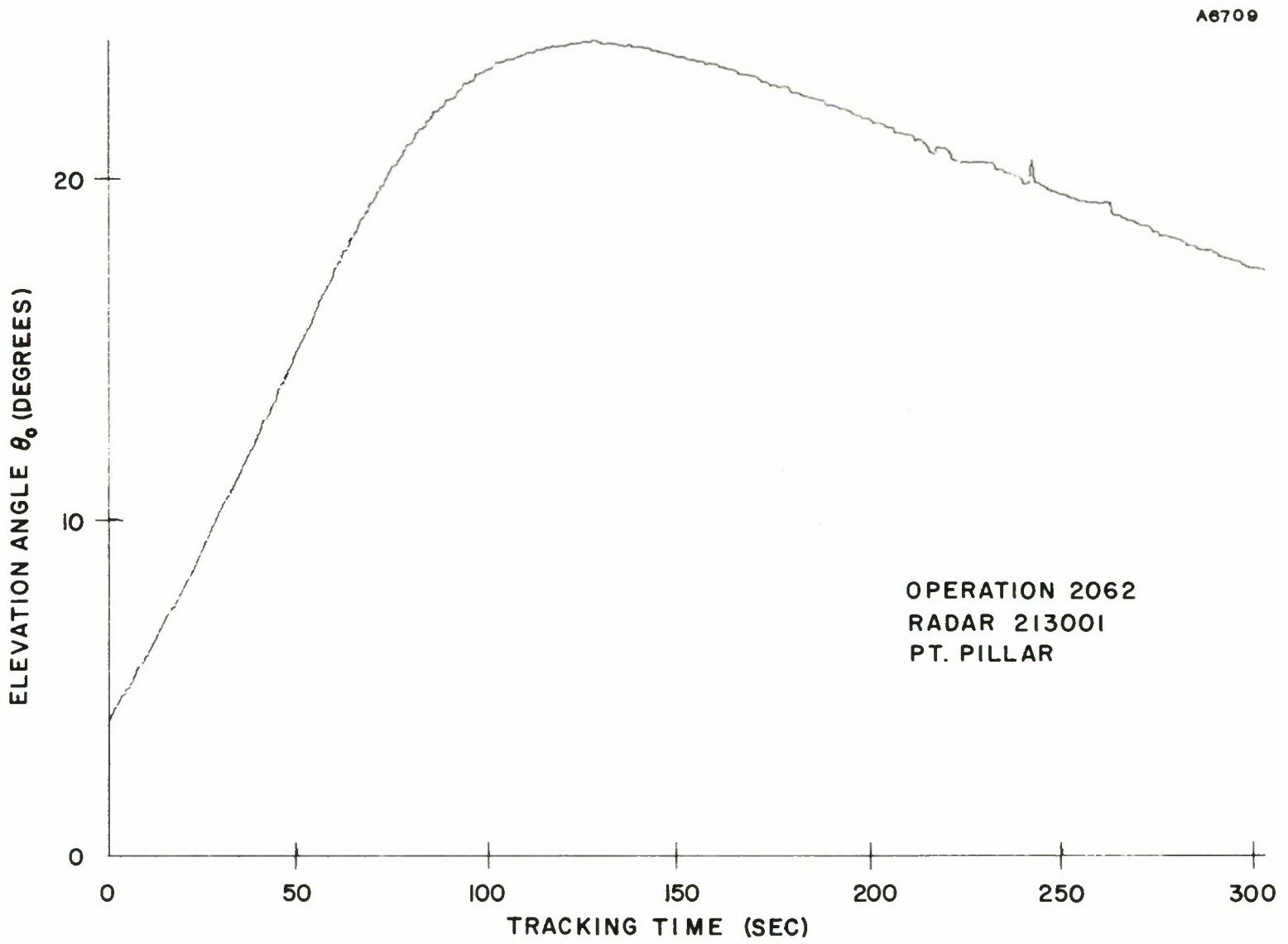

FIGURE 29. ELEVATION ANGLE VS. TIME (OP2062 PT. PILLAR)

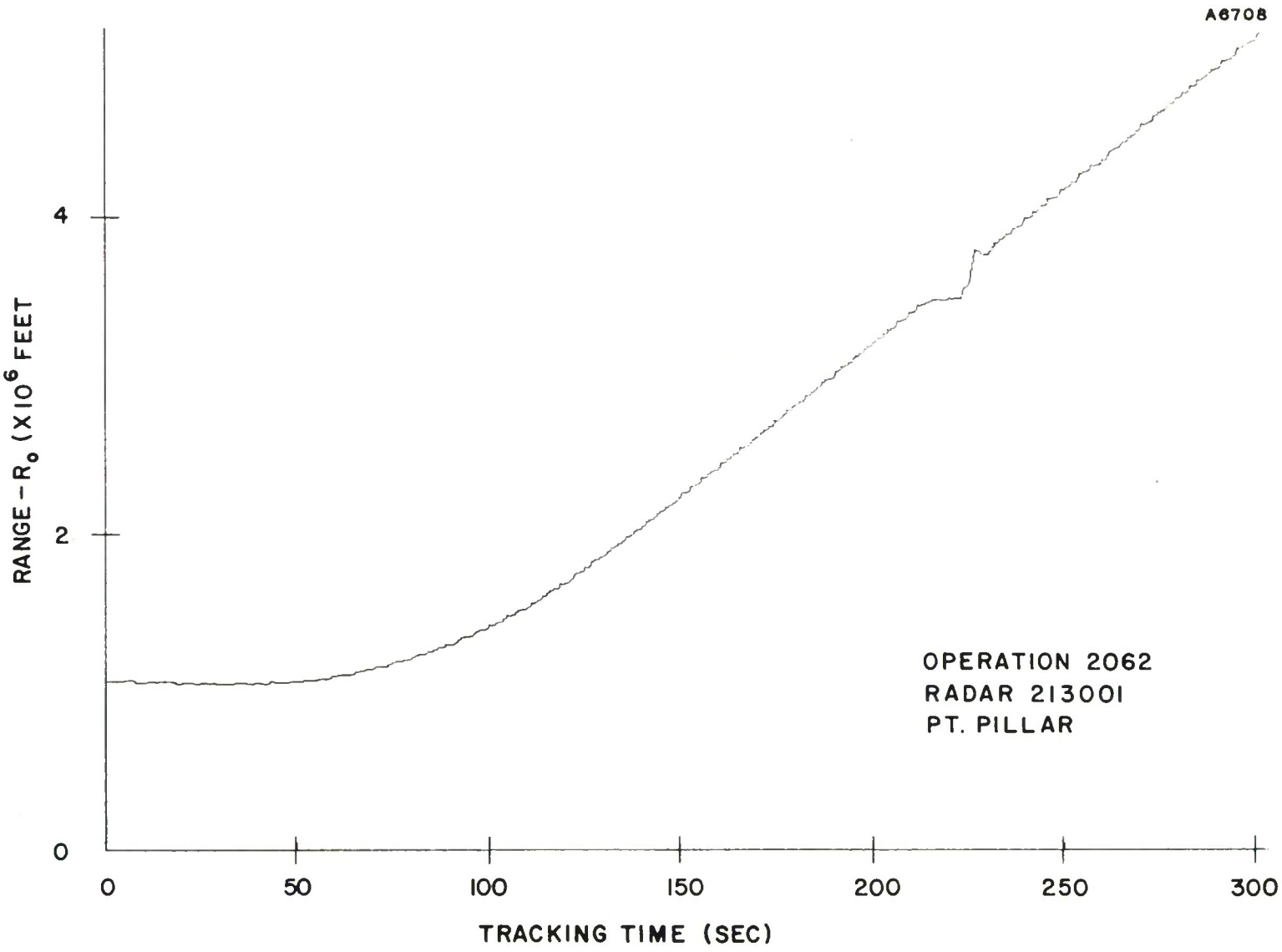

FIGURE 30. RANGE VS. TIME

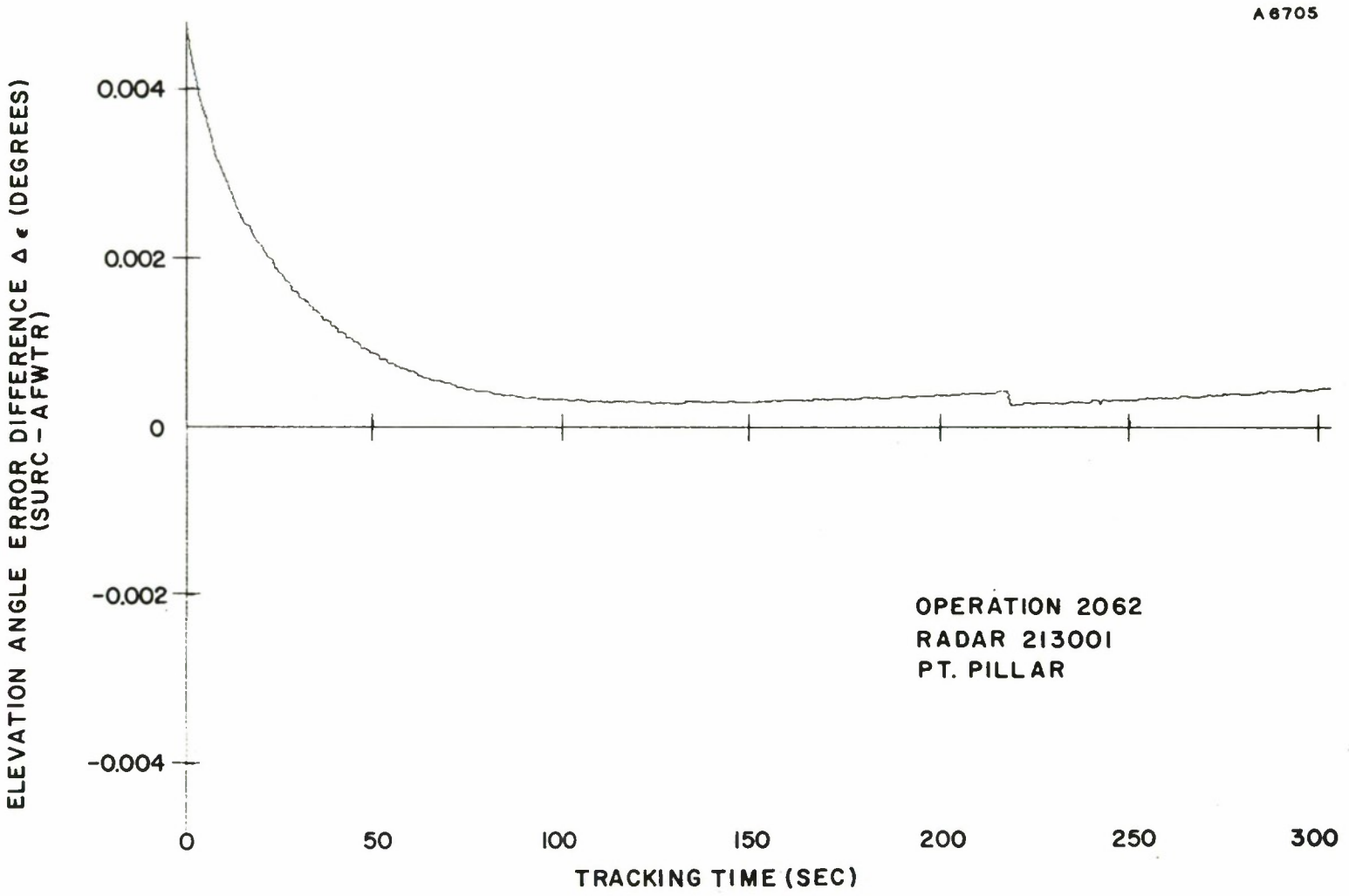

FIGURE 31. DIFFERENTIAL CORRECTED ELEVATION ANGLES VS. TIME

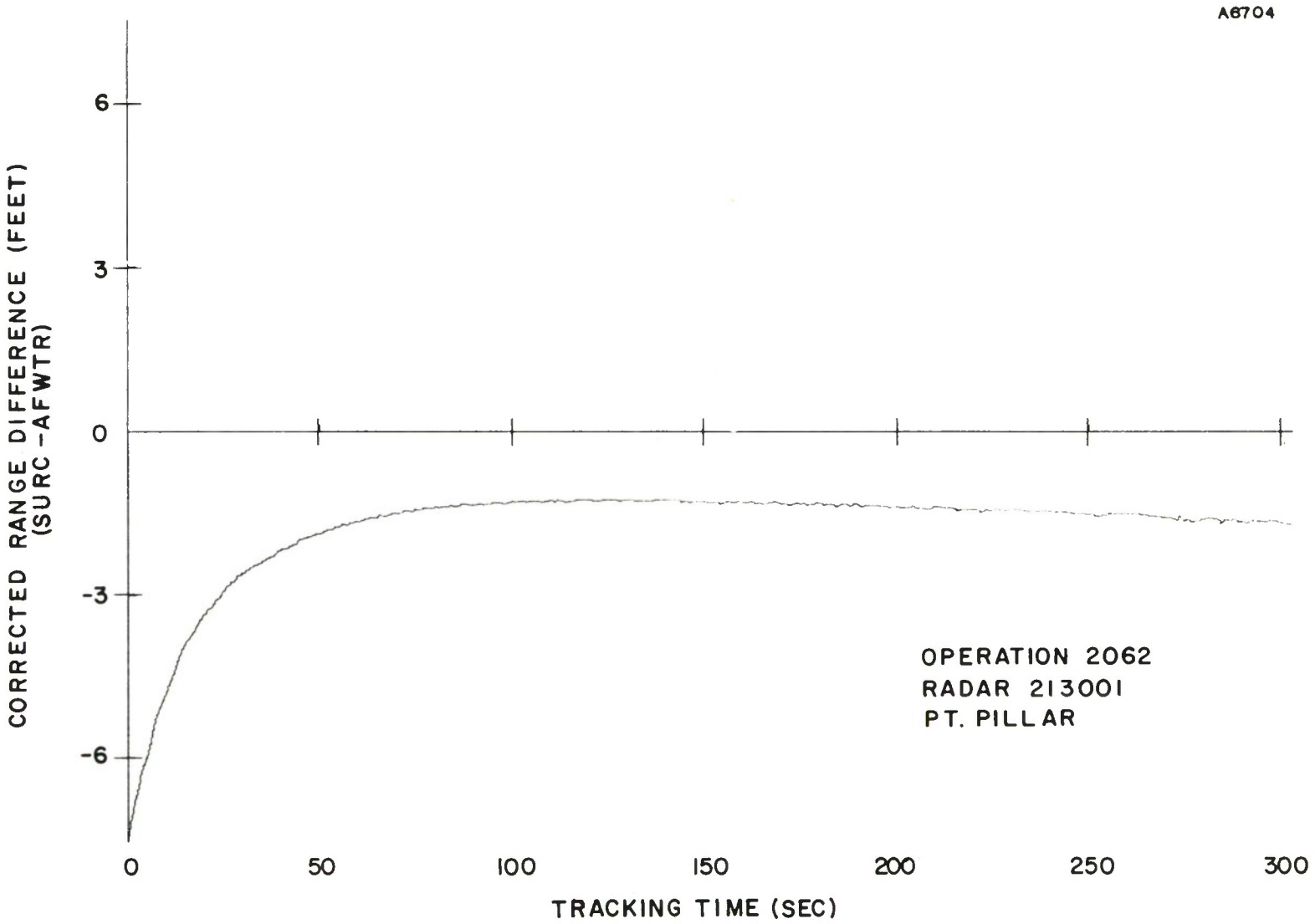

FIGURE 32. DIFFERENTIAL CORRECTED RANGES VS. TIME

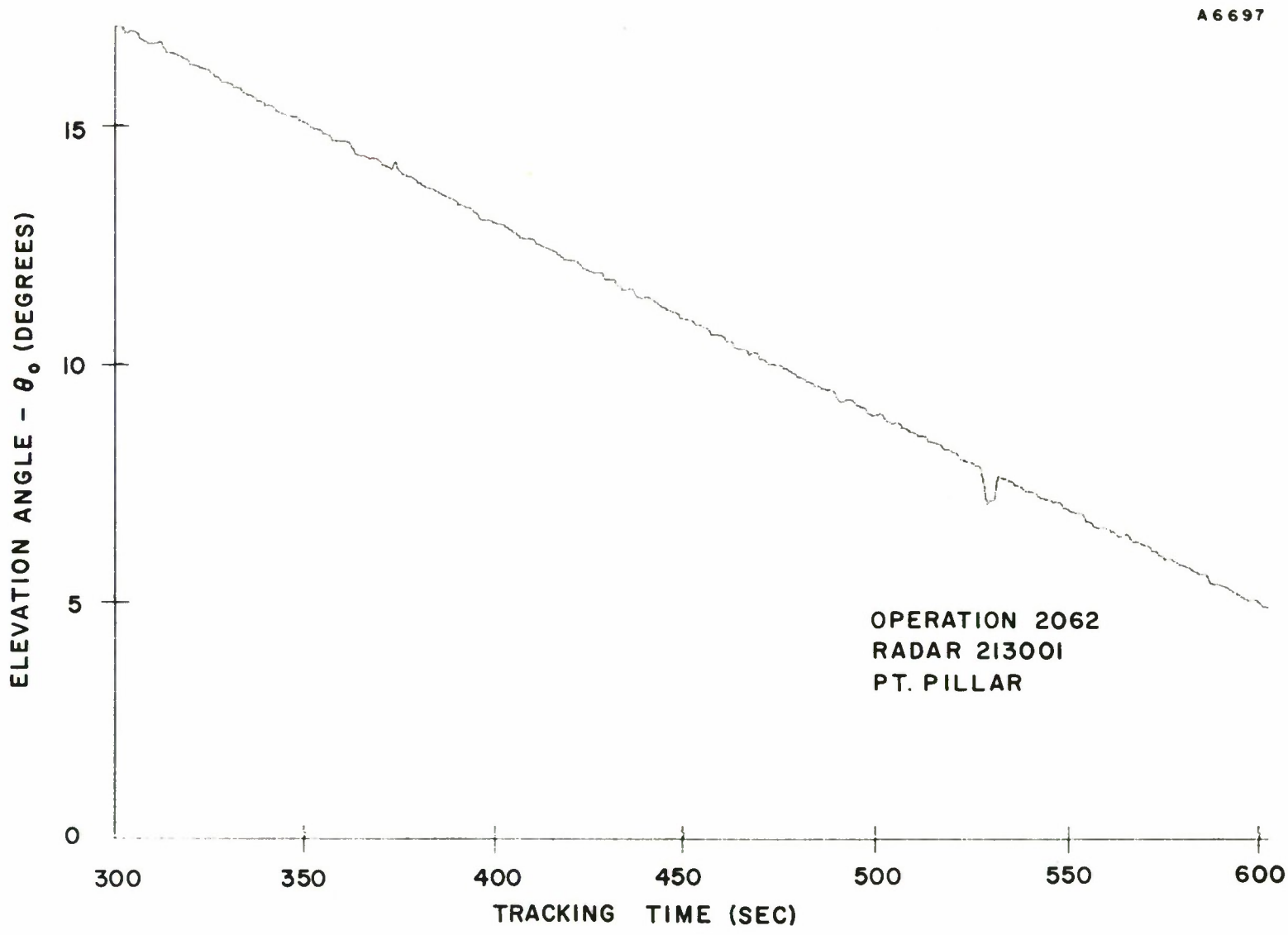

FIGURE 33. ELEVATION ANGLE VS. TIME (OP2062 PT. PILLAR - EXTENDED RANGE)

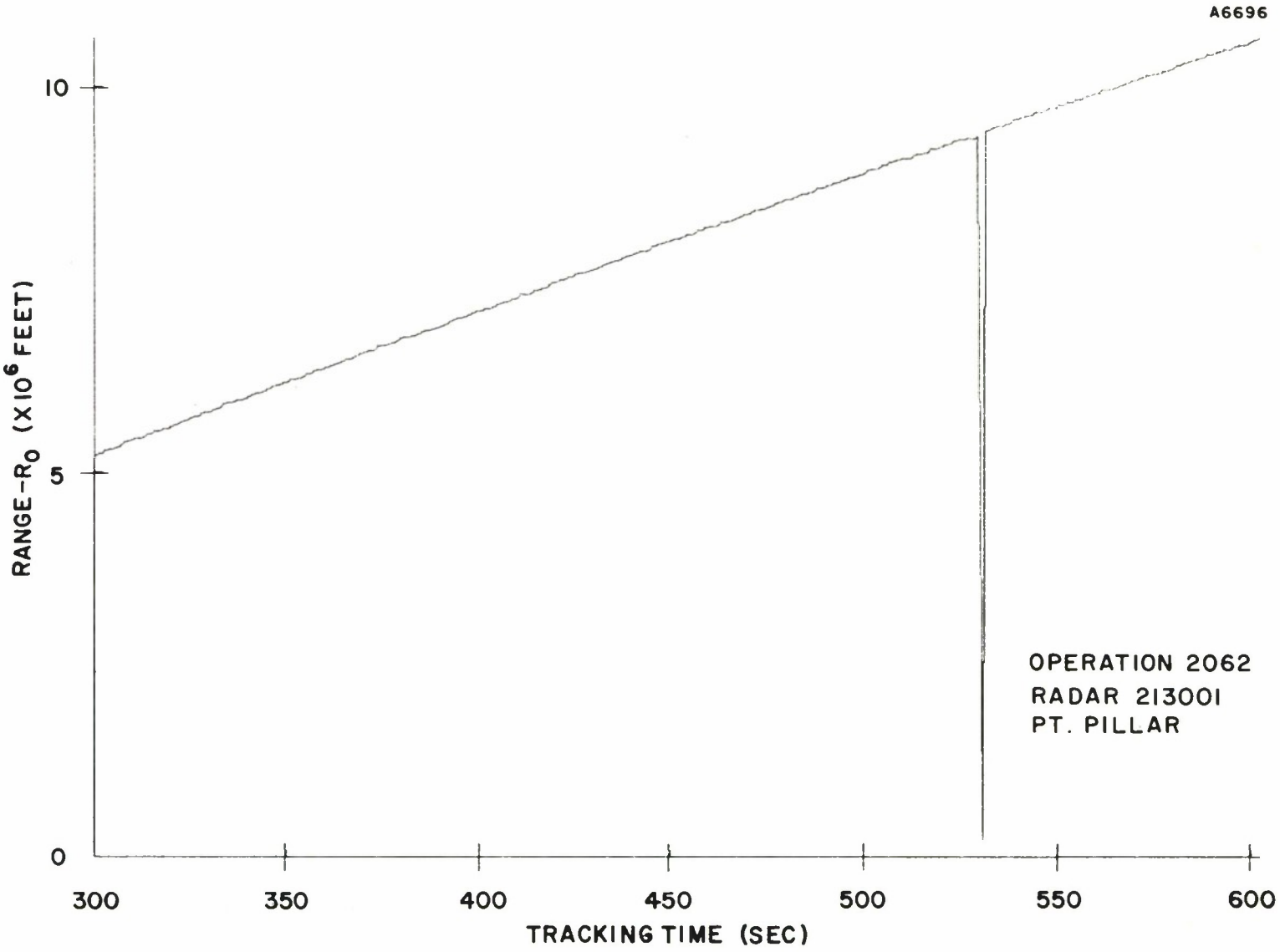

FIGURE 34. RANGE VS. TIME

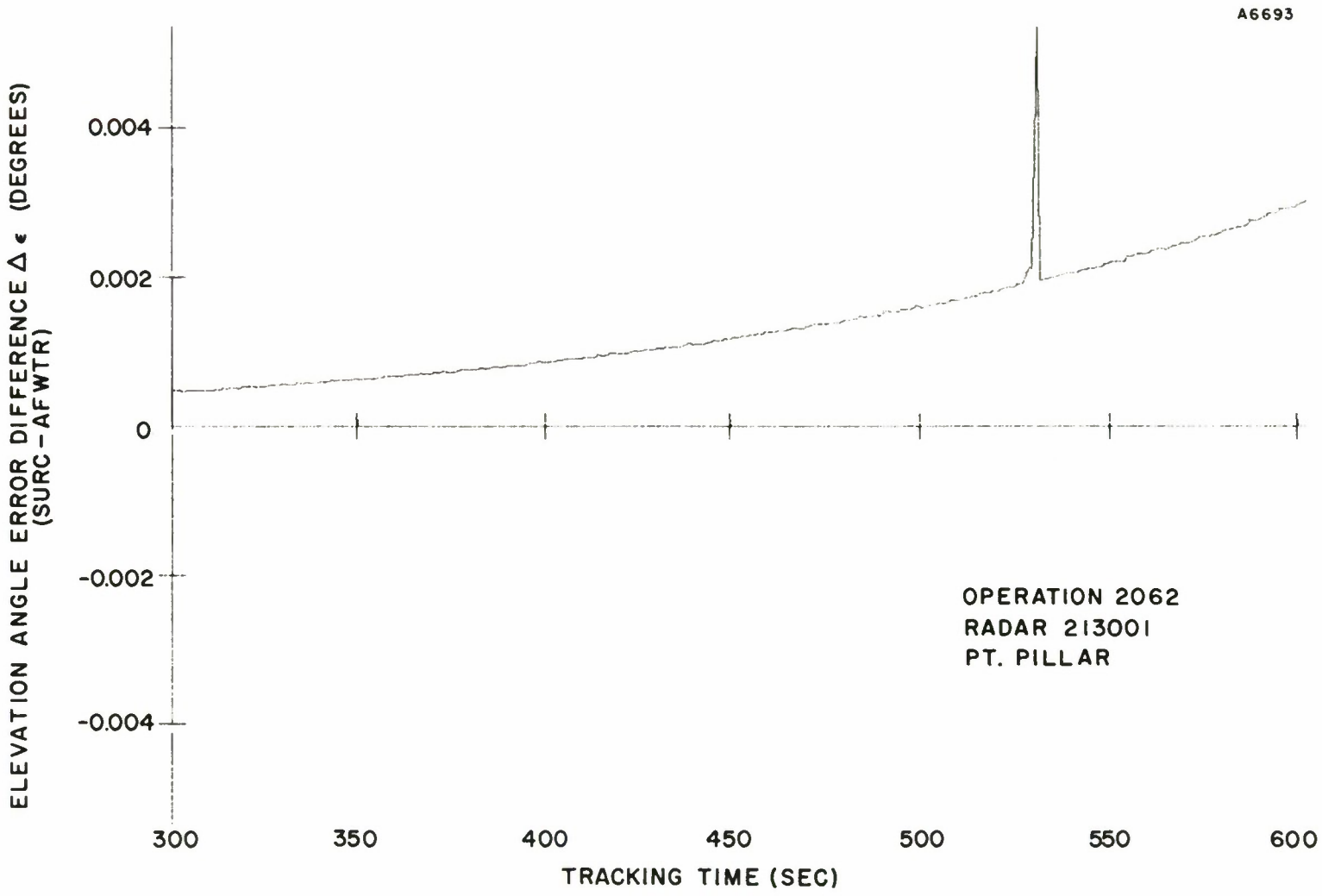

FIGURE 35. DIFFERENTIAL CORRECTED ELEVATION ANGLES VS. TIME

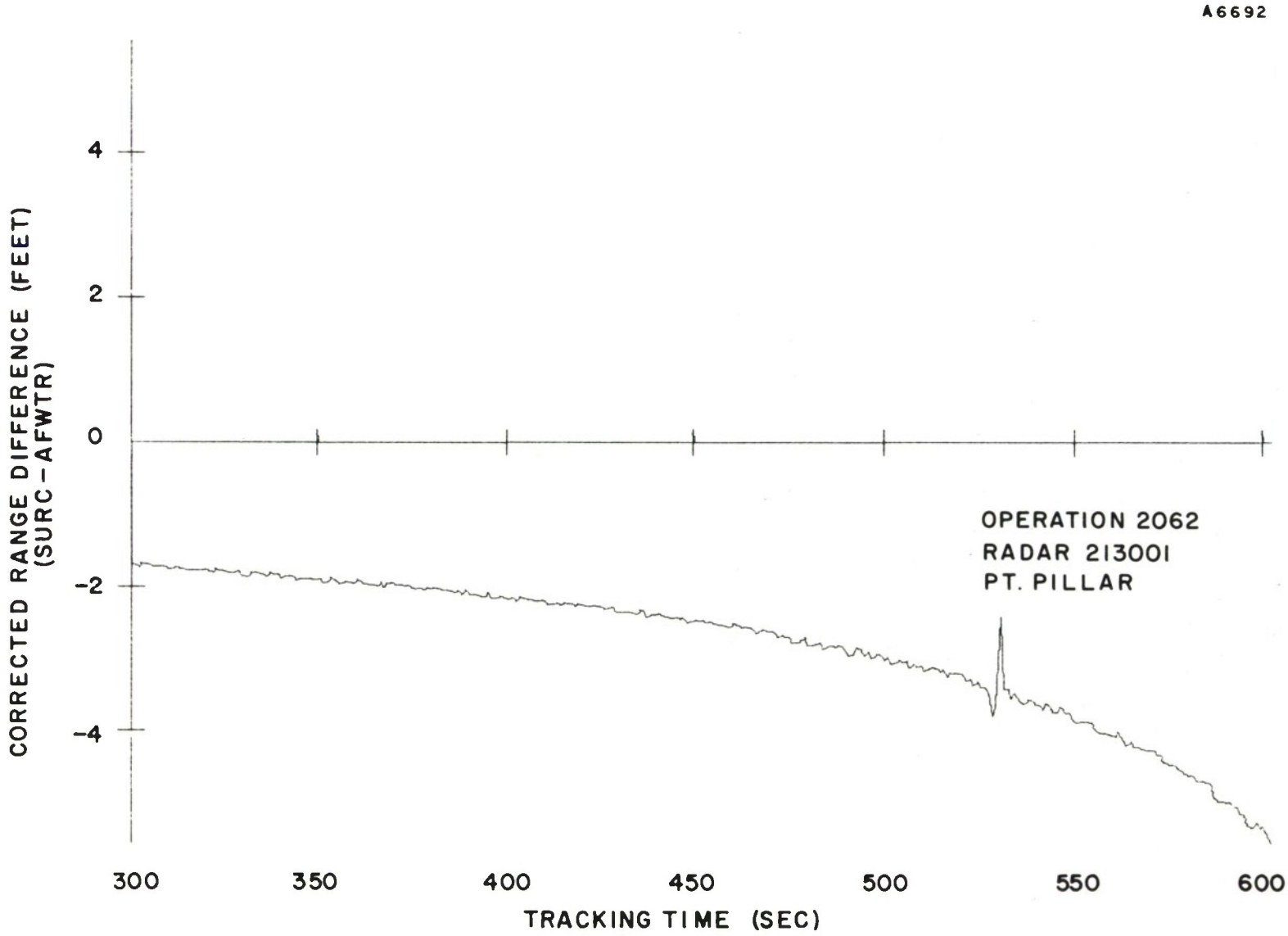

FIGURE 36. DIFFERENTIAL CORRECTED RANGES VS. TIME

As the tracking elevation angle decreases towards five degrees the elevation angle difference (figure 35) increases to a value around 0.003 degrees (0.0525 mr) which is still less than the reported angular resolution of the tracker. The range difference (figure 36) increases towards a value of about five feet at a vehicle range of 10 million feet.

4.1 Some Comments on the Analysis of Operation 2062

Basically, the analytical results of Operation 2062 confirm that the SURC equations can provide refraction-induced error data in agreement with ray-traced results. As the tracking elevation angle decreases below five degrees the differences between the radiosonde refractivity measurements and the CRPL exponential atmosphere become more apparent. This subject will be treated in greater detail in the conclusions.

It is noteworthy that the agreement between methods is also very good at long tracking ranges as shown by the final set of results. As the elevation angle from the Point Pillar tracker decreased below five degrees the tracking data became erratic probably due to multipath effects. Therefore, the plots were terminated at 600 seconds.

SECTION V

COMPARISON OF TRACKING ERRORS BETWEEN SURC CALCULATIONS AND GERTS FLIGHT DATA - OPERATION 7335

Figures 37 and 38 show the elevation angle and range of the vehicle from the GERTS system (Vandenberg). Figure 39 shows the elevation angle error calculated with the SURC equations where from Appendix II the associated radiosonde data did not indicate any elevated layer or non-standard refractivity behavior. However, figure 40, which shows the GERTS elevation angle error calculations, indicates a peak in the region of 5 seconds. This behavior is difficult to explain since both range and elevation angle are monotonically increasing.

Figure 41 shows the difference between the true elevation angle calculations and the minimum around 5 seconds is clearly due to the GERTS calculation described above. The angle difference decreases rapidly to a negligible amount after 25 seconds. The initial maximum difference of about -0.010 degrees is comparable with the results of the previous operation.

Figure 42 shows the corrected range difference which decreases rapidly after the first 20 seconds of flight. Since the GERTS tracker is particularly interested in range-rate data it is significant to note that the difference in calculation is not only small but remains essentially constant after forty seconds of flight.

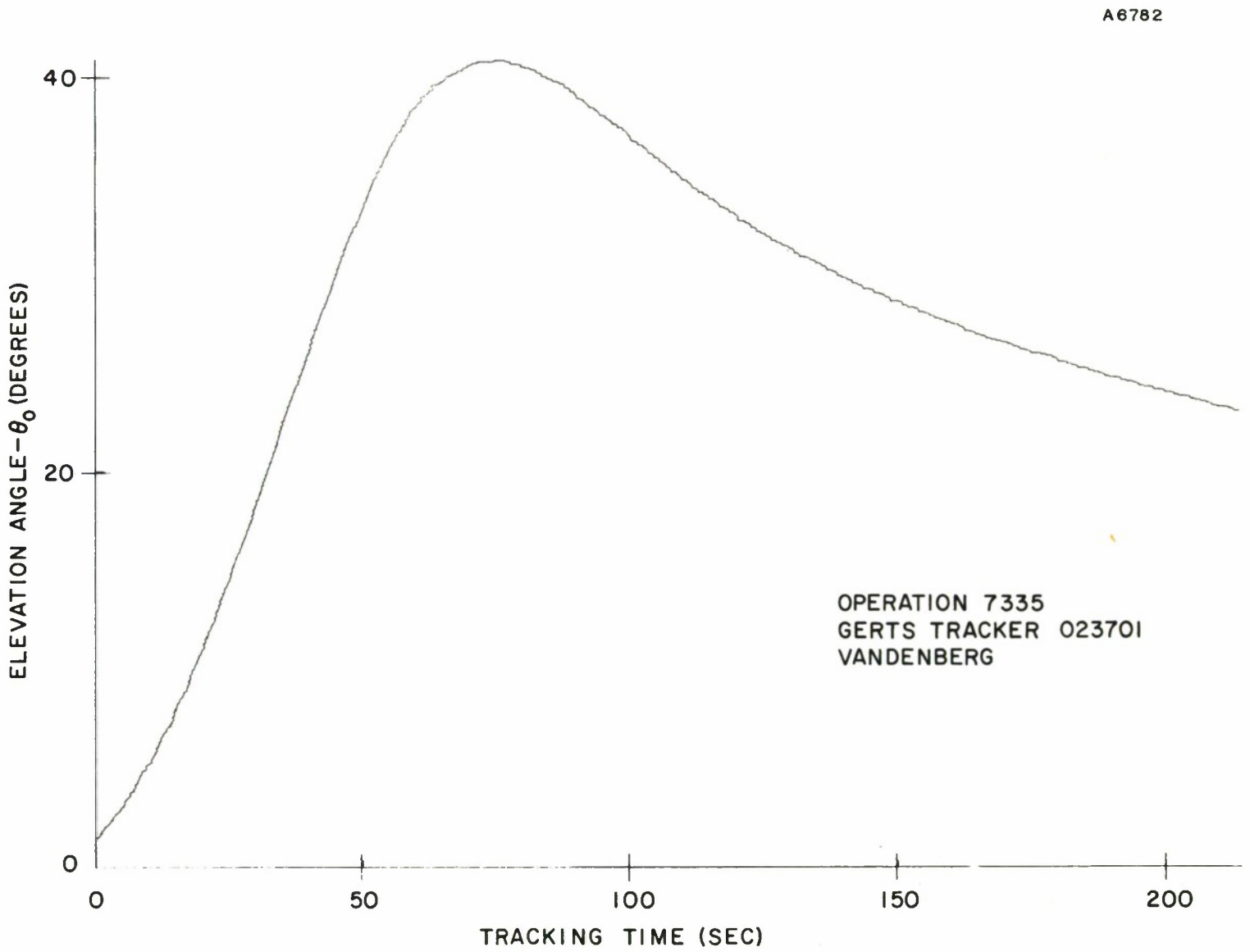

FIGURE 37. ELEVATION ANGLE VS. TIME (OP7335 - GERTS)

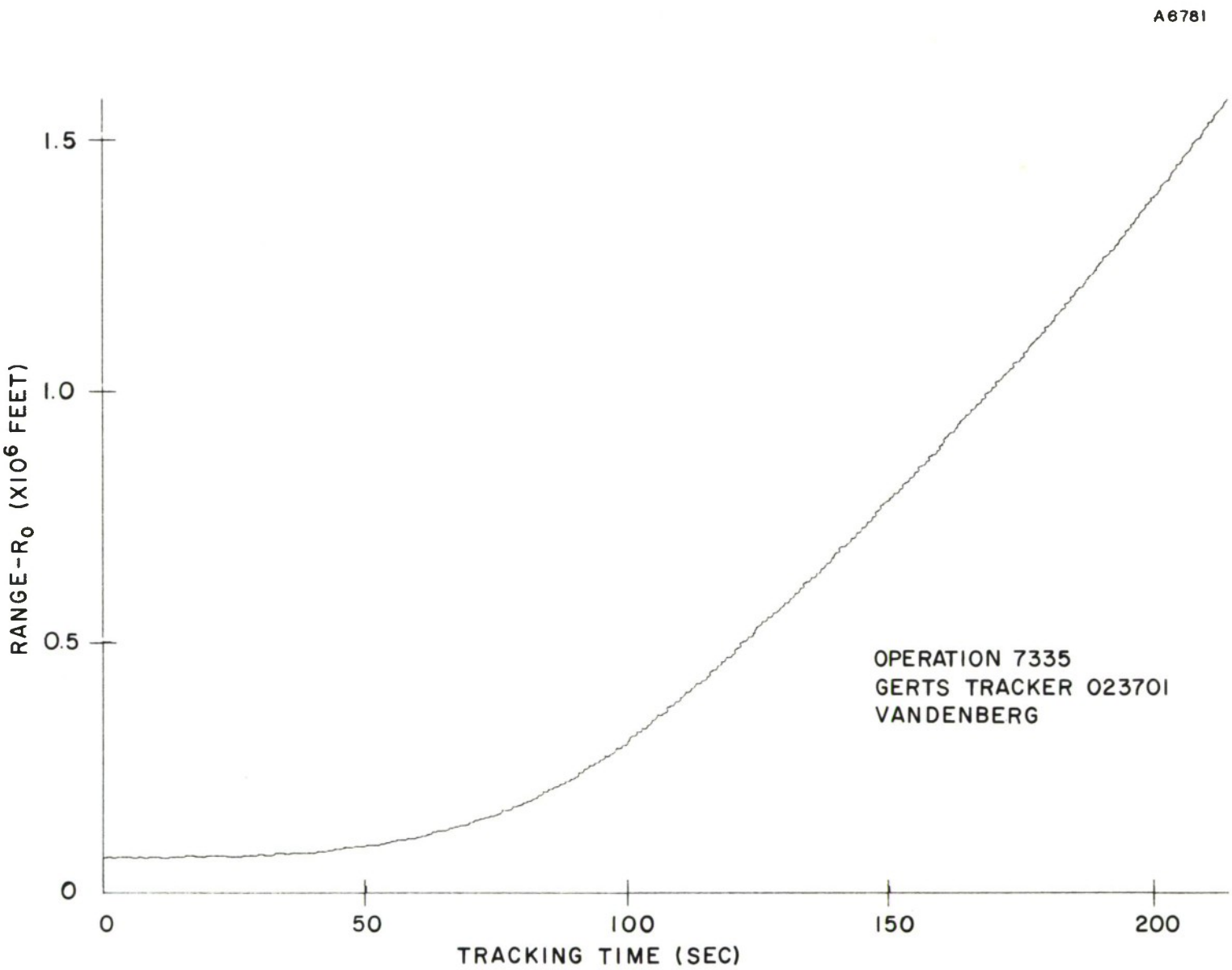

FIGURE 38. RANGE VS. TIME

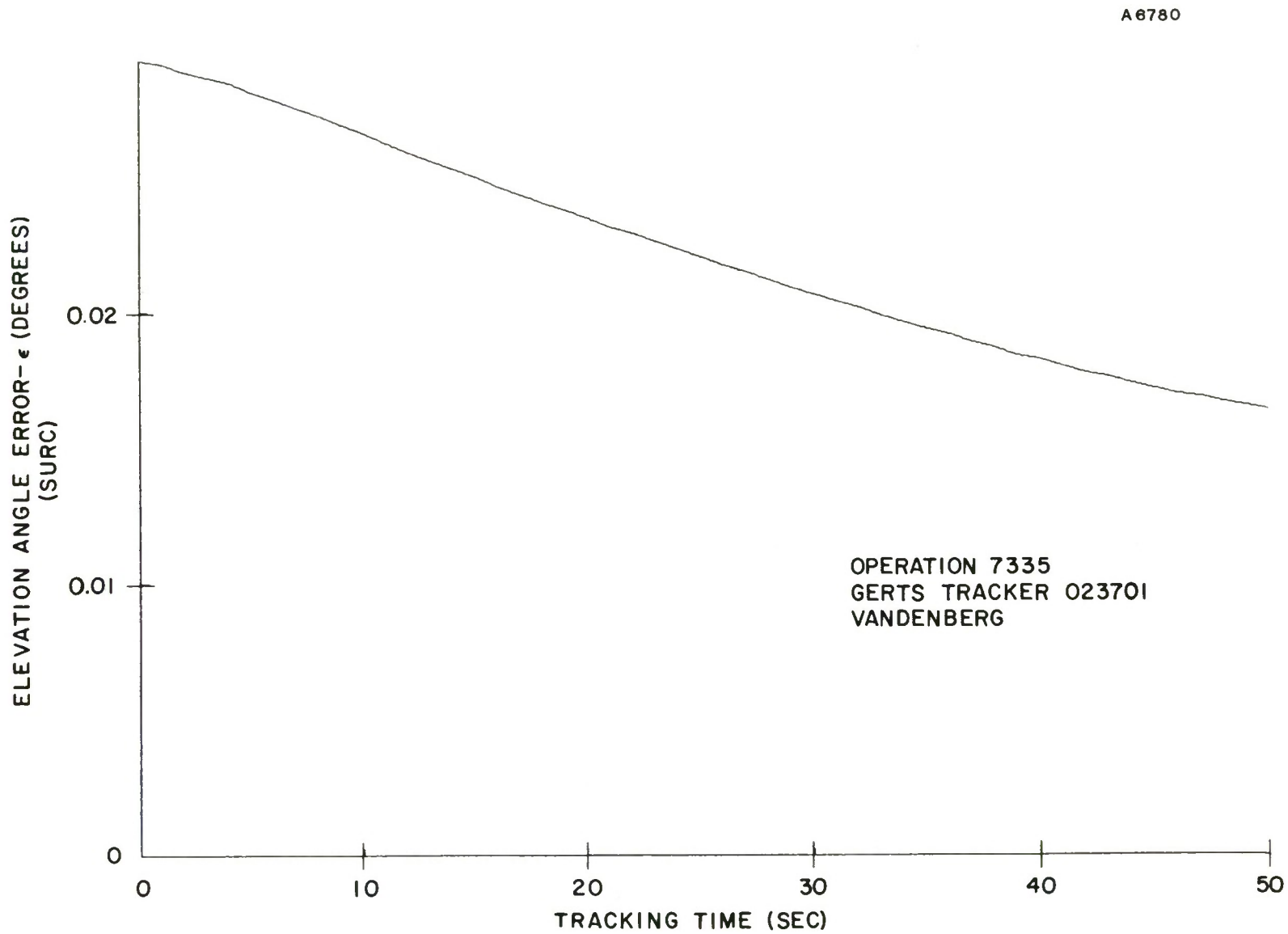

FIGURE 39. ELEVATION ANGLE ERROR VS. TIME (SURC)

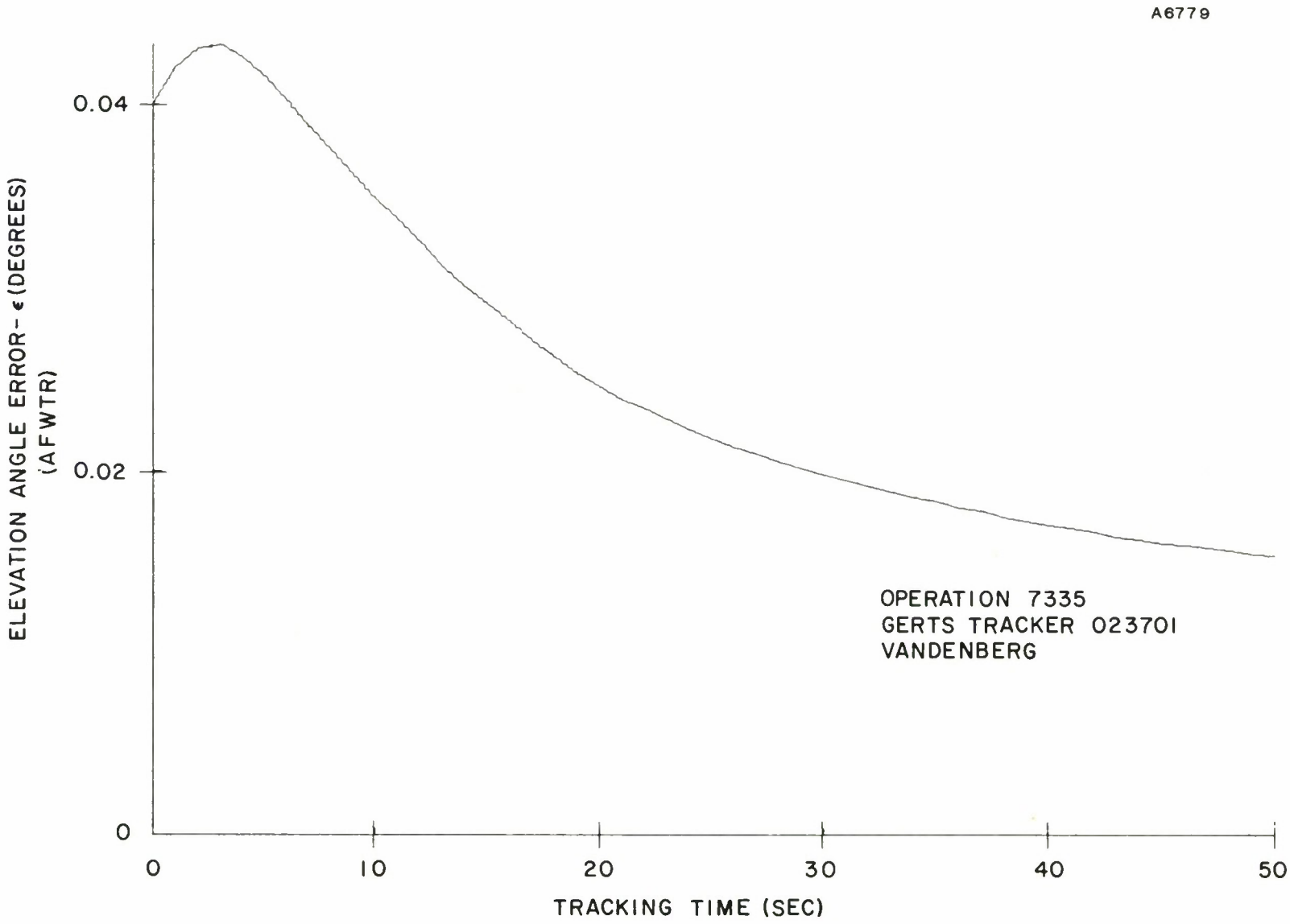

FIGURE 40. ELEVATION ANGLE ERROR VS. TIME (GERTS)

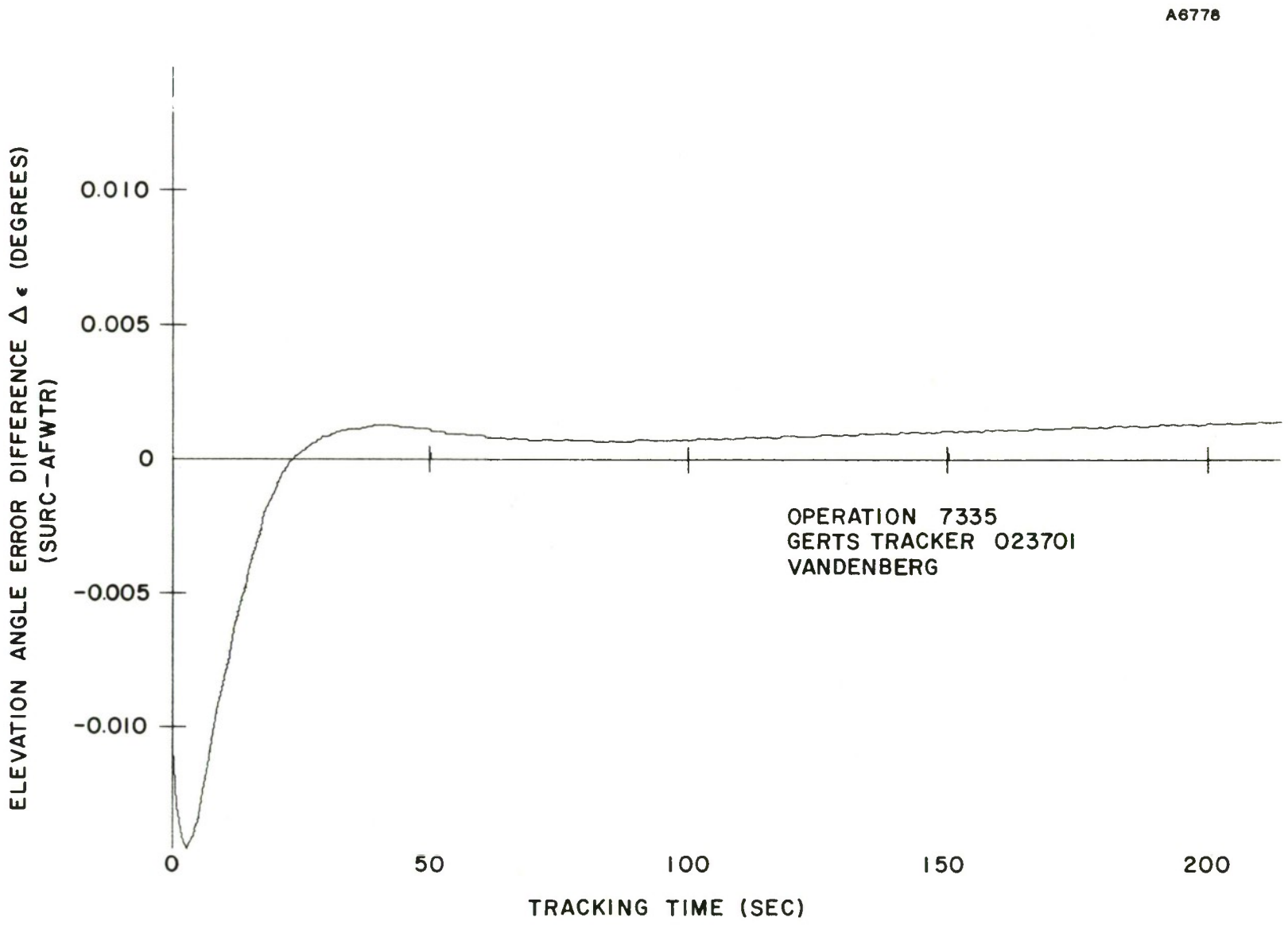

FIGURE 41. DIFFERENTIAL CORRECTED ELEVATION ANGLES VS. TIME

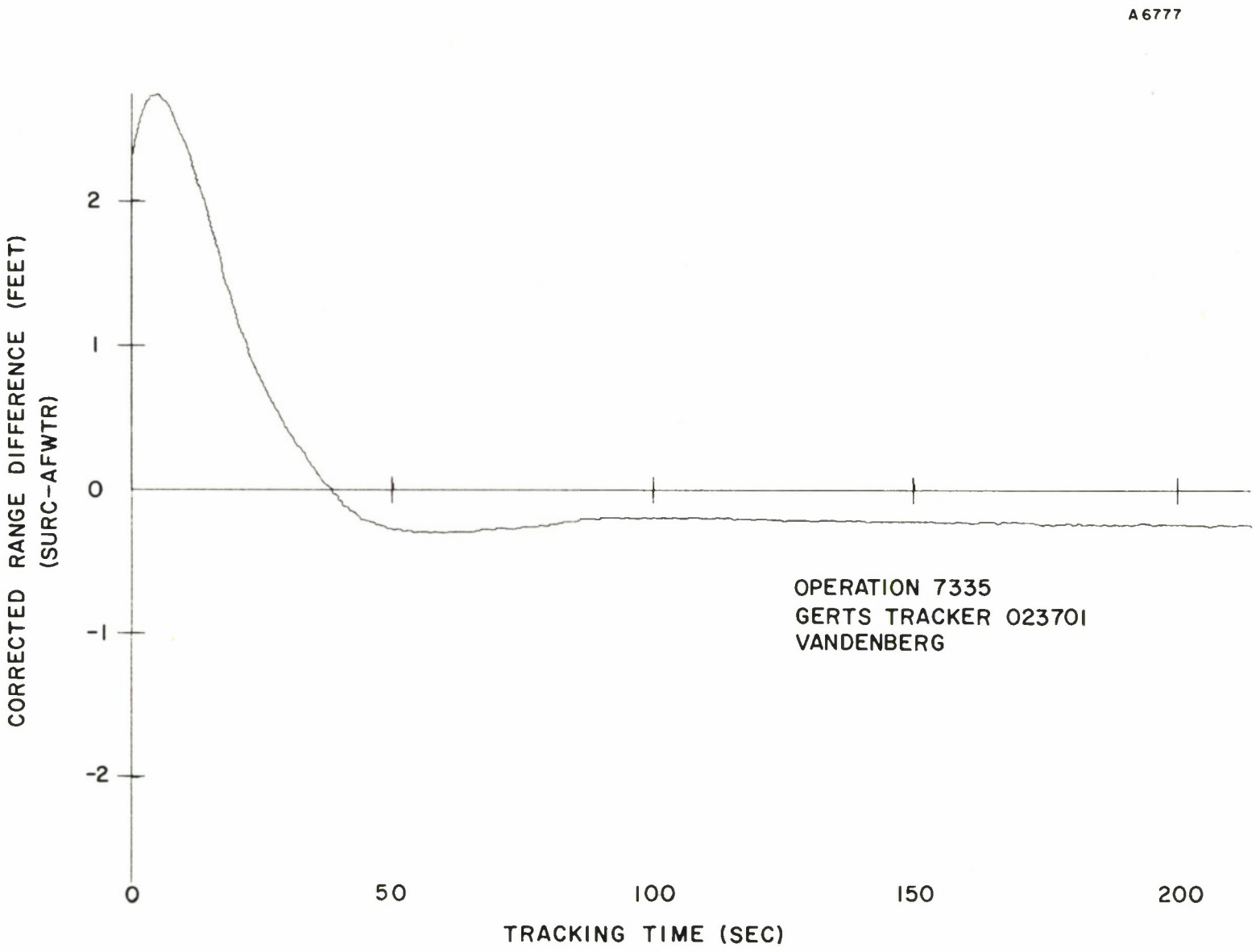

FIGURE 42. DIFFERENTIAL CORRECTED RANGES VS. TIME

SECTION VI

SOME COMMENTS ON THE GERTS REAL-TIME CORRECTION METHOD

The GERTS radar data was corrected using a real-time method. These equations are derived from Snell's law for refraction in spherical coordinates.[4] To calculate the true elevation angle an expression is used, where

$$\bar{n} \sin E_o' = n_o \sin E_o. \tag{12}$$

and

E_o' = the true elevation angle

E_o = the measured elevation angle

n_o = the surface refractive index

$\bar{n}$ = the average index of refraction between the missile and the tracker.

This equation can be developed using small angle approximations to give an expression for the elevation angle error, ΔE, in microradians, where

$$\Delta E = \tan E_o (N_o - \bar{N}) \tag{13}$$

and

N_o = the surface refractivity

$= (n_o - 1) \times 10^6$

and

$\bar{N}$ = the average index of refractivity between the missile and the radar, where

$\bar{N} = (\bar{n} - 1) \times 10^6$

The problem is to find values for $\bar{N}$ which provide meaningful values for the refraction-induced error data. By assuming an exponential refractivity model of the CRPL type[2] the average refractivity over the path is approximated by

$$\bar{N} \simeq \frac{N_o}{C_e \cdot H} \tag{14}$$

where C_e is the surface dependent exponential scale height and the target height H is found from apparent radar data.

There are certain limitations imposed by this method of development which can limit the usefulness of these real-time equations.

In the first place, Snell's Law is not expressed in terms of the average of refractivity (12),but it defines the relationship of the index of refraction and the local elevation angle of a ray at a point in space. Second, the target height used in (14) is calculated from apparent radar data which is meaningful only at large elevation angles. The calculated elevation angle errors using these equations must, therefore, be in error. By relating the data with accurate ray-traced results certain empirical corrections can be added to these equations to obtain meaningful data, which is apparently what has been done.

The comparison between these calculations and the SURC results, (figure 41), indicates that the GERTS equations provide very good error data for this particular operation.

The major difficulty will be realized if it is required to extend the use of these equations to low elevation angles and to provide meaningful data when a strong inversion is present.

The most serious limitation is that the doppler error angle, δ, (figure 1) cannot be calculated from the GERTS equation, where,

$$\delta = \tau - \epsilon. \tag{15}$$

These equations do not permit a calculation of the ray path bending, τ. Since the doppler error angle, δ, corrects velocity measurements obtained from doppler or range-rate measurements a knowledge of this angle is necessary to obtain accurate tangential velocity information at low tracking angles.[3] This situation occurs when a high trajectory object is being tracked at low elevation angles over the radar horizon.

It is sufficient to note that the SURC equations have none of these limitations since they are derived in direct relationship to the physical principles of ray behavior in a refractive medium, including the effect of an elevated layer. It is, therefore, advantageous to use these SURC equations if their execution time can be made compatible with the overall mission requirements. These equations can be directly extended for use in the optical tracking region should such a requirement arise.

SECTION VII

SUMMARY COMMENTS

The analysis of three AFWTR missions demonstrates that the SURC equations can be used in near-real-time to correct refraction-induced tracking errors. The corrected tracking data using these equations is comparable in accuracy with the use of ray-tracing correction methods. They can be used with a minimum of meteorological support and can take account of additional effects produced by an elevated layer. This latter ability gives them a distinct advantage over the present GERTS real-time correction method. Also, the GERTS equations do not provide a correction to velocity errors, which are introduced because of ray-bending. This inability may become significant if greater velocity accuracy is required in future missions.

Since any computational method requires some finite execution time, there is no direct method to obtain truly real-time error data. However, the SURC equations can be programmed for use with a raw radar data rate of greater than ten points per second. A simple linear extrapolation of the error data would permit equivalent real-time error data to be made available. Since the required extrapolation period is set by the particular processing machine we have not attempted to introduce this relatively simple function in the present program.

The question of the magnitude of residual tracking errors following corrections for refraction was covered in the previous report.[1] Unless the two dimensional structure of refractivity in height and distance could be measured instantaneously, there is no analytical method to determine the magnitude of these residual errors. For example, figure 43 shows the nature of the horizontal changes in refractivity which were measured with a refractometer-equipped aircraft. The vertical variations of refractivity near the antenna have the greatest effect on the magnitude of height errors. However, variations progressively further away from the radar contribute in a range-weighted manner to the final overall height errors. Therefore, increasing the detail of refractivity structure near the radar site will not necessarily decrease the overall height error directly.

A sensible approach to the determination of residual errors in real-time tracking operations is to confront the corrected radar position data with independent measurements of target position. As mentioned in the introduction, radar-altimeter equipped aircraft and established satellite orbital parameters could be used to fix the target locations.

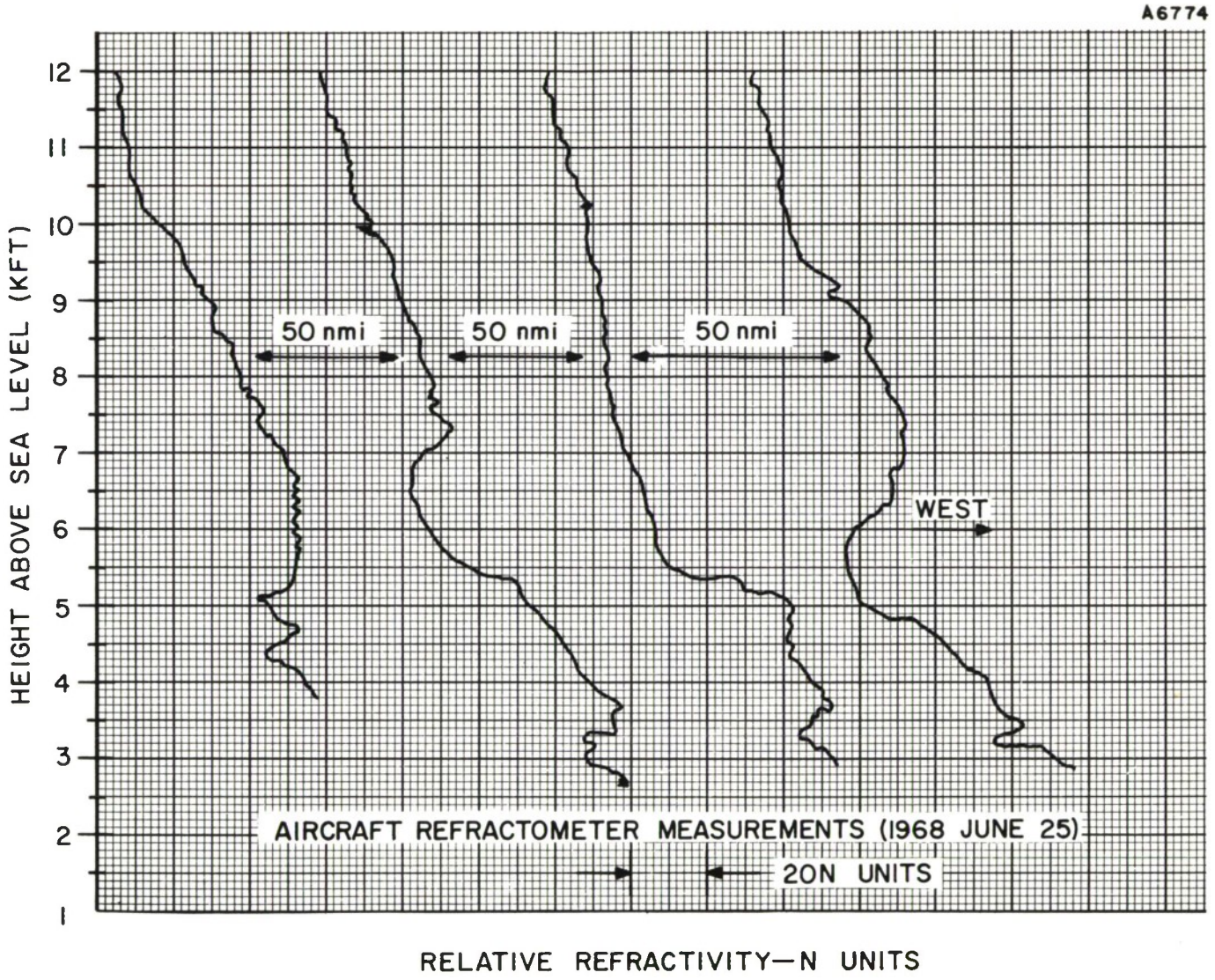

FIGURE 43. SPATIAL VARIATION OF RADIO REFRACTIVITY

Measurements of this kind have already been carried out with aircraft[5] where a sea-reflection interferometer was used to measure the angle of arrival of the signal. In general, the receiving system must be able to resolve angles of arrival of at least 0.05 milliradians to be able to discriminate the effect of residual refraction errors. This accuracy requirement essentially rules out using the FPS-16 radars in such an experiment.[6]

The exponential model atmosphere including the effect of the inversion layer has demonstrated an ability to represent propagation conditions by comparison with ray-traced results. The effect of the layer is covered in Appendix I. It appears from analysis covered in the previous report[1] that in the climatological environment peculiar to the coast of California, that the CRPL exponential could be adjusted to provide better agreement with ray-traced results. By establishing the relationship between surface values and the initial gradient over the first one kilometer height section, a regression analysis can be carried out using available radiosonde data. The indication based on previous analysis is that the exponential decay constant, c, used with the exponential model should be slightly smaller for the California coastal area than is given by the CRPL model. To this end, data which has been collected by ray-tracings of radiosonde and aircraft measurements is compiled in an addendum of which a limited number of copies are available for this type of further analysis. Since this type of information is not of general interest, the data is not included with this report.

SECTION VIII

RECOMMENDATIONS

1. Since the SURC refraction-correction program can be used in near-real-time to correct range, angle and velocity data, it is recommended that it be initially implemented on the AFWTR SDS-930 computer for further evaluation. The program was run on the SURC SDS-930 using AFWTR radar data tapes. Additional evaluation of the program should be made by AFWTR particularly when tracking is performed in the presence of a strong elevated layer (inversion).

2. The program operators should become completely confident with the program and evaluate it under various optional methods of inputing meteorological data. It is then recommended that an evaluation be made of the reduced running time possible through the use of machine language operation on other superior software.

3. An evaluation of the limitations of the electromechanical angle accuracy of the FPS-16 trackers should be carried out to determine if they can be used to experimentally determine the residual errors after real-time corrections are applied. If the accuracy is well under 0.1 milliradians it would be useful to compare the corrected radar data using the SURC program with independently determined target position data. Airborne radar altimeters should be able to give target (aircraft) heights to within 50 feet. The possibility of using satellite targets should be considered.

4. Presently available radiosonde data can be used to perform a correlation analysis of the initial 1 km gradient with surface data. In this way it appears possible to improve the correction available with the SURC program by determining an exponential model more suited to the seasonal characteristics in the Vandenberg area.

5. It is recommended that AFWTR consider using the consultation of SURC in these areas in view of our present experience with the nature of refraction errors affecting the AFWTR tracking system.

REFERENCES

1. Rowlandson, L. G., and J. R. Herlihy, "Refraction-Induced Tracking Errors and Correction Methods for the Air Force Western Test Range," December 1968, ESD (USAF)-TR-69-52, Syracuse University Research Corporation, Syracuse, New York.

2. Bean, B. R., and G. D. Thayer, "CRPL Exponential Atmosphere," NBS Monograph 4, October 1959.

3. Millman, G. H., "Atmospheric and Extraterrestial Effects on Radio Wave Propagation," General Electric Report No. R61EMH29, Technical Publication CSP9-12, Syracuse, New York.

4. AFWTR/WTOD, "GERTS Refraction Equations as Used in Real-Time at the AFWTR," Internal Memorandum.

5. Starkey, B. J., Rowlandson, L. G., and G. A. Fatum, "Cold Lake Radio Propagation and Meteorological Experiment – Description of a Radio-Meteorological Experiment to Measure Ray-Path Bending in the Troposphere With a Vertical Interferometer," 1 June 1967, MTR 118, Vol. I, The Mitre Corporation, Bedford, Massachusetts.

6. Barton, D. K., "Final Report, Instrumentation Radar AN/FPS-16 (XN-1) Evaluation and Analysis of Radar Performance," RCA, Moorestown, New Jersey, Contract DA 36-034-ORD-151, ASTIA Document AD 212 125.

APPENDIX I

A METHOD TO INCLUDE THE EFFECT OF AN ELEVATED LAYER AND TEST FOR TRAPPING

1.0 A METHOD TO INCLUDE THE EFFECT OF AN ELEVATED LAYER AND TEST FOR TRAPPING

On the average the exponential model atmosphere represents realistic conditions because of the exponential decrease of pressure with height. The model becomes very non-standard when an inversion exists, in which case the water vapor tends to remain under the inversion and then rapidly decreases with height through the inversion layer. In terms of refractivity, N, is

$$N \simeq \frac{77.6}{T}\left(p + \frac{4810e}{T}\right) \tag{1A}$$

where

p = the air pressure (mb)

T = the air temperature (° K)

e = the associated water vapor pressure (mb)

The rapid decrease of water vapor through the inversion causes N to also decrease thereby forming an elevated layer. This layer causes the ray-bending to increase above normal when the ray enters the layer at small angles of incidence. If the layer produces enough bending the ray does not immediately pass through the layer and a radio hole is formed.

Figure I-1 shows two refractivity profiles, one the CRPL exponential model and the other typical of propagation conditions in the presence of a strong inversion. The CRPL exponential is generated using the surface value of 345 N units.

Figure I-2 depicts the paths of two rays, one, S_e, propagated in an exponential atmosphere and the other, S_L, in the same atmosphere but with an elevated layer included. Due to the increased refractivity gradient in the inversion layer the ray, S_L, is bent significantly as it passes through the layer.

The bending in the layer produces a local elevation angle, θ_2, at the top of the layer, where

$$\theta_2 \simeq \left[\theta_1 + \frac{2DH}{r_o} - \frac{2DN}{10^6}\right]^{\frac{1}{2}} \tag{2A}$$

(see Radio Meteorology, page 83, NBS Monograph 92),

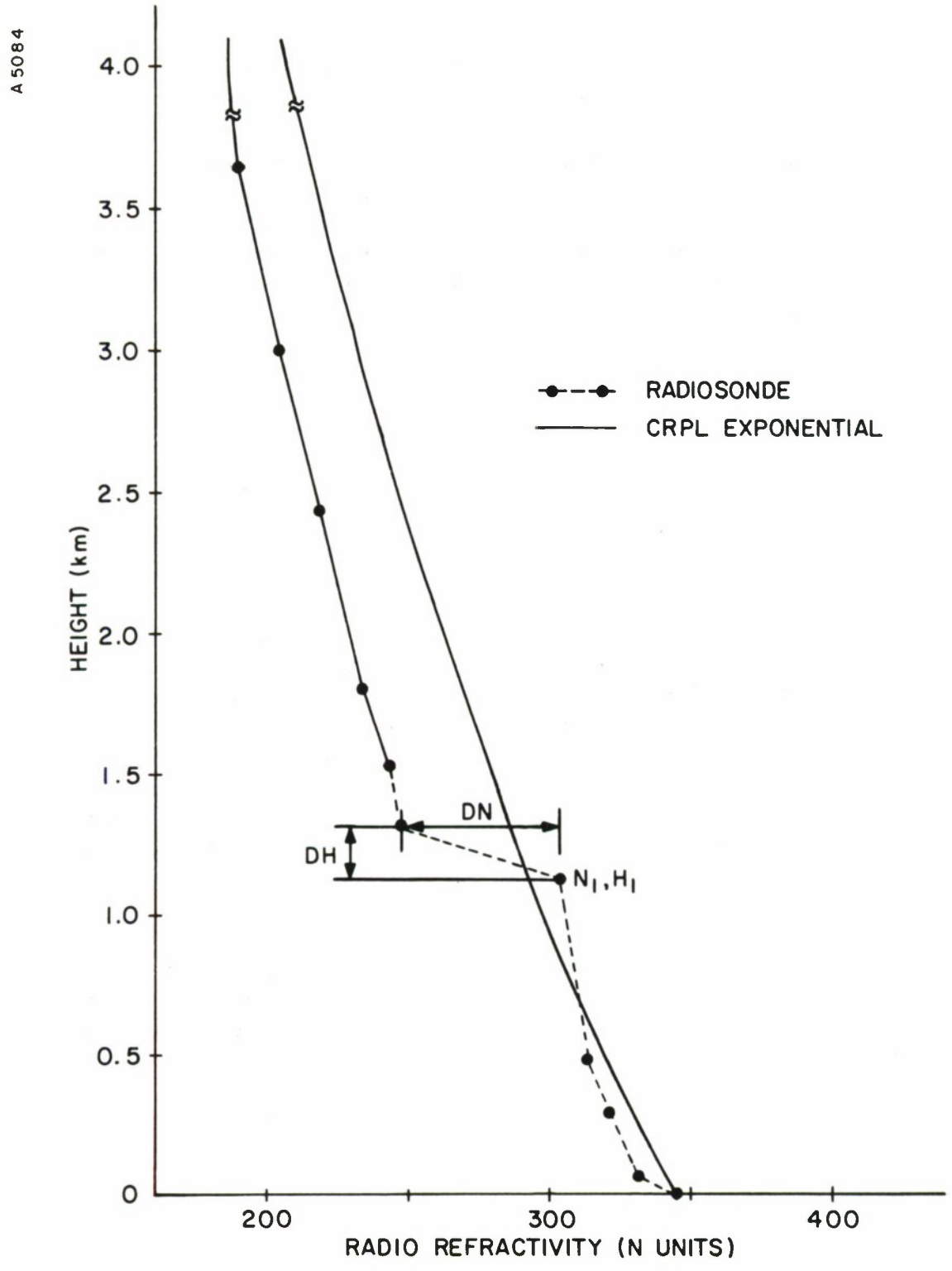

FIGURE I-1. THE EXPONENTIAL PROFILE AND A LAYERED MODEL

A5083

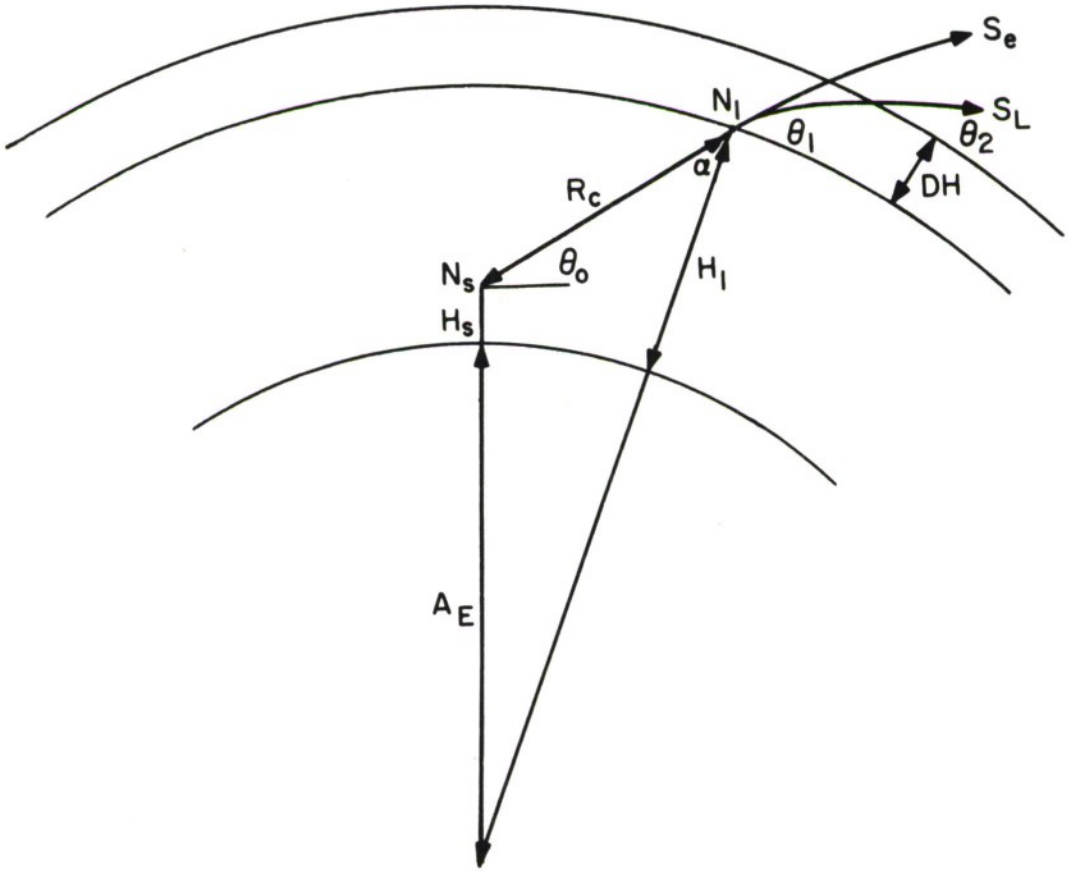

FIGURE I-2. RAY TRACING GEOMETRY IN A LAYERED MODEL

where

ϑ_1 = the local angle of incidence of the ray into the layer

DH = the layer thickness (positive)

DN = the change in N through the layer, and is defined here as positive.

Since the inversion tends to trap the water vapor under the layer the concentration of water vapor with height decreases slowly under the layer. Examination of meteorological data shows that the refractivity, N, then tends to decrease almost linearly with height under a strong inversion. It is, therefore, convenient to obtain a determination of θ_1, and the distance, RC, to the layer, RC, by using an effective earth radius approach.

Referring to figure I-2, the true earth's radius is replaced by an effective earth radius, AE, where (Schelleng, et al, Proc. IRE 21, March 1933).

$$AE \simeq \frac{r_o}{1 + \frac{r_o}{10^6} \cdot \left(\frac{N_1 - N_s}{H_1 - H_s}\right)} \tag{3A}$$

The angle of incidence, θ_1, is then given by

$$\theta_1 = \pi/2 - \alpha \tag{4A}$$

where

$$\alpha = \sin^{-1}\left[\cos\theta_o \cdot \frac{AE + HS}{AE + HI}\right] \tag{5A}$$

The range, RC, where the ray enters the layer is then

$$RC = (AE + HI) \cdot \cos\alpha - (AE + HS) \sin\theta_o. \tag{6A}$$

It is mathematically convenient to concentrate the bending produced by the layer on S_L at the point where the ray enters the layer. In other words, as the ray S_L enters the layer at an angle, θ_1, assume that it abruptly changes its direction to a new angle, θ_2, given by (2A). Now compare the remaining bending, τ, between S_e and S_L over the remaining range R - RC. If the value of refractivity, N_T, at the target is very small compared to the value, N_1, at the base of the layer, then,*

$$\tau \simeq N_1 \cot\theta_i \times 10^{-6} \tag{7A}$$

where θ_i is the initial elevation angle of the ray at the base of the layer.

*Bean, B.R. and E.J. Dutton, "Radio Meteorology," NBS Monograph 92, March 1966, p. 53.

Therefore, over the remaining path, R - RC,

$$\tau_L \simeq N_1 \cdot \cot \theta_2 \times 10^{-6} \text{ for } S_L \tag{8A}$$

where N_1 is the value of refractivity at the base of the layer obtained from radiosonde data (figure I-1) and for the other ray S_e in the exponential atmosphere,

$$\tau_e \simeq N_1 \cdot \cot \theta_1 \times 10^{-6} \tag{9A}$$

Taking the ratio of (8A) and (9A) the bending of the ray S_L over the remainder of the path, R - RC, is changed from its normal bending, τ_e, in the exponential atmosphere where

$$\tau_L \simeq \tau_e \cdot \frac{\cot \theta_2}{\cot \theta_1} \tag{10A}$$

Since the effect of bending is only significant at small angles of incidence then using small angle approximations

$$\tau_L \simeq \tau_e \frac{\theta_1}{\theta_2} \tag{11A}$$

where τ_e is obtained directly from (3) over the path where the range, R, exceeds, RC.

Therefore, (8) (Section 2.0), can be redefined when a layer is present by setting

$$\sum_{i=1}^{n} \sin (\theta_0 - \tau_i) \, \delta R_i = \sum_{i=1}^{n} \sin (\theta_0 - \tau_i \cdot m) \, \delta R_i \tag{12A}$$

where

$$m = 1 \text{ for } R < RC \tag{13A}$$

$$m = \theta_1/\theta_2 \text{ for } R > RC \tag{14A}$$

2.0 A COMPARISON OF CALCULATIONS INCLUDING A LAYER WITH RAY-TRACING ANALYSIS

Let the radiosonde data of figure I-1 describe propagation conditions in the presence of a strong inversion. Figure I-3 shows a comparison of results with the layer present between the SURC calculations and ray-traced results where the tracking station height is at 0.5 km above sea level. With the layer not included the error angle is seen to be significantly less at small elevation angles.

The elevation angle error, ϵ, from SURC calculations is given by

$$\epsilon = \theta_0 - \sin^{-1}\left[\frac{1}{R}\sum_{i=1}^{n} \sin(\theta_0 - \tau_i \cdot m)\,\delta R_i\right] \tag{15A}$$

where

$$m = 1 \text{ for } R < RC \tag{16A}$$

$$m = \theta_1/\theta_2 \text{ for } R > RC \tag{17A}$$

and RC, θ_1 and θ_2 are determined from (6A), (4A), and (2A), respectively, and τ_i by (3). The range intervals, δR_i, were found from (10) using nine intervals or N equals 10 in equation (11).

For the station height of 0.5 km the station value, N_s is 313 and all other parameters, c, k_0, k_1, k_2, k_3, are related to this value of N_s as previously reported.

Figure I-4 shows a comparison where the station height is increased to 1 km above the surface. As the distance between the base of the inversion and the station decreases, the effect of the layer on ray-bending becomes greater. The calculations with the layer excluded (that is, m is set equal to unity for all ranges (16A)) shows very much less angle error at small elevation angles. This data is equivalent to an exponential atmosphere.

Obviously, including the effect of the layer in the SURC equations gives a first order improvement to the prediction of bending errors when a layer is present. It is also apparent and previously reported that even the effect of a strong layer has relatively little effect on ray-bending until the elevation angle decreases below two degrees (35 mr).

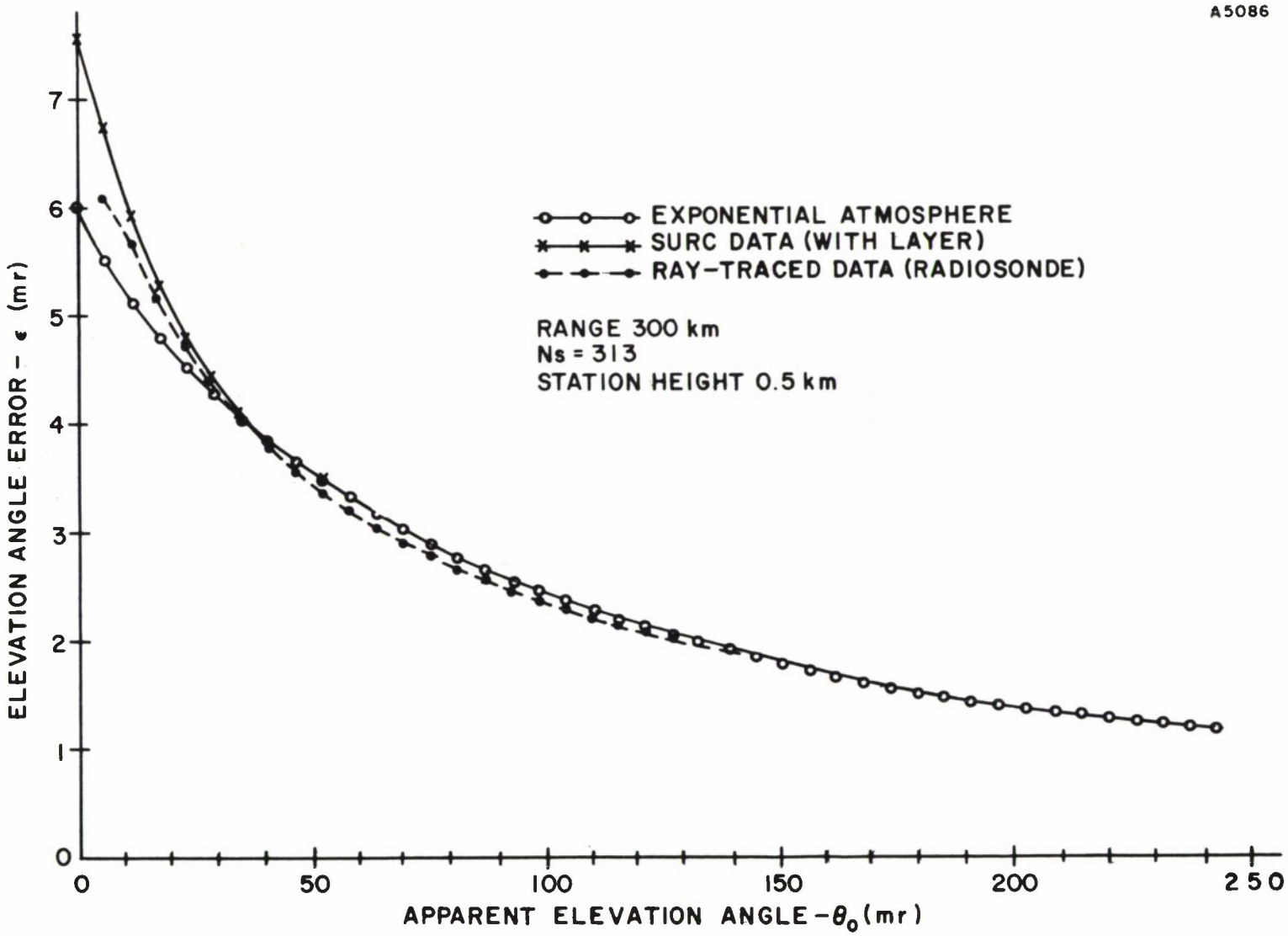

FIGURE I-3. A COMPARISON OF ELEVATION ANGLE ERRORS

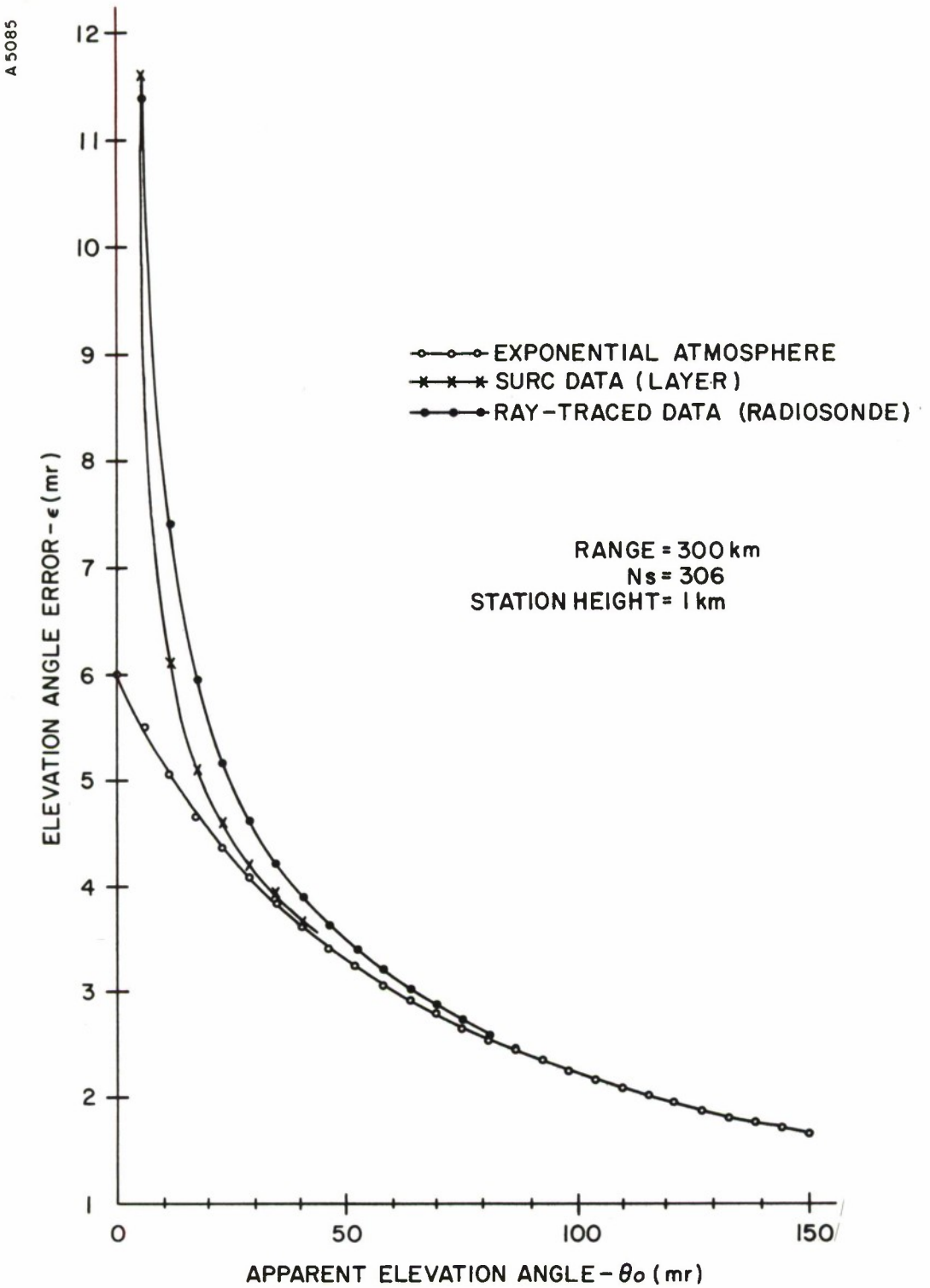

FIGURE I-4. A COMPARISON OF ELEVATION ANGLE ERRORS

Referring to (10) the range increments, δR_i, are fairly large in which case the effect of the layer is generally not introduced into (15A) until after the range, R, exceeds RC. This effect compensates for the assumption made in the derivation that the bending produced by the layer is concentrated at the point where the ray enters the layer. Also, the assumption that the ray-bending is directly proportional to, $\cot \theta_i$, (7A) is true only when the range is very large. Therefore, the above comparative results (figures I-3 and I-4) are most applicable when tracking a vehicle near the radar horizon. However, the target height error, for a given elevation angle error, ϵ, is almost directly proportional to range. That is, the height error, Δh, is

$$\Delta h \simeq \epsilon \cdot R \tag{18A}$$

Therefore, the errors in calculating the effect of a layer from (15A) at short tracking ranges is much less serious than if these errors were implicit in the calculations for long ranges.

To increase the accuracy of these calculations at short range would require using the expression for τ_i from (3), then

$$\tau_L \simeq N_1 \cot \nu_2 \times 10^{-6} \left[1 - \frac{g_1}{k_1 + g_1} e^{-k_1^2} - 2k_1 g_1\right] \tag{19A}$$

where ν_2, g_1, and k_1 are associated with the angle, θ_2.

Also

$$\tau_e \simeq N_1 \cot \nu_1 \times 10^{-6} \left[1 - \frac{g_2}{k_2 + g_2} \cdot e^{-k_2^2} - 2k_2 g_2\right] \tag{20A}$$

where ν_1, g_2, and k_2 are associated with the angle θ_1. Since the range, R - RC, is equal in (19A) and (20A), then neglecting second order effects,

$$\tau_L \simeq \tau_e \cdot \frac{\cot \nu_2}{\cot \nu_1}$$

$$\simeq \tau_e \cdot \frac{\nu_1}{\nu_2} \tag{21A}$$

For example, ν_1, for small elevation angles is essentially

$$\nu_1 \simeq \theta_1 + (k_0 + k_2 e^{-k_3 (R - RC)}) e^{-k_1 \theta_1} \tag{22A}$$

For real-time application where these SURC equations are most useful, complicating the summation in (15A) through the use of equation (21A) is not justified.

Furthermore, the characteristics of the layer generally change significantly with distance from the radar. The radiosonde measurement of the layer characteristics near the site may be unrelated to the layer conditions at the range RC. Therefore, including the layer in the SURC equations only provides a first-order correction in any case and in the same way even if ray-tracing calculations are used the same problems in defining the layer apply. However, for very small elevation angles the elevation angle error, ϵ, can be partly compensated by including the factor, θ_1/θ_2, in the bending equation when the range exceeds, RC.

3.0 A TEST FOR TRAPPING CONDITIONS

When the measured characteristics of a layer are introduced the preceding analysis shows that a first-order correction to ray-bending can be made. Possibly of equal importance is the fact that these equations can be used to give a prediction of the tracking elevation angle where trapping could occur. For example, setting θ_2 equal to zero in (2A) defines a limiting condition where the ray would be trapped for a value of θ_1 less than

$$\theta_1 \leq \left[\frac{2DN}{10^6} - \frac{2DH}{r_o}\right]^{\frac{1}{2}} \tag{23A}$$

Obviously, since θ_1 has to be a real number the first condition to produce trapping is that

$$\frac{DN}{10^6} \geq \frac{DH}{r_o} \tag{24A}$$

If these conditions are satisfied then θ_o is found from an expanded form of Snell's law in polar coordinates where

$$n_s\, r_s \cos \theta_o = n_1\, r_1 \cos \theta_1 \tag{25A}$$

and since

$$n_s = 1 + N_s/10^6$$

$$r_s = r_o + H_s$$

$$n_1 = 1 + N_1/10^6$$

$$r_1 = r_o + H_1$$

neglecting second order effects

$$\cos \theta_{oT} \simeq \frac{\cos \theta_1}{\left[1 + \frac{N_s - N_1}{10^6} - \frac{H_1 - H_s}{r_o}\right]^{\frac{1}{2}}} \tag{26A}$$

For a real value θ_{oT} the right hand side of (26A) must be less than one. If it is, then θ_{oT} is determined and represents the largest apparent elevation angle which could be trapped. The radar operator is then alerted to the fact that the target signal may be lost for tracking angles less than θ_{oT}.

With the radar at 0.5 km above sea level both the ray-tracing analysis and the SURC equation (26A) indicate that the trapping angle, θ_{oT}, was zero degrees, or in other words, no ray would be trapped for apparent elevation angles above zero degrees. With the radar at 1 km above sea level ray-tracing results show, θ_{oT} equals 0.2817 degrees (4.92 mr) and the SURC equations give 0.2480 degrees (4.335 mr). Such close agreement indicates that the SURC equations can be used to give a very good estimate of the trapping angle, θ_{oT}, compared to ray-tracing methods. However, again it should be emphasized that whether or not these results are meaningful depends upon the spatial characteristics of the layer.

APPENDIX II

RADIOSONDE PROFILES

SOUTH VANDENBERG WEATHER PROFILE OP-5265

ALTITUDE	REFRACTIVE INDEX
0	319
327	315
400	304
500	300
600	299
700	298
800	297
900	297
1000	296
1100	295
1200	294
1300	292
1400	291
1500	290
1600	290
1700	289
1800	288
1900	288
2000	287
2100	287
2170	288
2200	287
2300	286
2400	285
2500	283
2600	282
2700	281
2800	280
2900	279
3000	278
4000	274
5000	262
6000	254
7000	243
8000	223
9000	214
10000	207

SOUTH VANDENBERG WEATHER PROFILE OP-5265

ALTITUDE	REFRACTIVE INDEX
11000	200
12000	195
13000	187
14000	181
15000	177
16000	170
17000	164
18000	159
19000	154
20000	149
21000	143
23000	133
24000	130
25000	124
26000	120
27000	115
28000	112
29000	107
30000	104
35000	81
40000	65
45000	50
50000	39
55000	31
60000	25
65000	20
70000	15
75000	12
80000	10
85000	7
90000	5
95000	4
100000	3
105000	3
110000	1
120000	0
120100	0

SOUTH VANDENBERG WEATHER PROFILE OP-5265

ALTITUDE	REFRACTIVE INDEX
120200	0
1000000	0
10000000	0

POINT MUGU WEATHER PROFILE OP-5265

ALTITUDE	REFRACTIVE INDEX
12	313
100	304
200	301
300	298
320	297
400	297
500	297
600	296
700	296
800	295
900	294
1000	292
1100	291
1200	290
1300	288
1400	287
1500	287
1600	286
1700	285
1800	282
1900	280
2000	278
2100	277
2200	276
2300	274
2400	273
2500	271
2600	271
2700	270
2800	269
2900	269
3000	268
3100	267
3200	265
3300	264
3400	263
3500	262

POINT MUGU WEATHER PROFILE OP-5265

ALTITUDE	REFRACTIVE INDEX
3600	261
3700	260
3800	260
3900	259
4000	258
4100	256
4200	255
4300	255
4400	254
4500	253
4600	252
4700	251
4800	251
4900	250
5000	249
6000	240
7000	230
8000	218
9000	212
10000	204
11000	197
12000	190
13000	185
14000	179
15000	173
16000	168
17000	163
18000	159
19000	153
20000	148
21000	142
22000	139
23000	133
24000	129
25000	124
26000	120
27000	115

POINT MUGU WEATHER PROFILE OP-5265

ALTITUDE	REFRACTIVE INDEX
28000	112
29000	106
30000	103
31000	98
32000	94
33000	90
34000	86
35000	81
40000	63
45000	50
50000	39
55000	31
60000	25
65000	21
70000	15
75000	12
80000	10
85000	6
90000	4
95000	3
100000	2
110000	1
120000	0
120100	0
120200	0
1000000	0
10000000	0

POINT PILLAR WEATHER PROFILE OP-5265

ALTITUDE	REFRACTIVE INDEX
0	319
140	309
198	309
200	307
300	305
400	302
500	300
600	299
700	298
800	297
900	296
1000	295
1100	294
1200	292
1300	291
1400	290
1500	289
1600	288
1700	288
1800	287
1900	287
2000	286
2100	285
2200	285
2300	283
2400	282
2500	280
3000	276
4000	268
5000	260
6000	249
7000	232
8000	221
9000	214
10000	207
11000	199
12000	193

POINT PILLAR WEATHER PROFILE OP-5265

ALTITUDE	REFRACTIVE INDEX
13000	187
14000	181
15000	177
16000	170
17000	164
18000	159
19000	154
20000	150
21000	144
22000	140
23000	134
24000	131
25000	125
26000	122
27000	116
28000	113
29000	107
30000	104
31000	99
32000	94
33000	90
34000	86
35000	81
36000	77
37000	74
38000	69
39000	67
40000	62
41000	59
42000	58
43000	54
44000	51
45000	49
46000	48
47000	44
48000	42
49000	40

POINT PILLAR WEATHER PROFILE OP-5265

ALTITUDE	REFRACTIVE INDEX
50000	39
51000	38
52000	35
53000	34
54000	32
55000	31
56000	30
57000	29
58000	28
59000	25
60000	23
65000	20
70000	14
75000	12
80000	10
85000	7
90000	5
95000	3
100000	2
105000	0
110000	0
115000	0
10000000	0

SOUTH VANDENBERG WEATHER PROFILE OP-2062

ALTITUDE	REFRACTIVE INDEX
000	330
240	322
300	308
400	306
500	303
600	301
700	299
800	297
900	294
1000	294
1100	293
1200	292
1300	291
1400	290
1500	289
1600	288
1700	288
1800	287
1900	286
2000	286
2100	285
2200	285
2300	284
2400	283
2500	282
2600	281
2700	280
2800	279
2900	278
3000	275
4000	266
5000	256
6000	248
7000	241
8000	234
9000	225
10000	217

SOUTH VANDENBERG WEATHER PROFILE OP-2062

ALTITUDE	REFRACTIVE INDEX
11000	209
12000	197
13000	186
14000	178
15000	171
16000	165
17000	159
18000	153
19000	148
20000	142
21000	137
22000	132
23000	128
24000	123
25000	120
26000	116
27000	112
28000	108
29000	104
30000	100
35000	83
40000	66
45000	53
50000	42
55000	33
60000	26
65000	20
69000	17
80000	10
90000	6
100000	3
105000	2
110000	1
120000	0
120100	0
120200	0
1000000	0

POINT MUGU WEATHER PROFILE OP-2062

ALTITUDE	REFRACTIVE INDEX
00	315
12	315
100	315
200	313
300	312
400	311
500	310
600	309
700	308
800	307
900	305
1000	304
1100	303
1200	302
1300	301
1400	300
1500	299
1600	298
1700	298
1800	297
1900	297
2000	296
2100	295
2200	294
2400	293
2500	292
2600	291
2700	290
2800	288
2900	287
3000	276
4000	264
5000	255
6000	245
7000	240
8000	229
9000	219

POINT MUGU WEATHER PROFILE OP-2062

ALTITUDE	REFRACTIVE INDEX
10000	212
11000	203
12000	195
13000	186
14000	180
15000	174
16000	167
17000	161
18000	155
19000	150
20000	144
21000	139
22000	134
23000	129
24000	125
25000	120
26000	117
27000	113
28000	109
29000	106
30000	101
35000	84
40000	66
45000	53
50000	42
55000	35
60000	26
65000	20
70000	16
75000	12
80000	10
85000	8
90000	6
95000	5
97000	4
100000	3
105000	2

POINT MUGU WEATHER PROFILE OP-2062

ALTITUDE	REFRACTIVE INDEX
110000	1
120000	0
120100	0
120200	0
1000000	0

POINT PILLAR WEATHER PROFILE OP-2062

ALTITUDE	REFRACTIVE INDEX
0	308
140	304
200	300
300	296
400	295
500	292
600	291
700	290
800	289
900	288
1000	287
1100	287
1200	286
1300	285
1400	283
1500	282
1600	281
1700	280
1800	279
1900	279
2000	278
3000	269
4000	260
5000	247
6000	239
7000	228
8000	222
9000	214
10000	206
11000	199
12000	195
13000	188
14000	182
15000	177
16000	170
17000	164
18000	159

POINT PILLAR WEATHER PROFILE OP-2062

ALTITUDE	REFRACTIVE INDEX
19000	154
20000	149
21000	142
22000	136
23000	130
24000	124
25000	120
26000	115
27000	111
28000	106
29000	102
30000	97
35000	79
40000	65
45000	51
50000	41
55000	32
60000	25
65000	21
70000	15
75000	12
80000	10
85000	7
90000	5
95000	4
100000	3
105000	3
110000	2
120000	1
120100	0
120200	0
1000000	0
10000000	0

SOUTH VANDENBERG WEATHER PROFILE OP 7335

ALTITUDE	REFRACTIVE INDEX
0	328
327	324
1000	315
2000	306
2170	302
3000	290
4000	260
5000	241
6000	233
7000	225
8000	217
9000	210
10000	205
11000	201
12000	195
13000	191
14000	190
15000	181
16000	176
17000	169
18000	164
19000	158
20000	150
21000	144
22000	140
23000	134
24000	130
25000	124
26000	120
27000	115
28000	112
29000	107
30000	104
35000	87
40000	71
45000	54
50000	42
55000	33
60000	26

SOUTH VANDENBERG WEATHER PROFILE OP 7335

ALTITUDE	REFRACTIVE INDEX
65000	21
70000	15
75000	12
80000	10
85000	7
90000	5
95000	4
100000	3
105000	3
106000	3
110000	2
115000	1
120000	0
120100	0
120200	0
10000000	0

APPENDIX III

DESCRIPTION OF THE SURC REAL-TIME REFRACTION CORRECTION TECHNIQUE

1.0 INTRODUCTION

The enclosed program used on the SDS-930 computer at SURC consists of several sections, each section individually numbered. For ease in explanation, the total package is also renumbered by consecutive pages from 94 through 120.

It should be pointed out that the actual real-time refraction correction program is described in pages 109 through 112 which is a small part of the program described herein.

The total package is actually two individual programs:

1. The initialization program, pages 94 through 108, reads the data cards, calculates some a priori parameters and outputs them on magnetic tape.
2. The actual refraction correction program, pages 109 through 120, reads in a priori parameters and the radar data, calculates the refraction error and outputs the results on either the printer or magnetic tape, whichever is selected by sense switch control.

2.0 THE INITIALIZATION PROGRAM

2.1 Pages 94 - 96 : Refraction Correction Initialization

This program computes coefficients which are required for use in the real-time running program (Refraction Correction - page 109). Meteorological information is entered at this point as well as the height of the radar above mean sea level, HS, in kilometers.

Several options are available for entry of meteorological data:

a. If the radar station value of refractivity, SNS, is known, enter it directly. In general this value would be obtained from a radiosonde profile where the value SNS is picked from the profile at the height, HS, of the particular radar above mean sea level. The radiosonde profile would be selected from the local launch station and as close in time to the launch as possible.

Using this method the radiosonde profile will indicate the presence or absence of the inversion layer. If the layer is present and above the height of the radar station, set NTRAP = 1. The measured characteristics of the layer must then be entered where,

H1 = The base height of the layer above mean sea level (kilometers).

SNI = The value of refractivity at the base of the layer.

DH = The thickness of the layer (kilometers).

DN = The change in refractivity through the layer (always a positive quantity for the inversion layer).

And refractivity, N, is defined by

$$N = \frac{77.6}{T}\left[p + \frac{4810\ e}{T}\right]$$

where

T = The air temperature (deg. Kelvin).

p = The air pressure (millibars).

e = The water vapor pressure (millibars).

AFWTR has programs already available to calculate N.

The local earth radius used is seen to be 6378.163 km (page 95) but can be redefined to suit local geographical latitudes.

If the characteristics of the inversion layer are included the program will indicate if the radar signal can be trapped and, if so, it will calculate the elevation angle at and below which trapping could occur.

If no layer is present, or if it is desired not to include the effect of the layer set, NTRAP = 0.

b. The second option assumes that there is no direct measurement of SNS or any radiosonde profile information available. In this case there must be a value of refractivity, SNL, obtained at the radiosonde launch site. This value, SNL, is set in and also the height above mean sea level, HL (km), where SNL is measured. Also, of course, set, NTRAP = 0, since no inversion layer information is used.

2.2 Pages 97 - 102: Generalized Mainline Program for Polynomial Curve Fit

This program is used to generate the values of four constants used in the real-time running program (page 110). These constants, CK0, CK1, CK2, and CK3 are functions of the equivalent radar station value of refractivity, SNS. They are used to provide an optimum calculation of refraction errors for short tracking ranges and small elevation angles. These constants can be obtained from graphs or tables in place of using this generating program. The program is included herein since it facilitates direct and accurate determination of these constants without manual intervention.

2.3 Pages 103 - 108: Complete Magnetic Tape Routines

This program is designed to handle all magnetic tape operations. It has been written in metasymbol making use of the interlace feature and the extended mode capability but does not use or affect the interrupt system in any way. It contains all of the present Fortran capabilities plus several more and will execute all magnetic tape operations much more rapidly and efficiently than do the Fortran routines.

It is used here to output the necessary parameters calculated in the initialization program.

3.0 THE REFRACTION CORRECTION PROGRAM

3.1 Pages 109 - 112: SURC Refraction Correction Program

This is the real-time refraction correction program. It will use constants derived from the Initialization Program (Section 2.1) and the Polynomial Program (Section 2.2). Given the uncorrected radar range, R (feet) and the uncorrected elevation angle, θ_0 (degrees), it will generate the refraction induced errors and provide corrected range and elevation angle data. It will also generate the doppler velocity error angle, δ (DELTA) which can be then used to correct doppler or range rate velocity measurement. (Reference: Rowlandson, L. G., and J. R. Herlihy, "Refraction-Induced Tracking Errors and Correction Methods for the Air Force Western Test Range," December 1968, ESD, TR-69-52.)

3.2 Pages 113 - 114: Converter Program

This program written in metasymbol for the SDS-930 is used to convert the radar data supplied on AFWTR tapes (FPS - 16 data, 36 bit floating point words) to a format compatible with the input requirements for the SDS-930 (48 bit floating point words).

3.3 Pages 115 - 120: Complete Magnetic Tape Routines

This program is identical with 2.3. It is used to input from magnetic tape the parameters from the initialization program and the raw radar data. Under sense switch control, this program will output the results for possible future display purposes.

4.0 COMMENTS

The above program is being used in the SDS-930 to analyze AFWTR radar tapes at a data rate of 8 radar data points per second (approximately 124 ms execution time per data point). If the program were run in machine language on the 930 it could readily handle a data rate of 10 points per second.

We believe that in machine language on the IBM computer at AFWTR the program should execute in less than 50 ms because of the reduced times required for division and multiplication.

This SURC refraction correction program does not smooth the radar data but gives a direct correction for refraction on a one-to-one relationship with the input data.

It should be pointed out that the program was developed for use in the metric system requiring that conversions be made from feet and degrees to kilometers and radians. This conversion is presently carried out within the program thereby making it directly compatible with AFWTR radar data for raw radar range input in feet and raw tracking angle in degrees. The metric system was used within the calculations because the CRPL exponential profile data and ray-traced error data were metric.

It should be repeated that all height information put into the initialization program (2.1) must be in kilometers. Of course, AFWTR may wish to make the conversion necessary to use height data in feet.

```
▵JØB.
▵REWIND BØ.
▵FØRTRAN BØ,LØ.
C           REFRACTIØN CØRRECTIØN
C              INITIALIZATIØN
C           Q0001-01  ---  PEISEL
C
C
C               THE INITIALIZATIØN PRØGRAM READS 9 DATA CARDS
C           PLUS A SET ØF DATA TØ BE USED BY THE PØLYNØMIAL
C           CURVE FIT SUBRØUTINE.  FRØM THESE IT CALCULATES
C           SØME NECESSARY PARAMETERS FØR THE  REFCØR
C           PRØGRAM AND ØUTPUTS THEM ØN TAPE UNIT 1.  THE 9
C           INPUT PARAMETERS TØ THIS PRØGRAM ARE IN F10.0
C           FØRMAT.  THE UNITS ARE KILØMETERS --
C
C               HS     = STATIØN HEIGHT ABØVE MEAN SEA LEVEL
C               HL     = RADIØSØNDE LAUNCH
                 STATIØN HEIGHT ABØVE SEA LEVEL
C               SNS    = STATIØN VALUE ØF REFRACTIVITY
C               SNL    = RADIØSØNDE LAUNCH
                 STATIØN VALUE ØF REFRACTIVITY
C               NTRAP = 1 IF LAYER IS
                 TØ BE INCLUDED,  0 IF NØT
C               H1     = LAYER HEIGHT ABØVE MEAN SEA LEVEL
C               SN1    = REFRACTVITY VALUE AT HEIGHT H1
C               DH     = THICKNESS ØF THE LAYER
C               DN     = CHANGE IN REFRACTIVITY
                 THRØUGH THE LAYER
C
C
      DIMENSIØN DATA(50),XXLG(10),YX(0/3)
      EQUIVALENCE (DATA(1),XXLG(1)),
                  (DATA(11),ANGL),(DATA(12),SNS)
      EQUIVALENCE (DATA(13),HS),(DATA(14),H1),(DATA(15),SN1)
      EQUIVALENCE (DATA(16),DH),(DATA(17),DN),(DATA(18),CC)
      EQUIVALENCE (DATA(19),CK0),(DATA(20),
                  CK1),(DATA(21),CK2)
      EQUIVALENCE (DATA(22),CK3),(DATA(23),
                  PI),(DATA(24),PIPI)
      EQUIVALENCE (DATA(25),PI2),(DATA(26),
                  DTØR),(DATA(27),RTØD)
      EQUIVALENCE (DATA(28),ERADIUS),
                  (DATA(29),SQ1),(DATA(30),SQ2)
      EQUIVALENCE (DATA(31),AE),(DATA(32),
                  DH2),(DATA(33),AEHS)
      EQUIVALENCE (DATA(34),AEH1),(DATA(35),
                  FTØKM),(DATA(36),AKTØF)
      EQUIVALENCE (DATA(37),ELTRAP),
                  (DATA(38),N),(DATA(39),NTRAP)
```

```
C
      PRINT 60
   60 FORMAT(1H1,//,20X,$REFRACTION CORRECTION$,
                 /,23X,$INITIALIZATION$,
     1///)
      READ 10,HS,HL,SNS,SNL,NTRAP,H1,SN1,DH,DN
   10 FORMAT(F10.0)
C
      PI=3.14159265
      PIPI=2.*PI
      PI2=PI/2.
      DTOR=PI/180.
      RTOD=180./PI
      AKTOF=3280.8236
      FTOKM=1./AKTOF
      ERADIUS=6378.163
      DH2=DH+DH
      ANGL=1.
      CCC=0.
      DNI=0.
      ELTRAP=0.
      N=10
      XN=N
      XXN=ALOGF(XN)
      DO 20 FI=2,N
   20 XXLG(FI)=1.-ALOGF(XN-FI+1.)/XXN
C
      IF(SNL)32,31,32
   32 DNI=-7.32*EXPF(.005577*SNL)
      CCC=ALOGF(SNL/(SNL+DNI))
      SNS=SNL*EXPF(-CCC*(HS-HL))
   31 DNN=-7.32*EXPF(.005577*SNS)
      CC=ALOGF(SNS/(SNS+DNN))
      SQ1=SQRTF(CC*ERADIUS*.5)
      SQ2=SQRTF(CC/(2.*ERADIUS))
      XK=1./(1.+(ERADIUS/1.0E 06)*((SN1-SNS)/(H1-HS)))
      AE=XK*ERADIUS
      AEHS=AE+HS
      AEH1=AE+H1
C
      IF(NTRAP)33,33,37
   37 IF(DN*1.0E-06-DH/ERADIUS)33,34,34
   33 PRINT 35
   35 FORMAT(5X,$NO TRAP$)
      GO TO 36
   34 EL1=SQRTF((2.*DN*1.0E-06)-(2.*DH/ERADIUS))
      ELTRAP=COSF(EL1)/(1.+(SNS-SN1)*
                1.0E-06-(H1-HS)/ERADIUS)
      ELTRAP=ATANF(SQRTF(1.-ELTRAP*ELTRAP)/ELTRAP)
```

```
      PRINT 38,ELTRAP
   38 FORMAT(5X,$TRAP$,5X,$ELEVATION = $,F12.6)
C
   36 CALL POLYFIT(SNS,YX)
      CK0=YX(0)*1.0E-02
      CK1=YX(1)
      CK2=YX(2)*1.0E-02
      CK3=YX(3)*1.0E-02
C
      PRINT 61,SNS,SNL,HS,HL,AE,CC,DNN,
                  CCC,DNI,CK0,CK1,CK2,CK3
   61 FORMAT(//,5X,$SNS = $,F12.5,/,
                  5X,$SNL = $,F12.5,/,5X,$HS  = $,
     1F12.5,/,5X,$HL  = $,F12.5,/,5X,
                  $AE  = $,F12.5,/,5X,$CC  = $,
     2F12.5,/,5X,$DNN = $,
     3F12.5,/,5X,$CCC = $,F12.5,/,5X,
                  $DNI = $,F12.5,/,5X,$CK0 = $,
     4F12.5,/,5X,$CK1 = $,F12.5,/,5X,
                  $CK2 = $,F12.5,/,5X,$CK3 = $,F12.5)
C
      CALL WBT(DATA(1),100,2)
C
      CALL ENDF(2)
      CALL REW(2)
      CALL EXIT
      END
```

```
      SUBROUTINE POLYFIT(SNS,YX)
C
C           GENERALIZED MAINLINE PROGRAM
C            FOR 'POLYNOMIAL CURVE FIT'
C
      DIMENSION YX(0/3)
      DIMENSION X(100),Y(100),A(11),
                KTITLE(10),XX(20),YY(20),ITAB(3)
      LL=0
C
C           FORMAT STATEMENTS
C
    1 FORMAT(10A4)
    2 FORMAT(2F10.0)
    3 FORMAT(4F10.0)
    4 FORMAT(////($  A($,I2,$) = $,E15.8 ))
    5 FORMAT(1H1,40X,10A4////$  THE
                COMPLETE SET OF DATA INCLUDES$,I5,$
     1 POINTS.$,10X,$X$,24X,$Y$//(45X,F20.8,5X,F20.8))
    6 FORMAT(///$  XMIN =$,F20.8,20X,
                $XMAX =$,F20.8/$  YMIN =$,F20.8,20X
     1,$YMAX =$,F20.8///)
   12 FORMAT( 1H1$  DATA POINT NUMBER$,
                I4,$  AND THE NEXT$,I5,$  CONSECU
     1TIVE POINTS WILL BE USED TO FIND THE CURVE FIT.$)
   14 FORMAT(//$  XTEST = $,E15.8/$
                 YTEST = $,E15.8/$  CALX  = $,E15.8)
   16 FORMAT(///////$  THE FOLLOWING
                ARE THE COEFFICIENTS OF A POLYNOMIA
     1L OF DEGREE$,I3,$  FOUND AS A
                CURVE FIT TO THE DATA POINTS GIVEN.$
     2)
   19 FORMAT(1H1,$******  THE CODE SPECIFIED
                BY THE USER IS NOT PERMISSI
     1BLE.$//1H1)
   26 FORMAT(////$  THESE POINTS ARE$,
                10X,$X$,24X,$Y$,//(15X,F20.8,5X,
     1F20.8))
   55 FORMAT(16I5)
   64 FORMAT(/////$  THE FOLLOWING CASES
                PROVIDE A CHECK FOR THIS POLYNO
     1MIAL CURVE FIT.$)
   67 FORMAT(///$ **********  X TEST
                VALUE EQUALING$,E15.8,$   IS OUTSID
     1E THE RANGE OF INPUT DATA, THUS
                NORMALIZING IS INCORRECT.$/$ THE R
     2ANGE OF THE X VALUES OF THE INPUT
                DATA IS$,E15.8,$   TO$,E15.8)
      ITAB(1)=4HSAME
```

```
      ITAB(2)=4HNEW
      ITAB(3)=4HEND
C
C
C
C
C           READ TOTAL NUMBER OF POINTS IN COMPLETE DATA SET.
C           READ PROBLEM TITLE.
C           READ COMPLETE SET OF DATA
                 POINTS (X,Y) TO BE USED.
C           DATA POINTS 1 THROUGH 'NUMBER' MUST BE READ IN
C               EVEN IF 'L', THE FIRST
C               DATA POINT TO BE USED, IS GREATER THAN 1.
C           EACH DATA CARD CONTAINS ONE
                 POINT THUS HAS AN X AND A Y.
C           DATA SHOULD BE ARRANGED IN ASCENDING ORDER.
C           THE CARD FORMAT IS (2F10.0).
C
    9 READ 1,KTITLE
      READ 55,NUMBER
      READ 2,(X(I),Y(I),I=1,NUMBER)
C     PRINT 5,KTITLE,NUMBER,(X(I),Y(I),I=1,NUMBER)
C
C
C
C           READ HIGHEST DEGREE OF FIT
                 DESIRED, THE NUMBER OF DATA POINTS
C               TO BE USED IN CURVE FITTING,
                    THE SUBSCRIPT OF THE FIRST
C               DATA POINT TO BE USED, AND THE
C               NUMBER OF TEST CASES.
C           READ XMIN, XMAX, YMIN, YMAX OF DATA SET.
C
   20 READ 55,MM,L,N,NCHECKS
      READ 3,XMIN,XMAX,YMIN,YMAX
      NN=N-1
C     PRINT 12,L,NN
C     PRINT 26,(X(I),Y(I),I=L,L+NN)
C     PRINT 6,XMIN,XMAX,YMIN,YMAX
C
C
C
C           NORMALIZE X AND Y VALUES OF DATA POINTS
C
      DO 101 I=L,L+NN
      X(I)=(X(I)-XMIN)/(XMAX-XMIN)
  101 Y(I)=(Y(I)-YMIN)/(YMAX-YMIN)
C
C
```

```
C           READ IN ALL TEST POINTS WHICH
                  WILL BE USED TO EVALUATE THE
C               RESULTING POLYNOMIAL.
C
      IF(NCHECKS)60,60,61
   61 XX(1)=SNS
      YY(1)=0.0
C
C
C
C           FIT A POLYNOMIAL OF DEGREE
                  M THROUGH THE SET OF DATA POINTS
C
   60 DO 21 M=2,MM
      DO 62 I=1,11
   62 A(I)=0.
C     PRINT 16,M
C
      CALL LSQ(M,N,L,X,Y,A)
C     PRINT 4,(I,A(I),I=1,M+1)
C
      IF(NCHECKS)21,21,11
C  11 PRINT 64
   11 CONTINUE
      DO 100 I=1,NCHECKS
C
C
C
C           NORMALIZE TEST VALUE OF XX
                  TO FIT WITHIN DATA RANGE AND
C               CALCULATE F(XX)
C
      CALX=0.
      XTEST=(XX(I)-XMIN)/(XMAX-XMIN)
      IF(XTEST)65,66,66
   66 IF(XTEST-1.)68,68,65
   65 TYPE  67,XX(I),XMIN,XMAX
      GO TO 100
   68 DO 63 J=1,M+1
   63 CALX=A(J)*XTEST**(J-1)+CALX
      CALX=CALX*(YMAX-YMIN)+YMIN
C     PRINT 14,XX(I),YY(I),CALX
      IF(M-3)401,400,401
C 400 TYPE 401,LL,CALX
  400 CONTINUE
      YX(LL)=CALX
  401 FORMAT(2X,$K$,I2,$ = $,E15.8)
  100 CONTINUE
C
```

```
   21 CONTINUE
      LL=LL+1
C
C
C
C           READ CODE CARD.  THE OPTIONS INCLUDE:
C               SAME DATA SET
C               NEW DATA SET
C               END
C
      READ 1,ICODE
      DO 17 I=1,3
      IF(ICODE-ITAB(I))17,18,17
   17 CONTINUE
      PRINT 19
      GO TO 1113
   18 IF(I-2)20,9,1113
 1113 RETURN
      END
```

```
      SUBROUTINE LSQ(M,N,L,X,Y,A)
C
C           LEAST SQUARES POLYNOMIAL CURVE FIT
C
C           FITS AN M-TH DEGREE POLYNOMIAL
C                 THROUGH N POINTS
C               STARTING WITH THE L-TH
C
      DIMENSION X(1),Y(1),A(1),B(11,12)
C
C           CLEAR THE MATRIX
C
      DO 2 I=1,M+1
      DO 2 J=1,M+2
    2 B(I,J)=0
C
C           FORM THE LOWER MATRIX
C
      DO 4 K=L,L+N-1
      XI=1
      DO 4 I=1,M+1
      XJ=1
      DO 3 J=1,I
      B(I,J)=B(I,J)+XI*XJ
    3 XJ=XJ*X(K)
      B(I,M+2)=B(I,M+2)+XI*Y(K)
    4 XI=XI*X(K)
C
C           MAKE MATRIX SYMMETRIC AND SOLVE
C
      DO 5 I=1,M+1
      DO 5 J=1,I-1
    5 B(J,I)=B(I,J)
      CALL SOLVELSQ(M+1,B,INDIC)
      IF(INDIC)7,7,8
C
C           MATRIX IS SINGULAR
C
    8 TYPE 50
   50 FORMAT(//$NO SOLN, EQS SINGULAR$//)
      RETURN
C
    7 DO 6 I=1,M+1
    6 A(I)=B(I,M+2)
C
      RETURN
      END
```

```
      SUBROUTINE SOLVELSQ(NA,A,INDIC)
C
C          MODIFIED VERSION OF SOLVE
C              FOR USE WITH  LSQ
C
      DIMENSION A(11,12)
      DO 205 I=1,NA
      IF(A(I,I))200,206,200
  200 P=1/A(I,I)
      DO 201 J=I,NA+1
  201 A(I,J)=P*A(I,J)
      DO 202 K=1,NA
      IF(I-K)203,202,203
  203 Q=A(K,I)
      DO 204 J=I,NA+1
  204 A(K,J)=A(K,J)-Q*A(I,J)
  202 CONTINUE
  205 CONTINUE
      INDIC=0
      RETURN
  206 IF(NA-I)300,304,300
  300 DO 303 L=I+1,NA
      IF(A(L,I))301,303,301
  301 DO 302 J=I,NA+1
      HOLD=A(I,J)
      A(I,J)=A(L,J)
  302 A(L,J)=HOLD
      GO TO 200
  303 CONTINUE
  304 INDIC=1
      RETURN
      END
```

```
△E0F.
△META920 SI,L0,B0.
*                COMPLETE MAGNETIC TAPE ROUTINES
*                        PEISEL
*
*             THESE ROUTINES ARE CAPABLE OF
*                        TRANSMITTING DATA TO
*          AND FROM MAGNETIC TAPE IN EITHER
*                        A BINARY OR DECIMAL MODE.
*          ANY NUMBER OF RECORDS OR FILES
*                        MAY BE SKIPPED IN EITHER
*          DIRECTION, THE TAPE UNIT MAY BE
*                        REWOUND, AN END-OF-FILE
*          MAY BE DETECTED OR WRITTEN IF DESIRED.
*                         IN ADDITION, IF
*          THE WORD-COUNT IN THE RECORD IS
*                        UNKNOWN, THE ENTIRE RECORD
*          MAY BE READ AND THE NUMBER OF WORDS
*                        RETURNED IN  KOUNT
*          BY ENTERING THE ROUTINE WITH  KOUNT
*                         = -1.  AN INDICATOR
*          IS INCORPORATED TO ALLOW RECOVERY
*                        FROM TRANSMISSION ERRORS.
*             THE FOLLOWING IS A LIST OF THE
*                         CALL STATEMENTS  AS
*          THEY SHOULD APPEAR IN THE FORTRAN
*                        PROGRAM WITH THE
*          ARGUMENTS DEFINED:
*             DATA = THE DIMENSIONED DATA ARRAY
*             KOUNT = WORD COUNT
*             MAGT = LOGICAL MAGNETIC TAPE UNIT
*             KFILE =    0  NORMAL CORRECT TRANSMISSION
*                   =   -1  READ ERROR
*                   =   +1  END-OF-FILE
*             N = + OR - THE NO. OF RECORDS
*                        OR FILES TO BE SKIPPED
*          CALL RBT(DATA(1),KOUNT,MAGT,KFILE)
*          CALL RDT(DATA(1),KOUNT,MAGT,KFILE)
*          CALL WBT(DATA(1),KOUNT,MAGT)
*          CALL WDT(DATA(1),KOUNT,MAGT)
*          CALL SKF(MAGT,N)
*          CALL SKRC(MAGT,N)
*          CALL ENDF(MAGT)
*          CALL REW(MAGT)
*
       RORG    0
TFT    OPD     04013610
$WBT   PZE                          WRITE TAPE BINARY ENTRY
       SKR     MEM
```

```
$WDT    PZE                     WRITE TAPE DECIMAL ENTRY
        SKR     MEM
$RBT    PZE                     READ TAPE BINARY ENTRY
        SKR     MEM
$RDT    PZE                     READ TAPE DECIMAL ENTRY
        LDA     ERCT            MAXIMUM
                              NUMBER OF TRANSMISSION ERRORS
        STA     ERRCT           ERROR COUNT
        LDA     MEM
        ADD     MEM             MULTIPLY BY 2
        RCH     0402            Q INTO B, A INTO X
        STB     MEM             RESTORE MEM TO ZERO
        ADD     THREE           READ OR WRITE SWITCH
        STA     CNTRL           SET SWITCH
        LDA     TOP12,2         RETRIEVE
                              PROPER TAPE OPERATION
        STA     RWT
        LDA     RDT,2           OBTAIN RETURN ADDRESS
        STA     RBT
        LDX     EOADR           ADDRESS - ERASABLE CORE
        SKN     CNTRL
        STB     *3,2            CLEAR KFILE INDICATOR
        LDA     *1,2            2ND ARGUMENT
        STA     RCOUNT          WORD COUNT
        ETR     MAXWC           CLEAR NEGATIVE WORD COUNT
        RSH     10              EXTENDED WORD COUNT
        MRG     TOP11           EXTENDED WORD COUNT-EOM
        STA     MODE
        STB     PWORD
        LDA     *EOADR          ADDRESS - 1ST ARGUMENT
        ETR     ADRMSK
        MRG     PWORD           NORMAL WORD COUNT
        STA     PWORD           INTERPLACE POT WORD
        LDA     *2,2            3RD ARGUMENT
        STA     MAGT            LOGICAL MAGTAPE UNIT
        MRG     RWT             MERGE WITH TAPE OPERATION
        STA     RWT
        SKN     CNTRL           READ - WRITE SWITCH
        BRU     RERUN
        LDA     TOP10           BEGINNING OF TAPE TEST
        MRG     MAGT
        STA     $+2
        BRM     DELAY
        NOP                     TAPE OPERATION
        BRM     ERAS
        BRU     RERUN
ERAS    PZE                     ERASE TAPE FORWARD
        LDA     TOP9
        MRG     MAGT
```

```
        STA     $+1
        NOP                     TAPE OPERATION
        POT     DUMMY
        BRR     ERAS
RERUN   BRM     DELAY
RWT     NOP                     TAPE OPERATION
MODE    NOP                     EXTENDED MODE EOM
        POT     PWORD
        LDA     TOP7
        MRG     MAGT
        STA     $+1
        NOP                     TAPE READY TEST
        BRU     $+3
        CZT     0               CHANNEL ZERO TEST
        BRU     $-3
        TFT     0               TAPE END-OF-FILE TEST
        BRU     FILE
        CET                     CHANNEL ERROR TEST
        BRU     TRERR
        SKN     CNTRL           READ - WRITE SWITCH
        SKN     RCOUNT
        BRR     RBT
        ASC
        PIN     RCOUNT          RETRIEVE LAST ADDRESS
        LDA     *EOADR
        ETR     ADRMSK
        SUB     RCOUNT          OBTAIN ACTUAL WORD COUNT
        CNA
        STA     *1,2            RETURN
                                COUNT TO MAIN PROGRAM
        BRR     RBT             RETURN
FILE    STA     *3,2            SET END-OF-FILE INDICATOR
        BRR     RBT             RETURN
TRERR   BRM     DELAY           TRANSMISSION
                                ERROR ROUTINE
        LDA     MAGT
        SKN     CNTRL           READ - WRITE SWITCH
        BRU     SCN
        MRG     TOP3            ERASE REVERSE TAPE
        STA     $+1
        NOP                     TAPE OPERATION
        EXU     MODE            EXTENDED MODE EOM
        POT     PWORD
        BRM     ERCNT
        BRU     RERUN           RETURN TO REWRITE
SCN     MRG     TOP4            SCAN REVERSE
        STA     $+1
        NOP                     TAPE OPERATION
        POT     ERR
```

```
        BRM     ERCNT
        BRU     RERUN           RETURN TO REREAD
ERCNT   PZE                     ERROR COUNT ROUTINE
        MIN     ERRCT
        SKN     ERRCT           ARE ERROR TRIALS DONE
        BRU     $+2
        BRR     ERCNT           TRY AGAIN
        SKN     CNTRL           FAILED AFTER 10 TRIES
        BRU     ERRD
        LDA     MAGT
        MRG     TOP9            ERASE TAPE FORWARD
        STA     $+2
        BRM     DELAY
        NOP                     ERASE PASSED BAD SPOT
        EXU     MODE
        POT     PWORD
        LDA     ERCT
        STA     ERRCT           RESTORE ERROR COUNT
        BRR     ERCNT           CONTINUE
ERRD    LDA     ONES
        BRU     FILE            RETURN WITH KFILE = -1
$SKT    RES     0
$SKF    PZE
        LDA     ONES            FILE SWITCH
        LDB     $-2             OBTAIN RETURN ADDRESS
        STB     $+2
        BRU     $+3
$SKRC   PZE
        CLA                     RECORD SWITCH
        STA     CNTRL           SET SWITCH
        LDX     EOADR           ADDRESS - ERASABLE CORE
        LDA     *0,2            1ST ARGUMENT
        STA     MAGT            LOGICAL MAG TAPE UNIT
        MRG     TOP6            SCAN FORWARD
        STA     SCAN
        STA     RDF
        LDA     *1,2            2ND ARGUMENT
        STA     RCOUNT          RECORD OR FILE COUNT
        SKN     RCOUNT          WORD COUNT
        BRU     $+6
        CAX
        LDA     TOP4            SCAN REVERSE
        MRG     MAGT
        STA     SCAN
        BRU     $+5
        SKG     ZERO
        BRR     SKRC            ZERO COUNT RETURN
        CNA                     SKIP FORWARD
        CAX
```

```
        BRM     DELAY
SCAN    NOP                     TAPE OPERATION
        POT     ERR
        SKN     CNTRL           RECORD OR FILE SWITCH
        BRU     SKR
        BRM     DELAY
        TFT     0               TAPE END-OF-FILE TEST
        BRU     $+2
        BRU     SCAN
        BRX     SCAN
        SKN     RCOUNT          RECORD OR FILE SWITCH
        BRR     SKRC            RETURN
RDF     NOP                     PLACE READ-
                              HEAD BEYOND FILE MARK
        POT     ERR
        BRR     SKRC            RETURN
SKR     BRX     SCAN-1
        BRR     SKRC            RETURN
$REW    PZE                     REWIND ENTRY
        LDA     *EOIND
        STA     MAGT
        MRG     TOP5            REWIND
        STA     $+2
        BRM     DELAY
        NOP                     REWIND TAPE
        BRR     REW             RETURN
$ENDF   PZE                     WRITE END-OF-FILE ENTRY
        LDA     *EOIND
        STA     MAGT
        MRG     TOP10           BEGINNING OF TAPE TEST
        STA     $+1
        NOP                     TAPE OPERATION
        BRM     ERAS
        LDA     MAGT
        MRG     TOP8            WRITE TAPE DECIMAL
        STA     $+2
        BRM     DELAY
        NOP                     WRITE END-OF-FILE
        POT     TMC
        BRR     ENDF            RETURN
DELAY   PZE                     TEST STATUS OF TAPE
        LDA     TOP7
        MRG     MAGT
        STA     $+1
        NOP                     TAPE READY TEST
        CAT                     CHANNEL ACTIVE TEST
        BRU     $-2
        BRR     DELAY
INTER   FORM    10,14           INTERLACE FORMAT
```

```
PWORD   INTER   0,0                     POT WORD
ERR     INTER   1,ERR+1                 SCAN POT WORD
        RES     1                       INPUT 1ST WORD FROM SCAN
DUMMY   INTER   600,0                   ERASE BEYOND LOAD POINT
TMC     INTER   1,TMC+1
        DATA    017000000
EOADR   EQU     071
EOIND   EQU     074
ADRMSK  EQU     027                     ADDRESS MASK
ZERO    EQU     023
ONES    EQU     026
THREE   EQU     0342
MAGT    RES     1
CNTRL   RES     1
RCOUNT  RES     1
ERRCT   RES     1
MEM     DATA    0
ERCT    DATA     -10
MAXWC   DATA    077777
TOP1    WTB     *0,0,4                  ----
TOP3    ERT     *0,0,4
TOP13   WTD     *0,0,4
TOP4    SRB     *0,0,4
TOP2    RTB     *0,0,4
TOP5    REW     0,0
TOP12   RTD     *0,0,4                  GENERAL TAPE OPERATIONS
TOP6    SFB     *0,0,4
TOP7    TRT     0,0
TOP8    WTD     *0,0,1
TOP9    EFT     *0,0,4
TOP10   BTT     0,0
TOP11   EOM     014000                  ----
        END
▵EOF.
▵REWIND BO.
▵FORTLOAD MAP,LMAP,BI.
```

```
△J00.
△REWIND 00.
△FORTRAN 00,L0.
C           REFRACTION CORRECTION
C                 REFCOR
C           Q0001-01  --  PEISEL
C
C
C              THE  REFCOR  PROGRAM READS THE PARAMETER LIST
C           OUTPUT FROM THE INITIALIZATION PROGRAM FROM TAPE
C           UNIT 1 AND THE MEASURED ELEVATION AND RANGE DATA
C           FROM TAPE UNIT 2.  IT THEN CALCULATES THE ERROR
C           AND PRINTS THE RESULTS IF SENSE SWITCH 4 IS SET
C           OR OUTPUTS THE RESULTS ON TAPE UNIT 3 IF SENSE
C           SWITCH 3 IS SET.
C
C
      DIMENSION DATA(50),XXLG(10),LDATA(12),KDATA(34)
      EQUIVALENCE (DATA(1),XXLG(1)),
                  (DATA(11),ANGL),(DATA(12),SNS)
      EQUIVALENCE (DATA(13),HS),(DATA(14),H1),(DATA(15),SN1)
      EQUIVALENCE (DATA(16),DH),(DATA(17),DN),(DATA(18),CC)
      EQUIVALENCE (DATA(19),CK0),(DATA(20),
                  CK1),(DATA(21),CK2)
      EQUIVALENCE (DATA(22),CK3),(DATA(23),
                  PI),(DATA(24),PIPI)
      EQUIVALENCE (DATA(25),PI2),(DATA(26),
                  DTOR),(DATA(27),RTOD)
      EQUIVALENCE (DATA(28),ERADIUS),
                  (DATA(29),SQ1),(DATA(30),SQ2)
      EQUIVALENCE (DATA(31),AE),(DATA(32),
                  DH2),(DATA(33),AEHS)
      EQUIVALENCE (DATA(34),AEH1),(DATA(35),
                  FTOKM),(DATA(36),AKTOF)
      EQUIVALENCE (DATA(37),ELTRAP),
                  (DATA(38),N),(DATA(39),NTRAP)
      EQUIVALENCE (KDATA(4),TIME),(KDATA(6),
                  VRANGE),(KDATA(10),VEL)
      EQUIVALENCE (KDATA(12),VCR),(KDATA(16),
                  VCEL),(KDATA(18),VDR)
      EQUIVALENCE (KDATA(20),VDEL),(KDATA(22),
                  CRANGE),(KDATA(24),CELEV)
      EQUIVALENCE (KDATA(26),DRANGE),
                  (KDATA(28),DELEV),(KDATA(30),RDIFF)
      EQUIVALENCE (KDATA(32),EDIFF),(KDATA(34),DELTA)
C
      PRINT 66
   66 FORMAT(1H1,//,48X,$COMPARISON$,
                  /,36X,$VANDANBERG METHOD  AND  SURC
```

```
     1 METHOD$,/,45X,$FOR CORRECTION
                    OF$,/,35X,$RANGE AND ELEVATION  REF
     2RACTION ERROR$,///)
       PRINT 68
    68 FORMAT(/,31X,  $---   VANDANBERG
                      ---$,8X,$---$,6X,$SURC$,7X,
     4$---$,8X,$SURC - VAN$,12X,$ANGLE$,
                    6X,$ELAPSE$,/,15X,$MEASURED$,
     58X,$CORRECTED$,8X,$ERROR$,8X,$CORRECTED$,
                    9X,$ERROR$,8X,
     6$DIFFERENCE$,12X,$DELTA$,7X,$TIME$,///)
       LNS=-13
C
       CALL RBT(DATA(1),100,2,KFILE)
       IF(KFILE)10,12,30
C
    12 CALL RBT(LDATA(1),12,1,KFILE)
       IF(KFILE)10,20,30
    10 TYPE 11
    11 FORMAT($READ ERROR$)
       GO TO 30
C
    20 CALL CONV(LDATA(1),KDATA(1))
       ELEV=VEL*DTOR
       RANGE=VRANGE*FTOKM
       SINEL=SINF(ELEV)
       SQ3=EXPF(-CK1*ELEV)
       IF(ELEV-ANGL)53,53,54
    54 SINGAM=SINEL
       LOP=1
       GO TO 55
    53 SINGAM=SINEL+(CK0+CK2*EXPF(-CK3*RANGE))*SQ3
       LOP=0
    55 COSGAM=SQRTF(1.-(SINGAM*SINGAM))
       TANGAM=SINGAM/COSGAM
       GG=SQ1*TANGAM
       TAUF=SNS*1.0E-06/TANGAM
       SK=RANGE*SQ2*COSGAM
       GK=GG+SK
       DRANGE=SNS*1.0E-06/(CC*SINGAM)*
                    (1.-GG*EXPF(-SK*(2.*GG+SK))/GK)
       KOP=-1
       IF(NTRAP)56,56,57
    57 ATP=ELEV
       IF(ELEV-ELTRAP)47,48,48
    47 ELEV=ELTRAP
    48 ALPHA=COSF(ELEV)*AEHS/AEH1
       ALPHA=ATANF(ALPHA/SQRTF(1.-ALPHA*ALPHA))
       EL1=PI2-ALPHA
```

```
      EL2=SQRTF(EL1*EL1-DN*2.0E-06+DH2/ERADIUS)
      RC=AEH1*C0SF(ALPHA)-AEHS*SINF(ELEV)
      TM=EL1/EL2
      ELEV=ATP
      K0P=0
   56 SINDEL=0.
      DR0=0.
C
      D0 40 I=2,N
      DR=RANGE*XXLG(I)
      DDR=DR-DR0
      DR0=DR
      DR=DR-DDR/2.
      IF(L0P)44,44,45
   44 SINGAM=SINEL+(CK0+CK2*EXPF(-CK3*DR))*SQ3
      C0SGAM=SQRTF(1-SINGAM*SINGAM)
      TANGAM=SINGAM/C0SGAM
      GG=SQ1*TANGAM
      TAUF=SNS*1.0E-06/TANGAM
   45 SK=DR*SQ2*C0SGAM
      GK=GG+SK
      TAU=TAUF*(1.-GG*EXPF(-SK*(SK+2.*GG))/GK)
      IF(K0P)41,42,43
   42 IF(DR-RC)41,43,43
   43 SINDEL=SINDEL+SINF(ELEV-TAU*TM)*DDR
      K0P=1
      G0 T0 40
   41 SINDEL=SINDEL+SINF(ELEV-TAU)*DDR
   40 C0NTINUE
C
      VDR=VRANGE-VCR
      CRANGE=(RANGE-DRANGE)*AKT0F
      DRANGE=DRANGE*AKT0F
      RDIFF=VCR-CRANGE
      CELEV=SINDEL/RANGE
      CELEV=ATANF(CELEV/SQRTF(1-CELEV*CELEV))
      DELEV=ELEV-CELEV
      DELTA=(TAU-DELEV)*RT0D
      DELEV=DELEV*RT0D
      CELEV=CELEV*RT0D
      VDEL=VEL-VCEL
      EDIFF=VCEL-CELEV
      IF(SENSE SWITCH 4)59,28
   59 IF(LNS)58,27,27
   27 PRINT 69
   69 F0RMAT(1H1)
      PRINT 68
      LNS=-16
   58 PRINT 61,VRANGE,VCR,VDR,CRANGE,
                  DRANGE,RDIFF,DELTA,TIME,VEL,VCEL,
```

```
     1VDEL,CELEV,DELEV,EDIFF
   61 FORMAT(2X,$RANGE$,F18.8,F17.8,
                F13.8,F17.8,F14.8,F15.8,F20.8,
     1F11.4,/,$ELEVATION$,F16.8,F17.8,
                F13.8,F17.8,F14.8,F15.8,/)
      LNS=LNS+1
   28 IF(SENSE SWITCH 3)31,12
   31 CALL WBT(KDATA(1),34,3)
      GO TO 12
C
   30 CALL REW(1)
      CALL REW(2)
      IF(SENSE SWITCH 3)32,33
   32 CALL ENDF(3)
      CALL REW(3)
   33 CALL EXIT
      END
```

```
△E0F.
△META920 SI,L0,B0.
*                    C0NVERTER
*          72 BIT FL0ATING P0INT W0RDS T0
*          48 BIT FL0ATING P0INT W0RDS
*               LDATA  T0  KDATA
*
        R0RG    0
$C0NV   PZE
        LDA     E0ADR               ADDRESS - ERASEABLE C0RE
        STA     KDATA
        LDA     *KDATA
        STA     LDATA               ADDRESS - LDATA
        MIN     KDATA
        LDA     *KDATA
        STA     KDATA               ADDRESS - KDATA
        LDA     =4
        STA     WCNT                4 TIMES
L00P    SKR     WCNT
        BRU     $+2
        BRR     C0NV                RETURN
        LDX     LDATA               PHASE 1
        LDA     0,2
        LRSH    15
        ETR     =0577
        STA     SAVE                EXP0NENT
        LDA     1,2
        ETR     =077770000
        CAB
        LDA     0,2
        ETR     =00077777
        LSH     8                   MANTISSA
        LDX     SAVE
        LDE                         EXP0NENT INT0 B
        LDX     KDATA
        STB     0,2                 ST0RE FL0ATING P0INT W0RD
        STA     1,2                 IN REVERSE 0RDER
*
        LDX     LDATA               PHASE 2
        LDA     1,2
        LRSH    3
        ETR     =0577
        STA     SAVE                EXP0NENT
        LDA     1,2
        LDB     2,2
        LSH     20
        ETR     =037777777          MANTISSA
        LDX     SAVE
        LDE                         EXP0NENT INT0 B
```

```
        LDX     KDATA
        STB     2,2             STORE FLOATING POINT WORD
        STA     3,2             IN REVERSE ORDER
        LDA     =3
        ADM     LDATA           MOVE LDATA POINTER
        LDA     =4
        ADM     KDATA           MOVE KDATA POINTER
        BRU     LOOP
*
*
SAVE    RES     1
LDATA   RES     1
KDATA   RES     1
WCNT    RES     1
EOADR   EQU     071
        END
```

```
▵E0F.
▵META920 SI,L0,B0.
*                COMPLETE MAGNETIC TAPE ROUTINES
*                          PEISEL
*
*            THESE ROUTINES ARE CAPABLE OF
*                          TRANSMITTING DATA TO
*          AND FROM MAGNETIC TAPE IN EITHER
*                          A BINARY OR DECIMAL MODE.
*          ANY NUMBER OF RECORDS OR FILES
*                          MAY BE SKIPPED IN EITHER
*          DIRECTION, THE TAPE UNIT MAY BE
*                          REWOUND, AN END-OF-FILE
*          MAY BE DETECTED OR WRITTEN IF DESIRED.
*                           IN ADDITION, IF
*          THE WORD-COUNT IN THE RECORD IS
*                          UNKNOWN, THE ENTIRE RECORD
*          MAY BE READ AND THE NUMBER OF WORDS
*                          RETURNED IN  KOUNT
*          BY ENTERING THE ROUTINE WITH  KOUNT
*                           = -1.  AN INDICATOR
*          IS INCORPORATED TO ALLOW RECOVERY
*                          FROM TRANSMISSION ERRORS.
*             THE FOLLOWING IS A LIST OF THE
*                           CALL STATEMENTS  AS
*          THEY SHOULD APPEAR IN THE FORTRAN
*                          PROGRAM WITH THE
*          ARGUMENTS DEFINED;
*             DATA = THE DIMENSIONED DATA ARRAY
*             KOUNT = WORD COUNT
*             MAGT = LOGICAL MAGNETIC TAPE UNIT
*             KFILE =    0  NORMAL CORRECT TRANSMISSION
*                   =   -1  READ ERROR
*                   =   +1  END-OF-FILE
*             N = + OR - THE NO. OF RECORDS
*                          OR FILES TO BE SKIPPED
*          CALL RBT(DATA(1),KOUNT,MAGT,KFILE)
*          CALL RDT(DATA(1),KOUNT,MAGT,KFILE)
*          CALL WBT(DATA(1),KOUNT,MAGT)
*          CALL WDT(DATA(1),KOUNT,MAGT)
*          CALL SKF(MAGT,N)
*          CALL SKRC(MAGT,N)
*          CALL ENDF(MAGT)
*          CALL REW(MAGT)
*
       RORG    0
TFT    OPD     04013610
$WBT   PZE                          WRITE TAPE BINARY ENTRY
       SKR     MEM
```

```
$WDT    PZE                     WRITE TAPE DECIMAL ENTRY
        SKR     MEM
$RBT    PZE                     READ TAPE BINARY ENTRY
        SKR     MEM
$RDT    PZE                     READ TAPE DECIMAL ENTRY
        LDA     ERCT            MAXIMUM
                              NUMBER OF TRANSMISSION ERRORS
        STA     ERRCT           ERROR COUNT
        LDA     MEM
        ADD     MEM             MULTIPLY BY 2
        RCH     0402            O INTO B, A INTO X
        STB     MEM             RESTORE MEM TO ZERO
        ADD     THREE           READ OR WRITE SWITCH
        STA     CNTRL           SET SWITCH
        LDA     TOP12,2         RETRIEVE
                              PROPER TAPE OPERATION
        STA     RWT
        LDA     RDT,2           OBTAIN RETURN ADDRESS
        STA     RBT
        LDX     EOADR           ADDRESS - ERASABLE CORE
        SKN     CNTRL
        STB     *3,2            CLEAR KFILE INDICATOR
        LDA     *1,2            2ND ARGUMENT
        STA     RCOUNT          WORD COUNT
        ETR     MAXWC           CLEAR NEGATIVE WORD COUNT
        RSH     10              EXTENDED WORD COUNT
        MRG     TOP11           EXTENDED WORD COUNT-EOM
        STA     MODE
        STB     PWORD
        LDA     *EOADR          ADDRESS - 1ST ARGUMENT
        ETR     ADRMSK
        MRG     PWORD           NORMAL WORD COUNT
        STA     PWORD           INTERPLACE POT WORD
        LDA     *2,2            3RD ARGUMENT
        STA     MAGT            LOGICAL MAGTAPE UNIT
        MRG     RWT             MERGE WITH TAPE OPERATION
        STA     RWT
        SKN     CNTRL           READ - WRITE SWITCH
        BRU     RERUN
        LDA     TOP10           BEGINNING OF TAPE TEST
        MRG     MAGT
        STA     $+2
        BRM     DELAY
        NOP                     TAPE OPERATION
        BRM     ERAS
        BRU     RERUN
ERAS    PZE                     ERASE TAPE FORWARD
        LDA     TOP9
        MRG     MAGT
```

```
         STA     $+1
         NOP                         TAPE OPERATION
         POT     DUMMY
         BRR     ERAS
RERUN    BRM     DELAY
RWT      NOP                         TAPE OPERATION
MODE     NOP                         EXTENDED MODE EOM
         POT     PWORD
         LDA     TOP7
         MRG     MAGT
         STA     $+1
         NOP                         TAPE READY TEST
         BRU     $+3
         CZT     0                   CHANNEL ZERO TEST
         BRU     $-3
         TFT     0                   TAPE END-OF-FILE TEST
         BRU     FILE
         CET                         CHANNEL ERROR TEST
         BRU     TRERR
         SKN     CNTRL               READ - WRITE SWITCH
         SKN     RCOUNT
         BRR     RBT
         ASC
         PIN     RCOUNT              RETRIEVE LAST ADDRESS
         LDA     *EOADR
         ETR     ADRMSK
         SUB     RCOUNT              OBTAIN ACTUAL WORD COUNT
         CNA
         STA     *1,2                RETURN
                                 COUNT TO MAIN PROGRAM
         BRR     RBT                 RETURN
FILE     STA     *3,2                SET END-OF-FILE INDICATOR
         BRR     RBT                 RETURN
TRERR    BRM     DELAY               TRANSMISSION
                                 ERROR ROUTINE
         LDA     MAGT
         SKN     CNTRL               READ - WRITE SWITCH
         BRU     SCN
         MRG     TOP3                ERASE REVERSE TAPE
         STA     $+1
         NOP                         TAPE OPERATION
         EXU     MODE                EXTENDED MODE EOM
         POT     PWORD
         BRM     ERCNT
         BRU     RERUN               RETURN TO REWRITE
SCN      MRG     TOP4                SCAN REVERSE
         STA     $+1
         NOP                         TAPE OPERATION
         POT     ERR
```

```
        BRM     ERCNT
        BRU     RERUN           RETURN TO REREAD
ERCNT   PZE                     ERROR COUNT ROUTINE
        MIN     ERRCT
        SKN     ERRCT           ARE ERROR TRIALS DONE
        BRU     $+2
        BRR     ERCNT           TRY AGAIN
        SKN     CNTRL           FAILED AFTER 10 TRIES
        BRU     ERRD
        LDA     MAGT
        MRG     TOP9            ERASE TAPE FORWARD
        STA     $+2
        BRM     DELAY
        NOP                     ERASE PASSED BAD SPOT
        EXU     MODE
        POT     PWORD
        LDA     ERCT
        STA     ERRCT           RESTORE ERROR COUNT
        BRR     ERCNT           CONTINUE
ERRD    LDA     ONES
        BRU     FILE            RETURN WITH KFILE = -1
$SKT    RES     0
$SKF    PZE
        LDA     ONES            FILE SWITCH
        LDB     $-2             OBTAIN RETURN ADDRESS
        STB     $+2
        BRU     $+3
$SKRC   PZE
        CLA                     RECORD SWITCH
        STA     CNTRL           SET SWITCH
        LDX     EOADR           ADDRESS - ERASABLE CORE
        LDA     *0,2            1ST ARGUMENT
        STA     MAGT            LOGICAL MAG TAPE UNIT
        MRG     TOP6            SCAN FORWARD
        STA     SCAN
        STA     RDF
        LDA     *1,2            2ND ARGUMENT
        STA     RCOUNT          RECORD OR FILE COUNT
        SKN     RCOUNT          WORD COUNT
        BRU     $+6
        CAX
        LDA     TOP4            SCAN REVERSE
        MRG     MAGT
        STA     SCAN
        BRU     $+5
        SKG     ZERO
        BRR     SKRC            ZERO COUNT RETURN
        CNA                     SKIP FORWARD
        CAX
```

```
        BRM     DELAY
SCAN    NOP                     TAPE OPERATION
        POT     ERR
        SKN     CNTRL           RECORD OR FILE SWITCH
        BRU     SKR
        BRM     DELAY
        TFT     0               TAPE END-OF-FILE TEST
        BRU     $+2
        BRU     SCAN
        BRX     SCAN
        SKN     RCOUNT          RECORD OR FILE SWITCH
        BRR     SKRC            RETURN
RDF     NOP                     PLACE READ-
                            HEAD BEYOND FILE MARK
        POT     ERR
        BRR     SKRC            RETURN
SKR     BRX     SCAN-1
        BRR     SKRC            RETURN
$REW    PZE                     REWIND ENTRY
        LDA     *EOIND
        STA     MAGT
        MRG     TOP5            REWIND
        STA     $+2
        BRM     DELAY
        NOP                     REWIND TAPE
        BRR     REW             RETURN
$ENDF   PZE                     WRITE END-OF-FILE ENTRY
        LDA     *EOIND
        STA     MAGT
        MRG     TOP10           BEGINNING OF TAPE TEST
        STA     $+1
        NOP                     TAPE OPERATION
        BRM     ERAS
        LDA     MAGT
        MRG     TOP8            WRITE TAPE DECIMAL
        STA     $+2
        BRM     DELAY
        NOP                     WRITE END-OF-FILE
        POT     TMC
        BRR     ENDF            RETURN
DELAY   PZE                     TEST STATUS OF TAPE
        LDA     TOP7
        MRG     MAGT
        STA     $+1
        NOP                     TAPE READY TEST
        CAT                     CHANNEL ACTIVE TEST
        BRU     $-2
        BRR     DELAY
INTER   FORM    10,14           INTERLACE FORMAT
```

```
PWORD   INTER   0,0                     POT WORD
ERR     INTER   1,ERR+1                 SCAN POT WORD
        RES     1                       INPUT 1ST WORD FROM SCAN
DUMMY   INTER   600,0                   ERASE BEYOND LOAD POINT
TMC     INTER   1,TMC+1
        DATA    017000000
EOADR   EQU     071
EOIND   EQU     074
ADRMSK  EQU     027                     ADDRESS MASK
ZERO    EQU     023
ONES    EQU     026
THREE   EQU     0342
MAGT    RES     1
CNTRL   RES     1
RCOUNT  RES     1
ERRCT   RES     1
MEM     DATA    0
ERCT    DATA     -10
MAXWC   DATA    077777
TOP1    WTB     *0,0,4                  ----
TOP3    ERT     *0,0,4
TOP13   WTD     *0,0,4
TOP4    SRB     *0,0,4
TOP2    RTB     *0,0,4
TOP5    REW     0,0
TOP12   RTD     *0,0,4                  GENERAL TAPE OPERATIONS
TOP6    SFB     *0,0,4
TOP7    TRT     0,0
TOP8    WTD     *0,0,1
TOP9    EFT     *0,0,4
TOP10   BTT     0,0
TOP11   EOM     014000                  ----
        END
▵EOF.
▵REWIND BO.
▵FORTLOAD MAP,LMAP,BI.
```

Security Classification

DOCUMENT CONTROL DATA - R & D

(Security classification of title, body of abstract and indexing annotation must be entered when the overall report is classified)

1. ORIGINATING ACTIVITY (Corporate author)	2a. REPORT SECURITY CLASSIFICATION
Syracuse University Research Corporation Merrill Lane, University Heights Syracuse, New York	Unclassified
	2b. GROUP

3. REPORT TITLE

ANALYSIS OF REAL-TIME REFRACTION CORRECTION METHODS FOR THREE MISSILE FLIGHTS FROM THE AIR FORCE WESTERN TEST RANGE

4. DESCRIPTIVE NOTES (Type of report and inclusive dates)

5. AUTHOR(S) (First name, middle initial, last name)

Lyall G. Rowlandson
John R. Herlihy

6. REPORT DATE	7a. TOTAL NO. OF PAGES	7b. NO. OF REFS
July 1969	120	6

8a. CONTRACT OR GRANT NO.	9a. ORIGINATOR'S REPORT NUMBER(S)
F19628-68-C-0209	ESD-TR-69-280
b. PROJECT NO.	
c.	9b. OTHER REPORT NO(S) (Any other numbers that may be assigned this report)
d.	

10. DISTRIBUTION STATEMENT

This document has been approved for public release and sale; its distribution is unlimited.

11. SUPPLEMENTARY NOTES	12. SPONSORING MILITARY ACTIVITY
	Aerospace Instrumentation Program Office Electronic System Division Air Force Systems Command, USAF L. G. Hanscom Field, Bedford, Mass 01730

13. ABSTRACT

An emphasis is placed on the real-time correction of refraction-induced tracking errors. With radar data from three missile trajectories the corrected range and angle data, using real-time equations, is compared with ray-traced data. It is shown that these equations can be effectively used to reduce the range and angle errors to about the resolution of the tracking radars; that is, approximately two feet in range and five thousands of a degree in angle. It is also shown that the effect of an elevated layer on tracking angle errors can be compensated using these equations.

DD FORM 1 NOV 65 1473

Security Classification

14. KEY WORDS	LINK A		LINK B		LINK C	
	ROLE	WT	ROLE	WT	ROLE	WT
Refraction Correction Radar Errors Missile Trajectory Ray Tracing						